University of Windsor
Scholarship at UWindsor

Electronic Theses and Dissertations

1998

Study of needle heating in industrial sewing.

Qingwen. Li
University of Windsor

Follow this and additional works at: http://scholar.uwindsor.ca/etd

Recommended Citation
Li, Qingwen., "Study of needle heating in industrial sewing." (1998). *Electronic Theses and Dissertations.* Paper 3653.

This online database contains the full-text of PhD dissertations and Masters' theses of University of Windsor students from 1954 forward. These documents are made available for personal study and research purposes only, in accordance with the Canadian Copyright Act and the Creative Commons license—CC BY-NC-ND (Attribution, Non-Commercial, No Derivative Works). Under this license, works must always be attributed to the copyright holder (original author), cannot be used for any commercial purposes, and may not be altered. Any other use would require the permission of the copyright holder. Students may inquire about withdrawing their dissertation and/or thesis from this database. For additional inquiries, please contact the repository administrator via email (scholarship@uwindsor.ca) or by telephone at 519-253-3000ext. 3208.

INFORMATION TO USERS

This manuscript has been reproduced from the microfilm master. UMI films the text directly from the original or copy submitted. Thus, some thesis and dissertation copies are in typewriter face, while others may be from any type of computer printer.

The quality of this reproduction is dependent upon the quality of the copy submitted. Broken or indistinct print, colored or poor quality illustrations and photographs, print bleedthrough, substandard margins, and improper alignment can adversely affect reproduction.

In the unlikely event that the author did not send UMI a complete manuscript and there are missing pages, these will be noted. Also, if unauthorized copyright material had to be removed, a note will indicate the deletion.

Oversize materials (e.g., maps, drawings, charts) are reproduced by sectioning the original, beginning at the upper left-hand corner and continuing from left to right in equal sections with small overlaps.

Photographs included in the original manuscript have been reproduced xerographically in this copy. Higher quality 6" x 9" black and white photographic prints are available for any photographs or illustrations appearing in this copy for an additional charge. Contact UMI directly to order.

Bell & Howell Information and Learning
300 North Zeeb Road, Ann Arbor, MI 48106-1346 USA
800-521-0600

UMI®

STUDY OF NEEDLE HEATING IN INDUSTRIAL SEWING

By

Qingwen Li

A Thesis
Submitted to the Faculty of Graduate Studies and Research
Through the Department of Industrial and Manufacturing Systems Engineering
In Partial Fulfillment of the Requirements for
The Degree of Master of Applied Science at the
University of Windsor

Windsor, Ontario, Canada

1998

© Qingwen Li, 1998

National Library of Canada
Acquisitions and Bibliographic Services
395 Wellington Street
Ottawa ON K1A 0N4
Canada

Bibliothèque nationale du Canada
Acquisitions et services bibliographiques
395, rue Wellington
Ottawa ON K1A 0N4
Canada

Your file Votre référence

Our file Notre référence

The author has granted a non-exclusive licence allowing the National Library of Canada to reproduce, loan, distribute or sell copies of this thesis in microform, paper or electronic formats.

L'auteur a accordé une licence non exclusive permettant à la Bibliothèque nationale du Canada de reproduire, prêter, distribuer ou vendre des copies de cette thèse sous la forme de microfiche/film, de reproduction sur papier ou sur format électronique.

The author retains ownership of the copyright in this thesis. Neither the thesis nor substantial extracts from it may be printed or otherwise reproduced without the author's permission.

L'auteur conserve la propriété du droit d'auteur qui protège cette thèse. Ni la thèse ni des extraits substantiels de celle-ci ne doivent être imprimés ou autrement reproduits sans son autorisation.

0-612-52598-8

Canada

ABSTRACT

With the use of synthetic fabric and thread as well as high speed sewing in sewing industry, needle heating due to friction between the needle and fabric becomes a serious problem. The high temperature in the needle can scorch the fabric as well as accelerate thread wear and damage the thread. It also causes wear at the needle eye, and may temper and weaken the needle itself. Experimental methods, such as infrared radiometry, infrared pyrometry, thermal couples, etc., have been applied to analyze this problem in previous studies. They revealed some important factors that affect the needle peak temperature. However, they provided limited information and were expensive to conduct. Therefore, it is desirable to develop analytical computer simulation models to study the needle heating problem.

In this thesis, three models are developed: a sliding model, a lumped model, and a Finite Element (FE) simulation model. In the sliding model and the lumped model, it is assumed that needle can be modeled as a cylinder and the effect of the thread can be ignored. These simplified analytical models focus on the needle-fabric interactions, especially the friction heat partition between needle and fabric.

In the FE model, both the detailed needle geometry characteristics and thread effects are considered. It models the needle-fabric interactions as a transient heat transfer process with time-dependent boundary conditions. It correlates various important factors that affect the needle heating, such as needle characteristics, fabric properties, and sewing operation conditions. The FE simulation is carried out using **ANSYS 5.3.** Given various needle geometry, sewing conditions, and fabric properties, the model can predict the

needle heating process, including the initial heating phase, the equilibrium phase, and the temperature distribution in the needle. It is found that sewing speed and fabric thickness are the most important factors that affect peak temperature. The trend of the simulation results closely resembles the experimental results.

DEDICATION

To my parents and grandparents

ACKNOWLEDGEMENTS

I wish to express my sincere and deep appreciation for my supervisor, Dr. R. Du, who has been giving me encouragement, support and insight guidance from the very beginning of my study in this department and throughout the thesis.

I am also cordially indebted to Dr. E. Liasi, who has been helping me during the entire course of this thesis, by answering my technical questions, providing experiment support, revising thesis draft at the early stages.

I would like to thank Professor J. Zhou, Mr. A. Chen for giving valuable suggestions on many points of this study. Deep thanks extends to E. Mallet for his patient help and providing constructive information.

I particularly want to thank Dr. N. Zamani, my committee member, for supporting and giving precious advices in preparing this thesis.

Thanks is also due to Dr. Fil. Salustri, for not only serving on my committee, but also helping me in many ways. Much thanks are due to Ms. Jacquie Mummery, Mr. Dave Mckenzie, Ram Barrakat, secretary and technicians of Industrial Engineering, for their support and friendly assistance during my two years study in this department.

The encouragement and suggestions from my group members are never forgettable. Finally I convey my deep gratitude to all those who helped me in various ways.

TABLE OF CONTENTS

ABSTRACT iii

ACKNOWLEDGMENTS vi

LIST OF FIGURES x

NOMENCLATURE xii

CHAPTER I - INTRODUCTION 1

1.1 Background and Objectives 1

1.2 The Basic Thermal Mechanics of the Needle Heating 4

1.3 Previous Analytical Models 8

1.4 Brief Description of Presented Work 9

CHAPTER II - SLIDING MODEL OF NEEDLE HEATING 13

2.1 Theory of Moving Heat Sources and the Temperature at Sliding Contacts 13

2.1.1 Model and Fundamental Solutions 13

2.1.2 Problems on Moving Plane Sources 14

The Steady Temperature Due to a Moving Band Source in Plane $z=0$ 14
The Steady Temperature Due to Rectangular Moving Heat Source 17

2.1.3 Stationary Sources 20

2.2 Sliding Model in Needle Heating 21

2.2.1 Development of the Model 21

Analysis and Assumptions 21
Temperature Development Between Needle and Fabric 23
Needle Temperature vs. Time During the Sewing Process 24

2.2.2 Simulation Results 25

CHAPTER III - LUMPED MODEL OF NEEDLE HEATING 29

3.1 Basic Principles 29

3.1.1 Unsteady Heating and Cooling in Lumped Variables Method 30

Temperature Increase at Heating Stage 30
Temperature Decrease at Cooling Stage 30

3.1.2 Temperature Development in a Contact Heated Contact Surface 31

3.2 Lumped Model in Needle Heating 34

3.2.1 Development of the Model 34

Temperature Rise in the Needle 35
Temperature Rise in the Fabric Contact Surface 36
Friction Heat Partition Ratio 37
Needle Temperature vs. Time During the Sewing Process 38

3.2.2 Simulation Results 38

CHAPTER IV - THE FEA MODEL 41

4.1 Definition of Geometric Configuration of the Model 42

4.2 Boundary Conditions 47

4.2.1 Heat Flux 48

Applying the Time-Dependent Heat Flux Layer by Layer 48
Calculation of the Heat Flux 51
Friction Heat Partition Ratio Between Fabric and Needle 54

4.2.2 Convection Boundary Condition 55

Applying Time-Dependent Convection Boundary Condition 55
Determination of Convection Coefficient 56

4.2.3 Heat Flow 57

Heat Flow Boundary Condition 57
Calculation of Heat Flow 57

4.3 FEA Simulation Results and Discussions 63

4.3.1 Simulation Results 63

4.3.2 Parameters Effects on Needle Heating 69

Effect of Sewing Speed 70
Effect of Fabric Thickness 71
Effect of Material Properties 72
Effect of Needle Geometry 73

4.4 Brief Comparison of FEA model and Simplified Models 74

CHAPTER V - CONCLUSIONS AND FUTURE WORK 76

5.1 Conclusions 76

5.2 Future Work 77

REFERENCES 80

APPENDIX A Matlab Program for Sliding Model.....84

APPENDIX B Analysis of Friction Heat Partition Ratio.....87

APPENDIX C Matlab Program for Lumped Model.....93

APPENDIX D ANSYS Program for FEA Model.....96

APPENDIX E FEA Simulation Results with Fabric Thickness at 2 mm 108

LIST OF FIGURES

Figure	Description	Page
1.1	Needle heating thermal system	5
1.2	Coordinate system for a needle heating model	7
2.1	Temperature calculation for intermediate L [Jager, 1942]	18
2.2	Sliding model of needle heating	22
2.3	Needle temperature vs. time in sliding model	26
2.4	Peak temperature from sliding model	27
2.5	Peak Temperature From Experimental Report [Hersh, 1969]	28
3.1	Streamlines Directed Radially from the b-hemisphere	32
3.2	Lumped model	35
3.3	Needle temperature vs. time in lumped model	39
3.4	Needle peak temperature from lumped model	40
4.1	Solid 70 3-D thermal solid element	42
4.2	Industrial sewing machine needle geometry	44
4.3	Needle meshing result	45
4.4	First section view of needle meshing	46
4.5	One cycle of needle sewing process	49
4.6	Applying heat flux boundary conditions layer by layer	51
4.7	Sketch for heat flux calculation	51
4.8	Friction force vs. time	52
4.9	Normal pressure vs. time	53

4.10	γ vs. sewing stitch cycle	55
4.11	Sketch of thread motion and tension in the thread	58
4.12	Sketch of thread tension vs. crank rotation angle	59
4.13	Sketch to calculate the heat flow	60
4.14	IR image of needle heating results	63
4.15	Reference nodes positions	64
4.16	Temperature vs. time, 2000 rpm, th=4mm	66
4.17	Experiment results of high speed sewing 2000 rpm	66
4.18	Temperature vs. time, 1000 rpm, th=4mm	67
4.19	Experiment results of medium speed sewing 1000 rpm	67
4.20	Temperature vs. time, 500 rpm, th=4mm	68
4.21	Experiment results of low speed sewing 500 rpm	68
4.22	Comparison of temperature values on needle center and outer surface	75
5.1	Proposed speed suggestion system	79
B.1	γ vs. sewing speed at different fabric thickness	86
B.2	γ vs. fabric thickness at different sewing speed	87
B.3	γ vs. fabric density at different initial temperature difference	88
B.4	γ vs. fabric specific heat	89
B.5	γ vs. needle specific heat	90
B.6	γ vs. needle density at different ΔT_0	91
E.1	Temperature vs. time, 2000 rpm, th = 2 mm	106
E.2	Temperature vs. time, 1000 rpm, th = 2 mm	107
E.3	Temperature vs. time, 500 rpm, th = 2 mm	108

NOMENCLATURE

Symbols Used in Program

For Needle Geometry and Sewing Operation

dp = punching-in length that the needle go in to the fabric *m*

dw = the idling distance

fcoef = convection coefficient on the needle outer surface $W/(m^2 \cdot ℃)$

hb = beginning position of the needle eye

he = end position of the needle eye

kp = number of load steps during punching

kw = number of load steps during idling

lgb = beginning position of the long groove

lge = end position of the long groove

L_step= index of multiple load step

ndiv = number of section divisions on the needle length

nlg = the needle length

nshf = number of sections experiencing heat flux at the same time

rad(i) = needle radius on the "*ith*" section, $i = 1,2,3, \ldots ndiv$

rpm = rotation speed of the punching crank *revolution/minute*

spd = needle punching speed *m/s*

th = fabric thickness

For Material Properties and Thermal Boundary Conditions

c1 = needle material specific heat $J/(kg \cdot ℃)$

c2 = fabric material specific heat $J/(kg \cdot ℃)$

gama = friction heat partition ratio

lmt1 = needle material heat conductivity $W/(m \cdot ℃)$

lmt2 = fabric material heat conductivity $W/(m \cdot ℃)$

rou1 = needle material density kg/m^3

rou2 = fabric density kg/m^3

Symbols Used in Equations

A = area m^2

f(t) = the friction force N

h_c = convection coefficient $W/(m \cdot ℃)$

P_f = friction power generated when the needle punching W

p = unit normal force acted on the needle cylinder N / m^2

q_{flux} = heat flux due to friction W/m^2

r = needle radius m

t = time Sec

T = needle temperature K

T_0 = the environment temperature K

T_{thread} = thread tension in sewing process N

v(t) = the needle punching speed m / s

V = velocity m/s

V_{ol} = the examined needle volume m^3

α = material diffusivity m^2/s

δ = fabric thickness

γ = friction heat partition ratio

k = needle thermal conductivity $W/(m \cdot ℃)$

μ = friction coefficient

ρ = needle material density kg/m^3

CHAPTER I

INTRODUCTION

1.1 Background and Objectives

Industrial sewing is one of the most commonly used manufacturing operations, especially in the automobile industry. Everyday, millions of products are sewn, such as automotive car-seat, cushions and backs, airbags, etc., which demand high sewing quality of good appearance and long-lasting stitches. The material been sewn includes single and multiple ply synthetic fabric, plastic, and leather, which are thick, making the sewing conditions harder than ordinary sewing applications.

In order to increase the sewing productivity, high speed sewing machines are used. Usually sewing speed range from 2000 rpm ~ 6000 rpm. A problem which accompanies the high speed sewing is broken thread, which is also the most common defect encountered in industrial sewing, and must be minimized. This problem may be caused by various reasons, but excessive needle heating is by far the most important. When the needle penetrates the fabric thousands of times per minute, needle heating due to the friction between the needle and the fabric, is very severe. The friction generates heat, part of the heat is absorbed by the fabric, part of it is absorbed by the needle. The heat absorbed by the fabric is spread out along the seam stitches, but the heat absorbed by the needle is accumulated while the needle penetrates and withdraws periodically. The highest needle temperature depending on sewing conditions ranges from 100 ^{0}C ~ 300 ^{0}C while the sewing speed ranges from 1000 rpm to above 3000 rpm.

The high temperature can weaken the thread since thread tensile strength is a function of temperature. Sometimes the temperature exceeds the melting point of the synthetic sewing thread, resulting in broken threads. The hot needle can cause the formation of creases in the sewing thread. Because of the crease, the loop formed by the sewing thread is improperly shaped and the hook will not enter the loop, resulting in skipped stitches. The hot needle can also initiate damage in the fabric, such as leaving burn marks on natural fibers, leaving weakened seam or melted residue on the fabric surface. Also, the heat may draw the temper of the needle and weaken it, so it may bend or fail by breaking easily. Decreasing the sewing speed can cool down the needle, in the mean time, it will decrease the operator's other handling activities, hence the sewing productivity is doubly decreased. Even though the typical sewing machine is made of hundreds of parts, only few parts come in contact with the fabric. The needle is the only part that goes into and out of the fabric. Clearly, understanding the needle-fabric interactions, optimizing sewing operations, minimizing the penetrating force and the peak temperature result in significant economic benefit.

Lots of efforts have been made to analyze the needle heating problems, trying to understand the mechanism of needle heating, correlating the factors of needle characteristic, operation conditions and fabric properties to the peak temperature. Most of these studies are using the experimental methods to measure the needle temperature, such as IR radiometry[Liasi, E, 1996], infrared pyrometry, attached thermocouple, separate thermocouple, temperature-sensitive material [Hersh, S. P. et al. 1969], etc. The experiment results reveal interesting information in correlating some important physical factors to needle heating.

However, the experimental methods have some shortcomings: [Hersh, S. P. et al. 1969]

(1) For the infrared pyrometer, there is a problem in calibrating. Because the amount of radiation emitted at higher temperature depends on the surface characteristics. The emissivity of each needle must be determined individually and, indeed, the emissivity might change during testing, a condition which would require further calibration. Therefore this technique for needle temperature measurements would be quite expensive. Since the needle moves very fast, it is difficult to get the temperature profile along the needle in this method.

(2) The attached thermocouple is usually done by soldering or welding a wire other than steel to the needle to form a thermocouple, with the needle itself serving as one of the junction metals. The major shortcomings of this technique are the mechanical problems associated with the wire leads to the needle and the relatively slow response to temperature changes.

(3) Measurements by separate thermocouple is done by touching a thermocouple to the hot needle after the sewing machine is stopped. The major problem with this technique is the delay in placing the thermocouple in contact with the needle. Even 1 sec delay in touching the needle will result in a decrease of 20% to 30% in the temperature reading.

(4) Another way to measure the needle temperature is to put the temperature sensitive material, such as waxes, lacquers and melting-point crayons in the needle groove. The materials melt or change color when they reach a specific

temperature. This procedure is obviously a hit or miss operation. If a wax is placed on the needle and does not melt, it must be replaced with another one that melts at lower temperature. If the wax melts, it must be replaced with one melting at a higher temperature. In this manner, it is possible to indicate the highest temperature reached by the needle, but it can't give any idea of the rates of heating.

Due to the shortcomings of the experimental methods, a numerical simulation model of needle heating problem is highly desired. With the theoretical simulation model, the temperature profile along the needle and the needle heating process can be obtained. In addition, one could easily analyze various factors' correlation with the needle heating results, determine the mechanism of the main effects in this problem, and hence, optimize the sewing operation. Furthermore, the simulation model can give some useful information in assisting the design of needle and needle-cooling systems. With the advent of a high speed computer and simulation software, the numerical solution of this problem is possible.

1.2 The Basic Thermal Mechanics of the Needle Heating

The actual needle heating process is rather complicated. Needle temperature arises as the sewing process starts and continues to arise until the equilibrium state attained. During the entire process, the needle temperature varies slightly at each stitch while the needle punching and withdrawing the fabric. Figure 1.1 illustrates the needle heating system. More specifically, the heat is generated from following sources:

- Heat flux generated from friction between fabric and needle outer surface. With the needle punching and withdrawing, the fabric position relative to the needle is changing, hence heat flux position is changing with time during one stroke.
- Heat flow from the friction between thread and needle-eye when thread is tightening. This is due to thread friction with the needle-eye. Since the thread tension is changing periodically during one stroke, therefore the heat flow value is time-dependent.

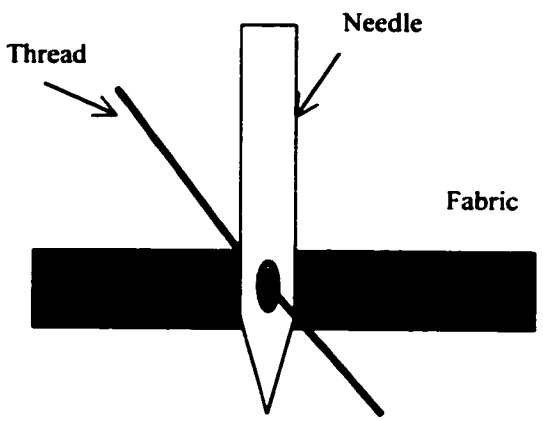

Figure 1.1 Needle Heating Thermal System

On the other hand, the heat sink includes:

- Convection of the outer surfaces of needle that are not contacting with the fabric. Since the relative position of the needle to the fabric is time-dependent, the convection is time-dependent.

- heat conduction in the needle from the higher temperature points to the lower temperature points, such as the needle shank.
- contact between thread and needle-eye when the thread loosely passes the needle-eye.
- radiation between the needle outer surfaces to the environment. According to the reports [Howard, G. M. 1968], radiation plays a minor role in needle cooling. Therefore, radiation is neglected in this study.

From the above, it is evident that both heat sources and heat sinks are time-dependent. Therefore, the needle heating is a transient heat transfer problem. As illustrated in Figure 1.2 coordinate system, the needle heating effect can be described as the conduction problem, with the boundary conditions as following:

$$\frac{\partial T}{\partial t} + U(t)\frac{\partial T}{\partial Z} = \frac{k}{\rho c}\left(\frac{\partial^2 T}{\partial r^2} + \frac{1}{r}\frac{\partial T}{\partial r} + \frac{1}{r^2}\frac{\partial^2 T}{\partial \theta^2} + \frac{\partial^2 T}{\partial Z^2}\right) \tag{1.1}$$

Initial condition : $T = T_0$, when $t = 0$, for all r, θ, Z

Boundary conditions : $k\frac{\partial T}{\partial r} + h(T - T_0) = 0$, when $r = r_0$, $Z \neq \pm\delta/2$,

$$k\frac{\partial T}{\partial r} + q(t) = 0, \quad \text{when} \quad r = r_0, \; Z = \pm\delta/2,$$

$$\frac{\partial T}{\partial Z} = 0 \qquad Z = a(\sin\omega t - \sin\omega_0 t) \quad r, \theta, t$$

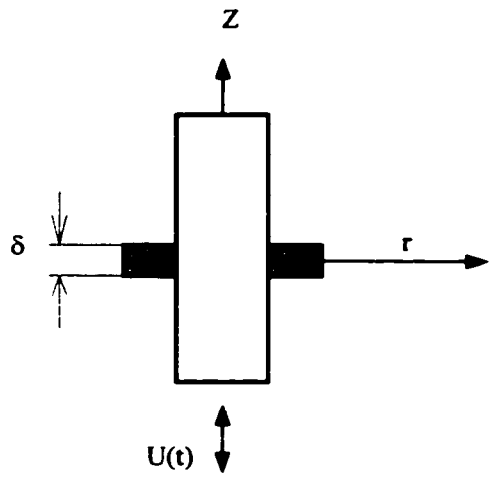

Figure 1.2 Coordinate System for a Needle Heating Model

Where, T is the needle temperature, K;

t is the time, *Second;*

k is the needle thermal conductivity, $W/(m \cdot K)$;

h is the convection coefficient, $W/(m^2 \cdot K)$;

ρ is the needle material density, kg/m^3;

c is the specific heat of needle, $W/(kg\ K)$;

r, θ, Z are cylindrical coordinates;

$U(t)$ is the velocity, m/sec;

a is the amplitude of sewing stroke, m;

ω is the frequency, rad/sec;

$q(t)$ is heat flux due to friction, W/m^2;

δ is the fabric thickness, m.

Since the boundary conditions are time-dependent and the needle geometry is not regular, it is very difficult to get an analytical solution for the model. Therefore either simplified methods are used in analyze this needle heating problem, or numerical technique is to be used, specifically, finite element analysis method is used in this thesis. During this thesis two basic assumptions are made: the different layers of fabric been sewn have uniform average material properties; the needle speed is assumed as constant during each cycle. The support of these assumptions are found in Jeager's study of contact sliding heat sources.

1.3 Previous Analytical Models

Even though previous efforts focused on experimental study, analytical methods have been used by Howard [1968] and Simmon [1980] in examine important factors that affect needle heating. In Howard study, a very simple model is established for estimating needle heat losses after the needle achieved equilibrium state. While Simmon developed a simple experience formula of exponential equation for needle heating process using regression method, which based on his experimental data.

These analytical models made no efforts in examine the friction heat partition between needle and fabric, which in fact is a function of material properties, sewing speed, fabric thickness, etc. Therefore it can hardly correlate the fabric properties to needle heating results theoretically. Also simulation of the transient stage while the

needle temperature building up has been a challenge to those efforts made by using the energy balance method at equilibrium stage.

But the previous efforts in experiments and theoretical analysis revealed very important information, which give author a good start point to establish simulation models described in this thesis. Among the several aspects that affect needle heating, their conclusions are :

- Sewing speed is the most important factor in peak temperature, but little effect on needle penetrating force.
- Radiation plays minor role on needle heat dissipation.
- Of the needle characteristics (including the needle finish, needle point shape, needle type), the needle finish has significant effect on equilibrium temperature, the effect of point type is minor.
- Fabric properties (including fabric structure, fabric finish, fabric composition,) have big effects on the final temperature: heat generation by frictional contact of needle and fabrics is primarily a function of fabric-surface frictional characteristics and of fabric tightness. The thickness of the fabric is also very important.
- Properly installed cooling systems have obvious results in decreasing high temperature.

1.4 Brief Description of Presented Work

In this thesis, the attempts were first made in establishing simplified analytical simulation model: sliding model and lumped model. In these models, the needle

geometry is assumed as an infinite cylinder, and the thread function in needle heating is ignored. The sliding model is based on the theory of moving heat source and temperature at sliding contact [Jaeger, 1942]. While the lumped model is based on the basic heat transfer principles.

These simplified models examined the needle heating phenomenon in one stitch, studied the friction heat partition ratio between needle and fabric, formulated heating and cooling equations. Then Matlab programs are developed in carrying on the calculation of needle temperature build-up in the whole sewing process.

Based on the information provided by the experiments and the simplified simulation models, the finite element analysis model for needle heating is established in considering needle geometry and thread function. This FEA model is a time dependent boundary condition problem. Since the position and value of the heat source and heat sink are changing with time, while needle penetrating the fabric.

Using **ANSYS 5.3** APDL *(ANSYS Parametric Design Language)* language, a program is written carrying out the FEA model simulations. In this FEA model, needle is meshed with solid element by direct nodes and elements generation method for the easy application of surface boundary conditions later on. The time dependent boundary conditions are applied using multiple load steps in transient heat transfer options. In post processing, the simulation results can reflect the temperature distribution in the needle, and the time history curves of needle heating process, including initial heating phase and equilibrium phase. The peak temperature and the time needed to go to the equilibrium state, which are of the two major interesting points for operators, can be obtained.

Since the heat due to friction between the needle and fabric is the major heat source, the friction force during needle penetrating and withdrawing must be studied. A sewing force model was developed by [Mallet, E. 1997], from which the necessary information related to needle heating are obtained, such as the friction force curve along the needle with different kind of needle characteristics, fabric properties.

Convection is the major part of heat dissipation. When there is a cooling system installed, forced convection applies, otherwise only free convection allowable for cooling. Since the sewing needle is punching at high speed, therefore the convection coefficient is affected by the sewing speed to some degree [Perry, 1963].

Sewing thread plays a complicated role in needle heating problem. Generally, the thread is a heat sink, because the thread goes through the hot needle eye in loosely contact most of the time during sewing. Therefore it takes some heat. It is reported that needle temperature decreased when sewing with thread [Hersh, S. P. ,et al. 1969].

In the meantime, the thread is a kind of heat source. It is observed that usually before the needle punches in the fabric, the needle temperature rises about 4 ^{0}C [Liasi, E. et al. 1996], which shows the friction between thread and needle is a heat source at some time, when tension is established in the thread to tighten the stitch.

In brief, these simulation models are developed to demonstrate the correlation between the important physical factors affect the needle heating, such as: needle characteristics, fabric properties, operation conditions, etc.. Given various needle geometry, sewing conditions, and fabric properties, the peak temperature and time span of initial heating process can be obtained.

In this study, the simulations are run at different sewing speeds with different fabric thickness. The trend of the simulation results match the experimental results [Liasi, E. et al. 1996]. The effects of sewing speed and fabric thickness on the peak temperature and time span are discussed.

This thesis are organized into five chapters. Chapter II and Chapter III proposes the simplified simulation methods: sliding model and lumped model. Chapter IV develops the FEA model. Finally the conclusions and future work are discussed in Chapter V.

CHAPTER II

THE SLIDING MODEL OF NEEDLE HEATING

2.1 Theory of Moving Heat Sources and the Temperature at Sliding Contacts

When one part is sliding against the other stationary part, heat is generated due to the friction between these two contacted parts. The temperature is developed in the contact surface, hence permeate into the body. The attempt was made in studying the temperature development of plane sliding mathematically by Jaeger, J.C. [1942]. Based on his theory and conclusions, the needle heating sliding model is proposed after some adjustments are made.

2.1.1 Model and Fundamental Solutions

The temperature at the point *(x, y, z)* at time *t* in an infinite solid, initially at zero temperature, due to a quantity of heat *Q* instantaneously liberated at the point *(x', y', z')* at zero time is:

$$\frac{Q\alpha}{8K(\pi\alpha t)^{3/2}}\exp\left(-\frac{(x-x')\ +(y-y')^2+(z-z')^2}{4\alpha t}\right) \tag{2.1}$$

where, $\alpha = \dfrac{k}{\rho c}$.

If *Q* is replaced by *Qdy'*, and the solution for instantaneous line source parallel to y-axis can be obtained by integrating Eq. (2.1) with respect to *y'* from $-\infty$ *to* $+\infty$. The temperature at the point *(x, y, z)* at time *t* due to this is:

$$\frac{Q}{4\pi kt}\exp\left(-\frac{(x-x')^2+(z-z')^2}{4\alpha t}\right) \tag{2.2}$$

The solutions for moving sources are obtained by integration of these fundamental solutions.

2.1.2 Problems on Moving Plane Sources

The calculation of the temperature in a semi-infinite solid, $z<0$, on which another body slides, has been the major part of this theory. The plane of sliding is taken as the plane $z=0$, and the sliding to be with constant velocity V along the axis of x. It is assumed that heat is liberated at a constant rate of q, per unit time, per unit area, over the instantaneous surface. If the sliding body were a non-conductor, the whole of the heat would be taken up by the solid $z<0$, and the problem would be that of a uniform source of heat moving in the surface $z=0$ of this region with no loss of heat from the surface.

1. <u>The Steady Temperature Due to a Moving Band Source in Plane $z=0$</u>

The band source parallel to the y-axis and of length $2l$ parallel to the x-axis is moving with velocity V in the plane $z=0$ of the semi-infinite solid $z<0$ with no loss of heat from the plane $z=0$. Heat is liberated at the rate q per unit time, per unit area, over the area of the source.

Suppose the motion has gone on infinitely long, so the steady conditions have been attained, and that at the instant considered, zero time, the center of the band is at the origin. The temperature at this time at the point $(x,0,z)$ is to be calculated. At time t

earlier, the center of the band was at *(-Vt)* and by (2.3) the temperature at zero time at the point *(x,0,z)* due to a line source of *2qdx'dt* heat units per unit length, parallel to the y-axis and through the point *(x'-Vt, 0,0)* is:

$$\frac{qdx'dt}{2\pi kt}\exp\left(-\frac{(x-x'+Vt)^2+z^2}{4\alpha t}\right) \tag{2.3}$$

To find the temperature at zero time for the band of length *2l* which has been moving for infinite time, integrate (2.4) with respect to x' from *-l to l*, and with respect to t from *0 to* ∞, and obtain:

$$\begin{aligned}\upsilon &= \frac{q}{2\pi k}\int_{-l}^{l}dx'\int_{0}^{\infty}\frac{dt}{t}\exp\left(-\frac{(x-x'+Vt)^2+z^2}{4\alpha t}\right)\\ &= \frac{q}{\pi k}\int_{-l}^{l}e^{-V(x-x')/2\alpha}K_0\left\{\frac{V}{2\alpha}\left[(x-x')^2+z^2\right]^{\frac{1}{2}}\right\}dx'\end{aligned} \tag{2.4}$$

where $K_0(x)$ is the modified Bessel function of the second kind of order zero.

Introducing the dimensionless quantities:

$$X=\frac{Vx}{2\alpha}\quad Y=\frac{Vy}{2\alpha}\quad Z=\frac{Vz}{2\alpha}\quad L=\frac{Vl}{2\alpha} \tag{2.5}$$

Eq. (2.4) becomes:

$$\upsilon=\frac{2q\alpha}{\pi kV}\int_{X-L}^{X+L}e^{-u}K_0(Z^2+u^2)^{1/2}\,du \tag{2.6}$$

Let $Z=0$, the temperature in the plane of the source are given by

$$\frac{\pi\ kV}{2\,q\,\alpha} = I\,(\,X\ +\ L\,)\ -\ I\,(\,X\ -\ L\,) \tag{2.9}$$

where,

$$I\,(\,x\,) = \int_0^x e^{-u}\,K_0\,(\,|u|\,)\,du \tag{2.10}$$

So that

$$I\,(-x\,) = -\int_0^x e^{u}\,K_0\,(\,|u|\,)\,du \tag{2.11}$$

Given small L, for small X, there is an approximate form:

$$\frac{\pi kV}{2q\alpha}\upsilon = -2.303(X+L)\log_{10}|X+L| + 2.303(X-L)\log_{10}|X-L| + 2.232\,L \tag{2.12}$$

Given large L, the approximate form is like:

$$\frac{\pi kV}{2q\alpha}\upsilon = \{2\pi(L-X)\}^{1/2}, \qquad -L<X<L \tag{2.13}$$

$$= (2\pi)^{1/2}\{(L-X)^{1/2} - (|X+L|)^{1/2}\}, \qquad X<-L$$

The above equations give the temperature value over the contact area and the nearby area the heat source passes by. From the equation (2.12), (2.13), the maximum and average steady temperatures over the area of source are obtained.

(i) If L is large, say $L>5$, the maximum temperature is (using 2.13):

$$\frac{4\,q\,\alpha\,L^{\frac{1}{2}}}{kV\,\pi^{1/2}} = \frac{2\,q}{k}\left(\frac{2\,\alpha\,l}{\pi\,V}\right)^{\frac{1}{2}} \tag{2.14}$$

and the average temperature over the area of the source is

$$\frac{8q\alpha L^{1/2}}{3kV\pi^{1/2}} = \frac{1.064q}{k}\left(\frac{\alpha l}{V}\right)^{1/2} \tag{2.15}$$

(ii) If L is small, say $L<0.1$, the maximum temperature is (using 2.12) :

$$\frac{4q\alpha}{\pi kV}\{-2.303L\log_{10}L + 1.116L\} \tag{2.16}$$

and the average temperature is:

$$\frac{4q\alpha}{\pi kV}\{-2.303L\log_{10}2L + 1.616L\} \tag{2.17}$$

For intermediate value of L, $0.1<L<5$, refer to Figure 2.1, curve I an II are the maximum and average temperature of a band source times $(\pi kV/2\alpha q)$ against L.

2. <u>The Steady Temperature Due to Rectangular Moving Heat Source</u>

The rectangular heat source of sides $2l$ and $2b$, parallel to the x and y axes respectively, is moving with velocity V along the x-axis in the plane $z=0$ of semi-infinite solid $z<0$ with no loss of heat from the plane $z=0$. Then the temperature at point (x, y, z), when the center of the source is at the origin,

$$\frac{\alpha q}{\pi kV}\int_{X-L}^{X+L} e^{-\eta}\, d\eta \int_{Y-B}^{Y+B} \frac{\exp\left\{-\left(\eta^2+\zeta^2+Z^2\right)^{1/2}\right\}}{\left(\eta^2+\zeta^2+Z^2\right)^{1/2}} d\zeta \tag{2.18}$$

Where, the notation (2.5) has been used, and $B=\frac{Vb}{2\alpha}$. In the plane $z=0$ there is a temperature variation in y as well as in x; the temperature is highest at points on the x-axis; Putting $Y=Z=0$ in (2.18), there is:

$$\begin{aligned}\frac{\pi kV}{2\alpha q}\upsilon &= \int_{X-L}^{X+L} e^{-\eta}\, d\eta \int_{0}^{B} \frac{e^{-(\eta^2+\zeta^2)^{1/2}}}{(\eta^2+\zeta^2)^{1/2}} d\zeta \\ &= \int_{X-L}^{X+L} e^{-\eta} K_0(|\eta|)\, d\eta - \int_{X-L}^{X+L} e^{-\eta}\, d\eta \int_{B}^{\infty} \frac{e^{-(\eta^2+\zeta^2)^{1/2}}}{(\eta^2+\zeta^2)^{1/2}} d\zeta\end{aligned} \tag{2.19}$$

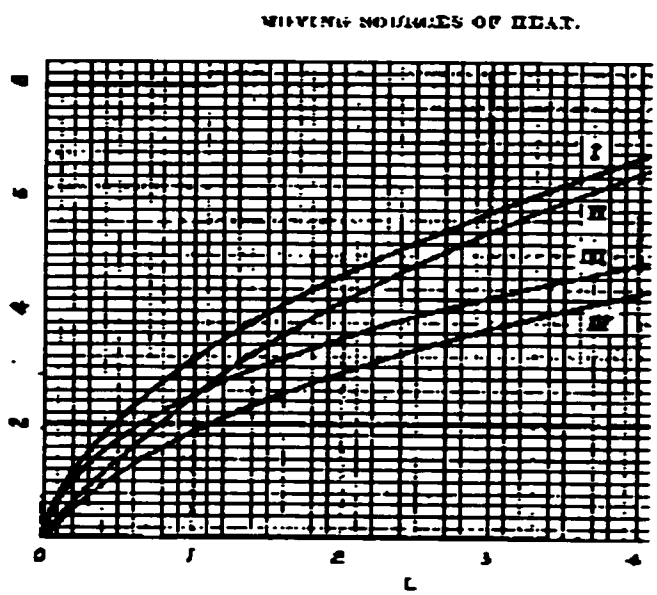

Figure 2.1 Temperature Calculation for Intermediate L [Jager, 1942]

For large B the result (2.19) tends to that for the band source (2.6), and for moderate values, the difference is small.

For small values of L, X and B, the exponential in (2.19) may be replaced by unity and obtain approximately:

$$\frac{\pi kV}{2\alpha q}\upsilon = (X+L)\log_e \frac{B+\left[(X+L)^2+B^2\right]^{1/2}}{X+L} + B\log_e \frac{X+L+\left[(X+L)^2+B^2\right]^{1/2}}{B}$$

$$+(L-X)\log_e \frac{B+\left[(L-X)^2+B^2\right]^{1/2}}{L-X} + B\log_e \frac{L-X+\left[(L-X)^2+B^2\right]^{1/2}}{B} \tag{2.20}$$

The maximum and average steady temperatures over the area of source are obtained as follows:

(i) If L is large, the maximum and average temperatures are nearly the same as those for a band source, namely, (2.14) and (2.15).

(ii) if L is small, them maximum temperature is, from (2.20):

$$\frac{8q\alpha L}{\pi kt}\log_e(1+\sqrt{2}) = 1.122\frac{ql}{k} \tag{2.21}$$

and the average temperature over the area of the source is:

$$\frac{8\alpha qL}{\pi kV}\left\{\log_e(1+\sqrt{2}) - \frac{\sqrt{2}-1}{3}\right\} = 0.946\frac{ql}{k} \tag{2.22}$$

For intermediate value of L, $0.1<L<5$, refer to figure 2.1, curve III an IV are the maximum and average temperature of a band source times $(\pi kV/2\alpha q)$ against L.

2.1.3 Stationary Sources

When the plane is a non-conductor, the whole of the heat would be taken up by the sliding body constantly, and the problem becomes a stationary source of heating. The temperature at time t, at the point (x,y,z), in the semi-infinite solid $z<0$ with no flow of heat over the surface $z=0$, due to heat supplied at the rate q per unit time per unit area over the square $-l<x'<l$, $-l<y'<l$, $z'=0$, commencing at zero time, when the solid is at zero temperature, is

$$\frac{q\alpha}{4k(\pi\alpha)^{1/2}}\int_0^t \frac{dt'}{(t-t')^{3/2}}\int_{-l}^{l} dx'\int_{-l}^{l} dy'\exp\left[-\frac{(x-x')^2+(y-y')^2+z^2}{4\alpha(t-t')}\right] \tag{2.23}$$

To find the steady temperature, put $t=\infty$ and obtain

$$\frac{q}{2k\pi}\int_{-l}^{l} dx'\int_{-l}^{l} dy'\{(x-x')^2+(y-y')^2+z^2\}^{-1/2} \tag{2.24}$$

The maximum temperature occurs at $x=y=z=0$ and is

$$\frac{4lq}{k\pi}\log_e(1+\sqrt{2})=1.122\frac{lq}{k} \tag{2.25}$$

The average temperature over the area of the source is

$$\frac{4lq}{k\pi}\left\{\log_e(1+\sqrt{2})-\frac{\sqrt{2}-1}{3}\right\}=0.946\frac{lq}{k} \tag{2.26}$$

2.2 Sliding Model in Needle Heating

The above theory is developed from the semi-infinite moving plane heat sources. Based on the conclusions from the theory, its applications to the cylinderic heat sources of needle heating are studied in this thesis after adjustments being made.

2.2.1 Development of the Model

The depth of the heat penetration is about 0.015mm after one sliding. This dimension is very tiny compared to the needle diameters. Therefore it can be assumed that the needle diameter is infinite compared to the heat penetrating depth. Hence the theory of semi-infinite plane can be applied.

1. Analysis and Assumptions

Taking one stroke of the needle punch as the study cycle, referring to figure 2.2, the fabric experiences the constant heat source. Therefore the fabric (substance 2), called slider here, with thermal properties k_2, α_2, slides with velocity V over the surface of the needle (substance 1), k_1, α_1, which is at rest.

Assume heat is generated at a uniform rate per unit time per unit area over the common surface, and there is no loss of heat from the portions of the surfaces which are not in contact. If either substance 1 or 2 is an insulator, the theory of stationary heat sources or moving heat sources can be applied. Since the fabric is not a perfect insulator, this practical case is much more difficult in which both bodies have finite conductivity and the sliding is repeated with the slider has environment temperature at the beginning of each cycle:

1. During the first cycle, the slider (fabric) is heated by the source and cooled by the coming cooler portions of substance 1, while the needle is heated both by the source and by conduction of slider.
2. After several stitches, the needle temperature increases, the slider is going to be heated both by the source and by the conduction of the needle, while the needle is heated by the source and cooled by the slider with relatively low temperature.

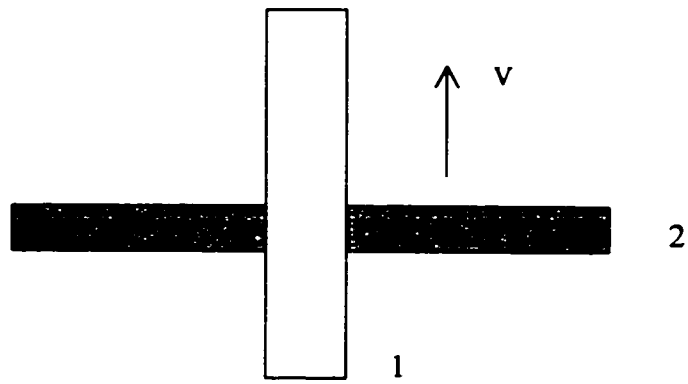

Figure 2.2 Sliding Model of Needle Heating

The exact discussion of this problem seems out of the question. Some efforts are made in giving exact treatment of particular models, but these are very cumbersome and add nothing to the general conclusions [Jaeger, 1942]. The approximate method is used.

Since sliding speed is very fast, contact conduction between two contacted substances won't have enough time to happen. Then, it would be safe to ignore the effect of heat conduction between needle and fabric. Therefore only friction heat are absorbed

in by the substances' contact surfaces. During each stroke, the contact surfaces of needle and fabric have an tendency to achieve the same average temperature at the end of the stroke. Assume a fraction γ of the heat q per unit time per unit area generated over the area of contact passes to the needle and the remaining fraction $(1-\gamma)$ to the fabric. The friction heat partition ratio γ will be calculated by the requirement that the average temperature over the area of contact calculated for a moving source γq in substance 1 equals the average temperature calculated for the substance 2 with a stationary source $(1-\gamma)q$. Since the two temperature distributions over the area of contact calculated in this way will be different, thus the reasonable criterion for calculating γ maybe used; Average temperature is chosen here because it is the best single representative of the temperature distributions.

2. Temperature Development Between Needle and Fabric

Suppose the fabric thickness is δ, then fabric is regarded as a band heat source with length of δ. Before selecting the right equations applied in this case, the dimensionless quantity L must be determined. With needle velocity at 500 rpm, fabric thickness at about 2mm, L is about 120. Hence the equation (2.15) is applied to obtain the average temperature over the contact area of needle, suppose the needle is at initial temperature of T_{01},

$$T_1 = T_{01} + 1.064\frac{\gamma q}{k_1}\left(\frac{\alpha_1 l}{V}\right)^{1/2} \tag{2.27}$$

While the average temperature over the contact area of fabric is obtained by (2.26), with fabric at initial temperature of T_{02},

$$T_2 = T_{02} + 0.946\frac{(1-\gamma)ql}{k_2} \tag{2.28}$$

Since T_1=T_2, friction heat partition ratio is obtained from (2.27) and (2.28):

$$\gamma = \frac{\frac{0.946ql}{k_2} - (T_{01} - T_{02})}{1.064\frac{q}{k_1}\left(\frac{\alpha_1 l}{V}\right)^{1/2} + \frac{0.946ql}{k_2}} \tag{2.29}$$

From the above, it is observed that γ is a function of material properties of both needle and fabric, sliding velocity, length of the band source, and the initial temperature difference between needle and fabric. The higher the velocity, the bigger the γ. The bigger initial temperature difference the smaller the γ.

3. Needle Temperature vs. Time During the Sewing Process

In this thesis, the simplified model is created to get a temperature vs. time curve in sewing process by taking one section of the needle as study object. Assume the needle is infinite long, and the conduction along the needle is neglected.

The heating process of this section when the fabric passes it has been studied in detail. The average temperature over the contact area is obtained by (2.27), and the friction heat partition ratio can be obtained from (2.29). Actually, γ will not be a constant during one stroke, since the initial temperature difference will change with slider moving further on the needle. γ calculated here is a kind of average value during one cycle, which indicates the heat partition tendency at each cycle. Therefore some adjustments will be made when applying in real case of needle heating.

After the heat source passes by, the cooling process begins at the examined section till the heat source comes back. During each cycle, this examined section is going to experience with two times heating while the needle punching and withdraw, and also two times cooling.

As stated above, the heat penetrating into the needle is shallow, the temperature falls to 1/10 of it's surface at the depth of 0.015mm when L=2, which is much smaller than our case. Suppose the needle has a diameter of 2 mm, therefore, no more that 2% depth of needle are activated by heating, and about 0.04% volume of that needle section are activated by heating. Therefore when the cooling process begin, only this part of volume in the needle is going to cool down. There is a coefficient β to adjust this particular volume in the program. Obviously β is dependent on the material's thermal properties. Here the equation of lumped variable method for unsteady cooling process is used:

$$T = T_{\infty} + (T_i - T_{\infty}) \exp(-\frac{h_c F}{\rho c V_{ol}}) \tag{2.30}$$

Where, T_{∞} is the temperature of environment

T_i is the initial temperature at the cooling begins,

h_c is the convection coefficient

F is the cooling area;

V_{ol} is the volume to cool down;

2.2.2 Simulation Results

Simulations are run at different sewing speed with different fabric thickness. Figure 2.3 is the temperature vs. time curves obtained at sewing speed 2000 rpm, 1000 rpm, 500 rpm with fabric thickness of 4 mm. The time constant[1] are also shown in the figure. These curves are verified by the experimental data [Liasi, 1996], which shows fairly good match.

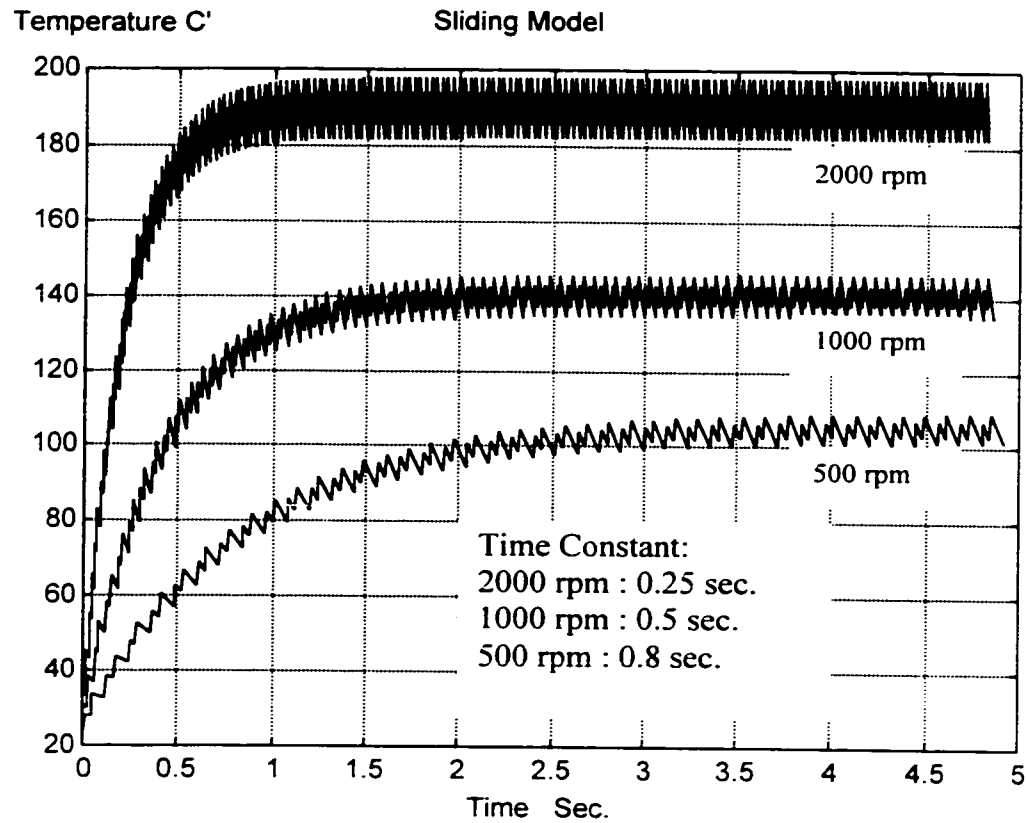

Figure 2.3 Sliding model temperature vs. time

Figure 2.4 is the needle average peak temperature obtained at speed range from 1000 rpm to 4000 rpm with fabric thickness from 2mm to 14 mm (1 ply to 7 plys). In

[1] Time constant is defined as the time period needed to achieve the 63.2% of the steady state value.

typical sewing industrial, when fabric thickness is about 2mm ~ 6mm, and sewing speed is within 3000rpm, needle peak temperatures from simulation give good results referring to the report [Hersh, S. P., 1969]. When sewing conditions exceed these ranges, peak temperatures from simulation are higher than that from reference.

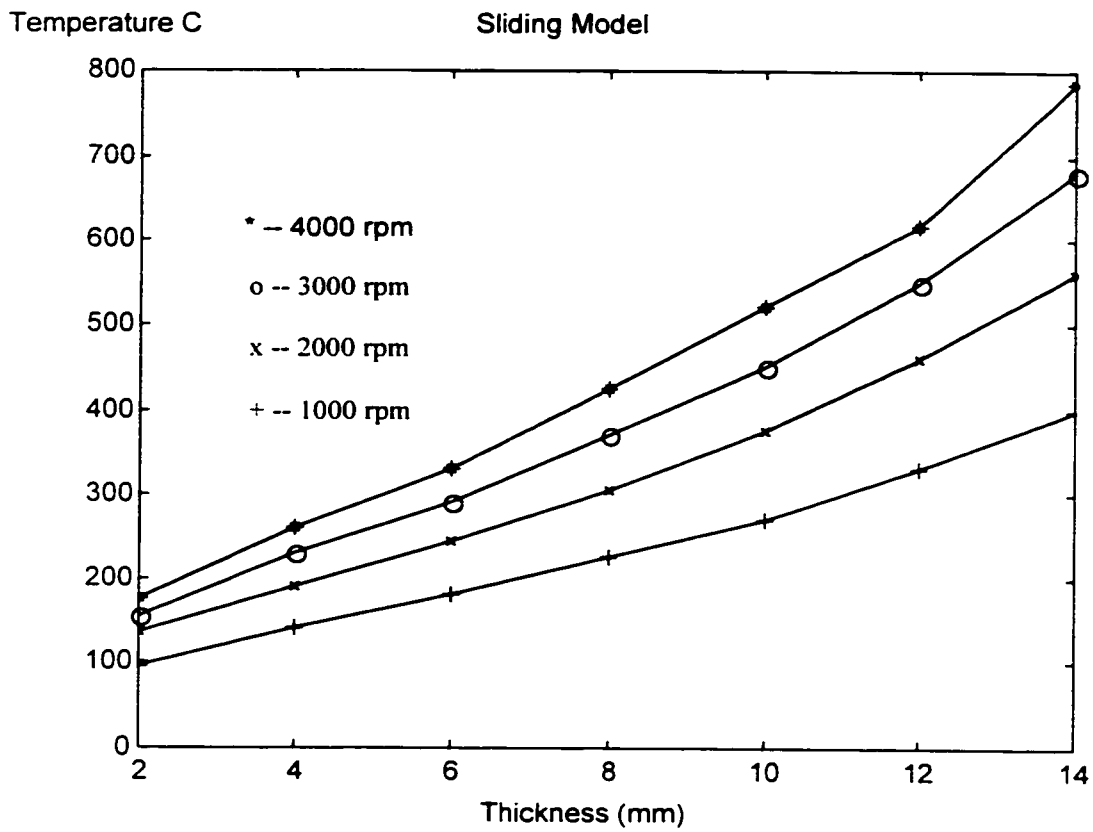

Figure 2.4 Peak temperature from sliding model

The reason for the difference is that the sliding model does not consider the heat conduction effect along and across the needle, which plays an important role in needle heat loss when the temperature goes higher. Also at higher temperature, the radiation plays important roles in heat loss too. Therefore the results from this sliding model tends

to make the peak temperature even higher as thickness and speed goes higher, which will result high temperature themselves.

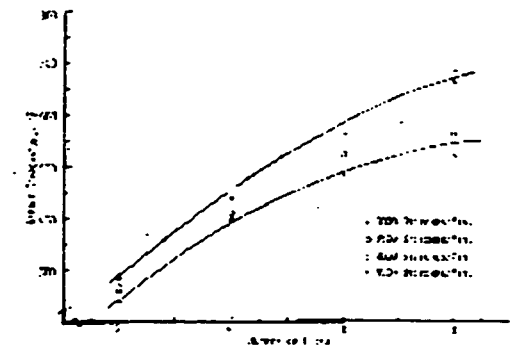

Figure 2.5 Peak Temperature From Experimental Report [Hersh, 1969]

Finally, when the thickness increases, the temperature distribution over the contact heat source will make bigger difference between the temperature in the area, since some points will experience longer heating time than others. This error will make the model violate the basic assumptions.

Comparing Figures 2.4 and Figure 2.5, it is seen that the two curves do not match well when the fabric thickness is big. This motivates the study of the lumped method in next chapter, which includes the heat conduction across the needle section of the contact heat area.

CHAPTER III

LUMPED MODEL OF NEEDLE HEATING

3.1 Basic Principles

Unsteady heat transfer problems are often simplified with three aspects before solving: boundary condition, geometry of the object, inner thermal resistance of the object.

When the surface of a substance suddenly experiences heating or cooling, the temperature distribution inside the solid depends on two ways: one is the thermal resistance between the environment and the object; the other is the inner thermal resistance of the substance. When the inner thermal resistance is small, the inside temperature gradient is very small, therefore it can be thought the whole substance reached the same temperature at the same time. It seems the continuous distributed mass converges to the one point, with the same temperature at one time. The method ignoring the substance's inner thermal resistance is called lumped variables.

If the object has relatively big conductivity with small geometry dimensions, or its surface heat transfer coefficient is relatively low, the lumped variable method can apply.

In this chapter every section in the needle experienced moving heat source is modeled as lumped model. And the temperature rise in fabric is calculated using the principles of the temperature development in a contact heated surface [Holm, 1948].

3.1.1 Unsteady Heating and Cooling in Lumped Variables Method

1. Temperature Increase at Heating Stage

Suppose the existing arbitrary shape solid, with volume V_{ol}, surface area F, has uniform initial temperature T_0. Then it will experience constant heat Q (W) from zero time. Assume the solid is wrapped around the heat source and there is not heat loss through convection or radiation. The substance temperature T after a time period t can be obtained from the following analysis.

Since all the energy absorbed are used in increasing the substance's inner energy, therefore the following equation is obtained:

$$Q = \rho c V_{ol} \frac{dT}{dt} \tag{3.1}$$

$$t = 0, \qquad T = T_0$$

With the solution as:

$$T = T_0 + \frac{Q}{\rho c V_{ol}} t \tag{3.2}$$

The temperature increase is a function of material property, heating time, heating intensity, and substance's initial temperature.

2. Temperature Decrease at Cooling Stage

Suppose the existing arbitrary shape solid, with volume V_{ol}, surface area F, has uniform initial temperature T_0. Then it is exposed in the environment with temperature at T_∞ to cool down ($T_0 > T_\infty$). The convection coefficient is h_c. The substance's temperature after some time can be obtained in the following way.

Since all the heat loss through convection is reduced to the substance's inner energy decrease, hence the equation exists:

$$\rho c V_{ol} \frac{dT}{dt} = -h_c F (T - T_\infty)$$
$$t = t_0, \quad T = T_0 \tag{3.3}$$

The solution for this equation is :

$$T = T_\infty + (T_0 - T_\infty)\exp(-\frac{h_c F}{\rho c V_{ol}} t) \tag{3.4}$$

The above equation's exponential coefficient can be transformed as:

$$\frac{h_c F}{\rho c V_{ol}} t = \frac{h_c V_{ol}}{kF} \cdot \frac{kF^2}{\rho c V_{ol}^2} t = \frac{h_c (V_{ol}/F)}{k} \cdot \frac{\alpha t}{(V_{0l}/F)^2} = Bi_v Fo_v \tag{3.5}$$

Where Fo_v is Fourier number, dimensionless time; Bi_v is the Biot number, indicateing the ratio of inner thermal resistance to the external thermal resistance. From previous study, when

$$Bi_v = \frac{h_c (V_{ol}/F)}{k} < 0.1M \tag{3.6}$$

The temperature difference inside the substance is less than 5%. Where M is non-dimensionless value depending on the object geometry. For infinite plate M=1; infinite

cylinder M=1/2; sphere M=1/3; Therefore equation (3.6) can be used to judge whether the lumped variable method can be applied.

For an infinite cylinder, suppose the radius is r, there is:

$$Bi_v = \frac{h_c (V_{ol} / F)}{k} = \frac{r}{2}\frac{h_c}{k} \tag{3.6a}$$

In this needle heating problem, the radius is only about 0.001m, therefore the lump variables method can apply.

3.1.2 Temperature Development in a Contact Heated Contact Surface [Holm, 1947]

It is assumed that a semi-infinite body limited by a hemisphere surface with the radius *b* in which, from the time *t=0* on, heat is produced at the constant rate *Q* and uniformly distributed over the area. No heat may be lost to the surroundings. Figure 3.1.

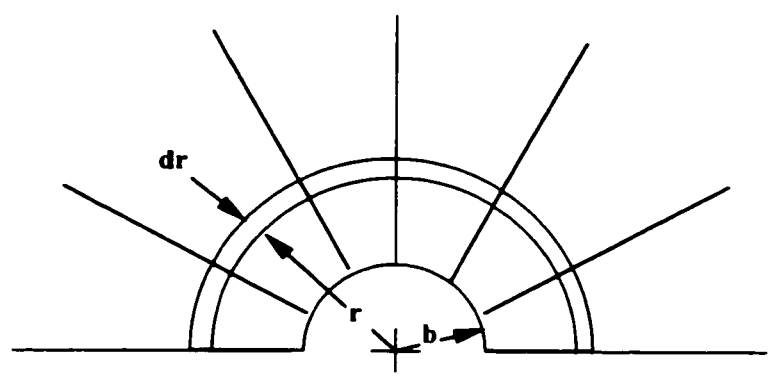

Figure 3.1 Streamlines Directed Radially from the b-hemisphere

This hemisphere may be regarded as an isotherm. Then all isotherms are concentric hemispheres. The equation defining the development of the temperature is readily found to be:

$$\frac{\partial^2 \upsilon}{\partial r^2} + \frac{2}{r}\frac{\partial \upsilon}{\partial r} = \frac{c}{k\rho}\frac{\partial \upsilon}{\partial t} \tag{3.7}$$

With initial conditions as: t=0, υ=0;

And boundary conditions as:

$$Q = -2\pi b^2 k\left(\frac{\partial \upsilon}{\partial r}\right) \qquad r = b, \qquad t > 0 \tag{3.8}$$

The substitutions of

$$y = \upsilon r - \frac{Q}{2\pi k}, \qquad and \qquad r = b(1+x) \tag{3.9}$$

transform Equation (3.8) to

$$\frac{k}{\rho c b^2}\frac{\partial^2 y}{\partial x^2} = \frac{\partial y}{\partial t} \tag{3.10}$$

with the conditions that:

at $t = 0$, $y = -Q/2\pi k$ for every x, and at $t > 0$, $(\partial y/\partial x)_{x=0} = y(0,t)$.

The solution is:

$$-y(x,t) = \frac{Q}{2\pi k}\left\{\Phi\left(\frac{x}{2(z)^{1/2}}\right) + e^{x+z}\left[1 - \Phi\left(\frac{x}{2(z)^{1/2}} + (z)^{1/2}\right)\right]\right\} = Y(x,z) \tag{3.11}$$

where

$$\Phi(x) = \frac{2}{(\pi)^{1/2}}\int_0^x e^{-\beta^2}\, d\beta \tag{3.12}$$

and

$$z = \frac{k}{\rho c b^2} t \tag{3.13}$$

Hence

$$\upsilon(r,z) = \frac{Q}{2\pi k r} - \frac{1}{r} Y(x,z) \tag{3.14}$$

Putting $x = 0$, i.e., $r = b$, it is found:

$$\upsilon(b,z) = \frac{Q}{2\pi k b}\left\{1 - e^{z}\left[1 - \Phi\left((z)^{1/2}\right)\right]\right\} = \theta(z) \tag{3.15}$$

It would be easily found the permanent super-temperature is

$$\theta(\infty) = Q/2\pi kb \tag{3.16}$$

3.2 Lumped Model in Needle Heating

3.2.1 Development of the Model

In this model, the continuous sliding motion between needle and fabric is simplified by the discrete motion of the fabric sliding through the needle layer by layer. Taking one needle section which has the same length of the fabric thickness for study, Figure 3.2, then the time during which friction heating happened between needle and fabric is to be calculated in such a way: $t = \delta / V$, where V is the average velocity. Therefore the one stitch cycle is comprised by several of this time period.

The temperature rise in the needle section and fabric surface is going to be calculated from the above principles. The friction heat partition ratio between the needle and fabric is going to be calculated in such a way that the temperature in the needle and the temperature in the fabric contact surface is going to achieve the same value after that

time period. The author met an interesting question: after several stitches sewing, the needle temperature goes very high, how about if all the friction heat goes to fabric and its surface temperature still can't achieve the same needle initial temperature of that first time period? Does the contact conduction from the needle to the surface happen? Here the author assume: NOT. The time that the contact conduction needs is not enough in our case, which the time period is only about 0.005s. Therefore, the fabric surface temperature will wait to rise to the same value as the needle during the following time periods.

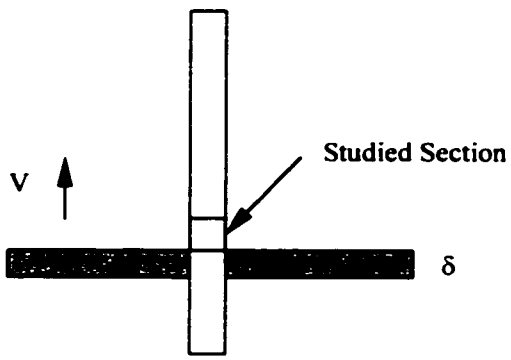

Figure 3.2 Lumped Model

1. Temperature Rise in the Needle

Ignoring the conduction along the needle from the studied section during the heating period, the temperature rise in the needle after the time period can be obtained from lumped variables method.

Assume the friction heat Q is generated uniformly per unit time and uniformly distributed over the contact area of that time period. The friction heat absorbed by the needle is γQ, then the fabric will absorb $(1-\gamma)Q$ friction heat. According to equation (3.2), the temperature rise in the needle will be:

$$T = T_{01} + \frac{\gamma Q}{\rho_1 c_1 V_{ol}} t \tag{3.17}$$

2. Temperature Rise in the Fabric Contact Surface

Assume there is no heat loss from the fabric surfaces that are not in contact with the needle. Its contact surface temperature can be obtained approximately from the equation (3.15) after making following adjustments. Suppose r is the needle radius, δ is the fabric thickness. The adjustment is based on two sides: the surface area of the cylinder contact is converted to the equal area of hemisphere; there is an coefficient ζ to adjust the shape transformation from hemisphere to cylinder which can be determined by experiment data later.

$$2\pi b^2 = \zeta(2\pi r \cdot \delta) \tag{3.18}$$

And therefore,

$$b = \zeta\sqrt{r \cdot \delta} \tag{3.18a}$$

From equation (3.15), suppose the fabric has initial temperature T_{02}, the surface temperature of the fabric after this temperature period will be:

$$T = T_{02} + \frac{(1-\gamma)Q}{2\pi k_2 b}\tau(t) \tag{3.19}$$

where,

$$\tau(t) = \{1 - e^{z}\left[1 - \Phi\left((z)^{1/2}\right)\right] \tag{3.20}$$

and $\Phi(x)$, z, b are defined by equation (3.12), (3.13), (3.18a).

From the above equation, it is found that the fabric contact surface temperature rise is a function of fabric material properties, heating time and heating intensity.

3. Friction Heat Partition Ratio

Friction heat going to each of the contact surfaces tends to make the temperature at the contact surface equal. Assume after the first time period, needle and fabric contact surface reaches the same temperature. Then, the friction heat partition ratio is calculated from (3.17) and (3.19):

$$\gamma = \frac{\dfrac{\tau(t)}{2k_2\pi b} - \dfrac{T_{01} - T_{02}}{Q}}{\dfrac{t}{\rho_1 c_1 V_{ol}} + \dfrac{\tau(t)}{2k_2\pi b}} \tag{3.20}$$

Suppose the needle is punching and withdrawing with uniform speed V, there are:

$$Q = f \cdot V, \quad t = \delta / V; \tag{3.21}$$

Therefore, equation (3.20) becomes :

$$\gamma = \frac{\dfrac{\tau(\delta/V)}{2k_2\pi b} - \dfrac{T_{01} - T_{02}}{f \cdot V}}{\dfrac{\delta/V}{\rho_1 c_1 V_{ol}} + \dfrac{\tau(\delta/V)}{2k_2\pi b}} \tag{3.22}$$

The friction heat partition ratio is a function of material properties of both needle and fabric, sewing speed, fabric thickness, needle diameter, initial temperature difference between needle and fabric (ΔT_0). In Appendix B, curves are obtained based on equation (3.22), showing that how γ is going to change with these parameters. Obviously, as sewing continues, ΔT_0 increases, therefore γ is going to decreases. It is found that γ is going to increase with the increase of sewing speed and fabric thickness.

Since assumptions have been made before deducing the equations, modification of γ may be made while applying in the real case.

4. Needle Temperature vs. Time During the Sewing Process

Similar to Chapter II, the Matlab (Appendix C) program is developed to obtain the temperature development in the studied needle section as sewing continues. The cooling process of the needle section is going to be defined by equation (2.30).

3.2.2 Simulation Results

Simulations are run at different sewing speed with different fabric thickness. Figure 3.3 is the temperature vs. time curves obtained at sewing speed 2000 rpm, 1000 rpm, 500 rpm with fabric thickness of 4 mm. These curves are verified by the experimental data [Liasi, 1996], which shows fairly good match.

Figure 3.4 is the needle average peak temperature obtained at speed range from 1000 rpm to 4000 rpm with fabric thickness from 2mm to 14 mm (1 ply to 7 plys). The results show fabric thickness makes peak temperature go higher as the speed increases.

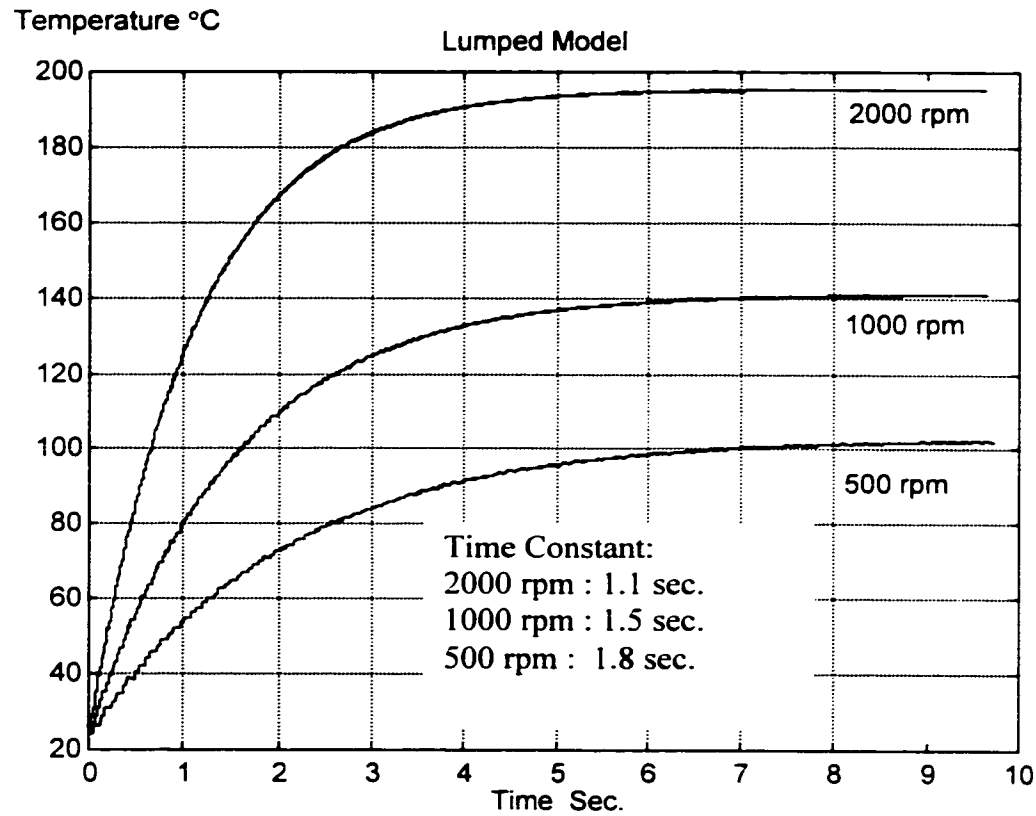

Figure 3.3 Needle temperature vs. time in lumped model

Within typical industrial sewing conditions, when fabric thickness is about 2mm ~ 6mm, and sewing speed is within 3000rpm, the needle peak temperatures from simulation give good results referring to the report [Hersh, S. P., 1969]. When sewing conditions exceed these ranges, peak temperatures from simulation are higher than that from reference.

The difference can be ascribed to the less information of Hersh's experiment, such as what kind of fabric he used, what is the exact thickness of his fabric ply. Also ignoring the conduction along the needle and radiation from the high needle temperature surface are the reasons too.

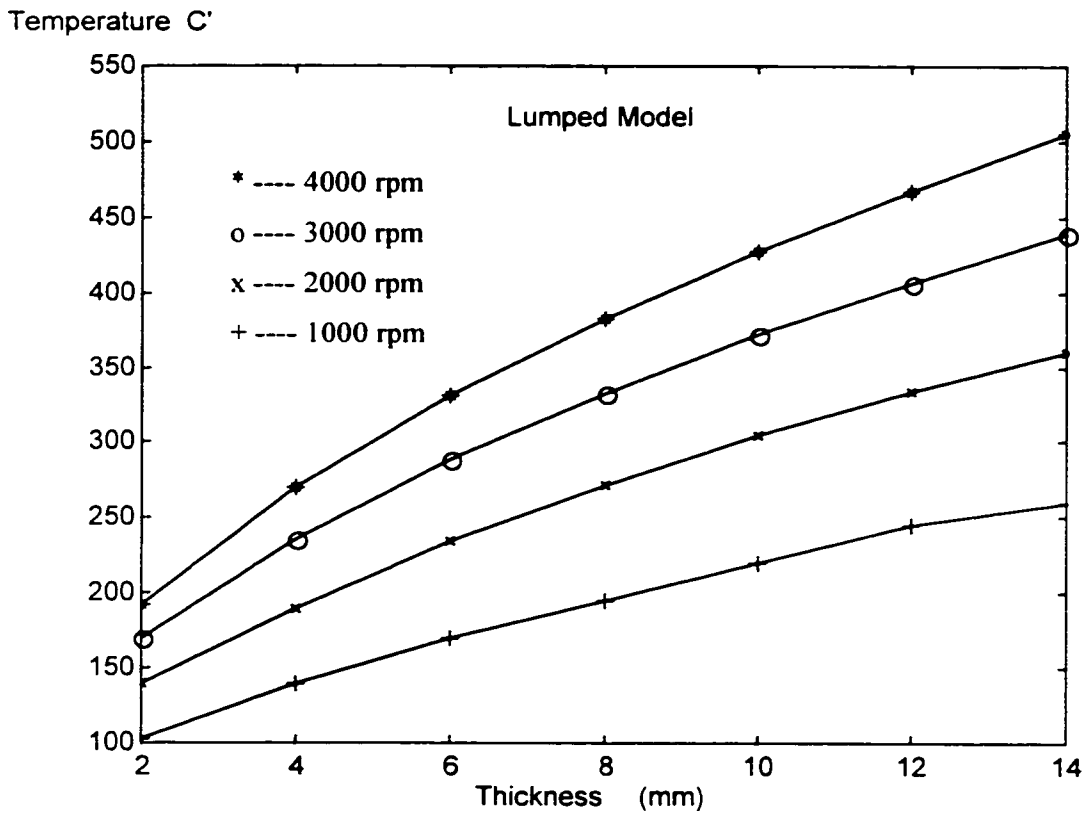

Figure 3.4 Needle peak temperature from lumped model

CHAPTER IV

THE FEA MODEL

Finite element analysis is to re-create mathematically the behavior of an actual engineering system. The analysis must be an accurate mathematical model of a physical prototype. The model comprises all the nodes, elements, fabric properties, real constants, boundary conditions, and other features that are used to represent the physical system. In this study, **ANSYS**, a commercial FEA software system, is used to get the numerical solution of this transient needle heating problem. The needle geometry is meshed into hundreds of elements composed of nodes. The time-dependent boundary conditions are applied by multiple load steps. The temperature values at these discrete nodes at each time step can be calculated, as a result the needle temperature distribution can be simulated. Hence the highest temperatures reached by the needle and their corresponding location can be obtained.

Using **ANSYS** APDL (Parametric Design Language) programming language, a program is created in order to establish the FEA model. The FEA model includes: establishing the needle geometry meshing, and applying the time-dependent boundary conditions. The model correlates the relationship between key parameters, such as: geometry parameters, material properties, operation conditions, etc., and presentation of the heating results. As a result, the temperature value at each node under certain operating conditions with different kinds of needle shape can be predicted. Following is a detailed description of the FEA model.

4.1 Definition of Geometric Configuration of the Model

Since the temperature distribution in the needle is the main concern, "**Solid70 3-D Thermal Solid**" is chosen to establish the meshing. Each element has eight nodes with a single degree of freedom, temperature, at each node. See Figure 4.1 for the element structure. This element is applicable to a three-dimensional, steady-state or transient thermal analysis.

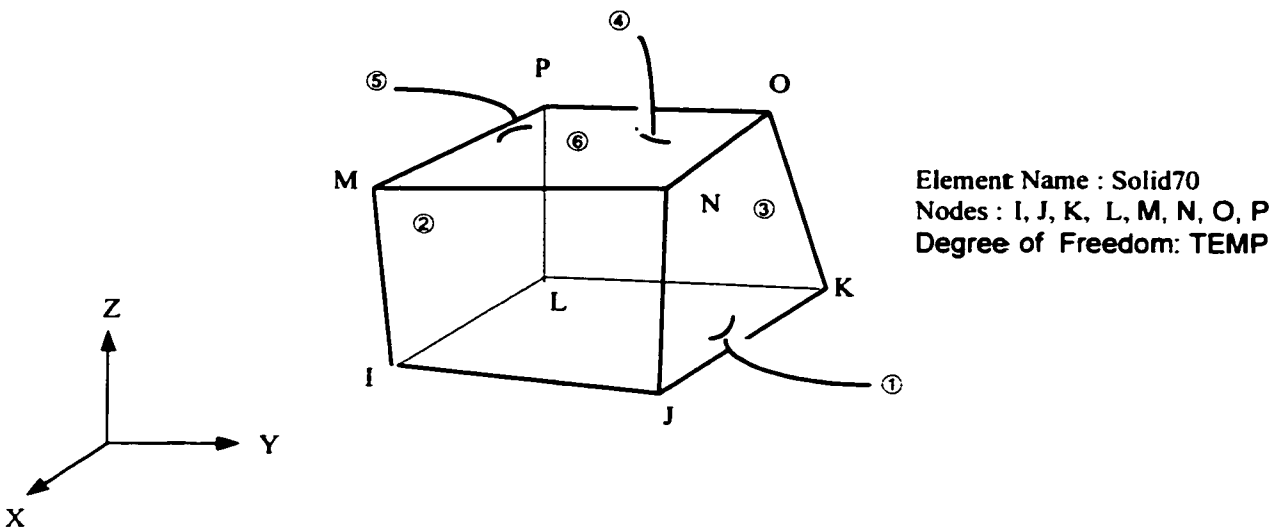

Figure 4.1 Solid 70 3-D thermal solid element

In **ANSYS**, there are two different methods to define the geometric configuration of the model's nodes and elements: solid modeling and direct generation. With "solid modeling", we can describe the geometric boundaries of the model, establish controls over the size and desired shape of our elements, and then instruct the **ANSYS** program to

generate all the nodes and element automatically. By contrast, with the "direct generation" method, the location of every node and the size, shape, and connectivity of the element are determined prior to defining these entities in our **ANSYS** model.

"Solid modeling" is convenient when dealing with large and complex models, because it allows relatively small number of data items. Also it also has some other advantages:

- It allows geometric operations that can't be done with nodes and elements.
- It supports the use of "primitive" areas and volumes and Boolean operations for "top down" construction of the model.
- It facilitates the use of **ANSYS** program's design optimization features, readily allowing the modifications to geometry, facilitating changes to element distribution, etc.

But it also has some disadvantages:

- requiring large amounts of CPU time
- cumbersome for small simple model's generation
- failing to generate the finite element mesh under certain circumstances.

While the direct manual generation is convenient for small and simple models, provides us with complete control over the geometry and numbering of every node and every element. In the needle heating problem, the surface loads are applied on the element face of the needle outer surface that experience heat flux or convection. For the easy of programming, the element face number that endure surface load must be controlled, therefore the "direct generation" is used here.

Figure 4.2 is a typical industrial sewing needle used in the experiments [Liasi,1996,1997]. It is defined by 15 parameters. The parameters, which determine the needle lead shape, needle eye position and size, long groove position and size, are related to needle heating.

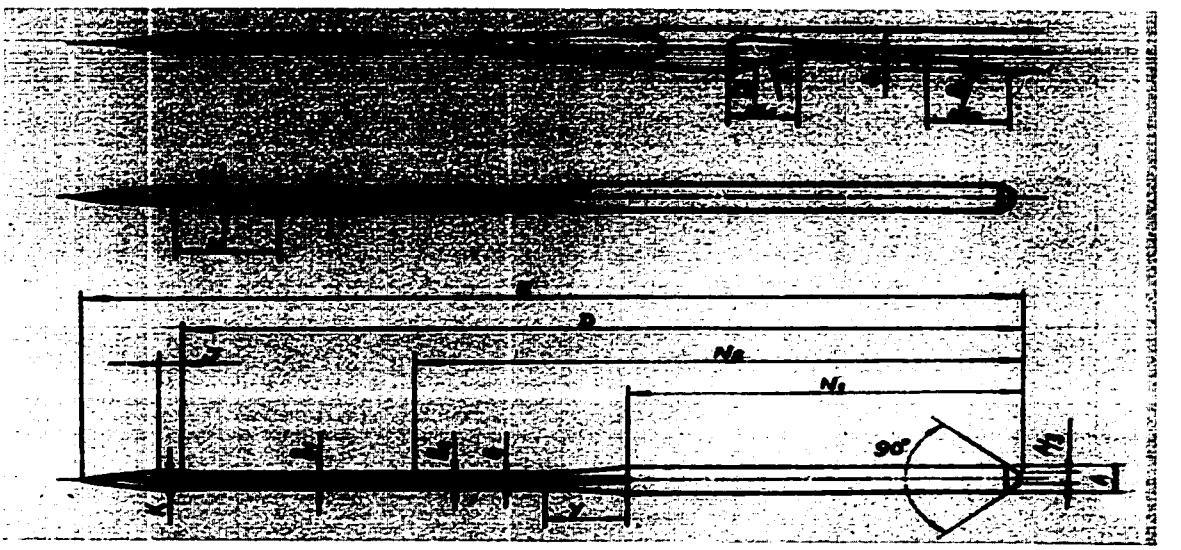

Figure 4.2 Industrial sewing machine needle geometry

Figure 4.3 is the needle meshing results from the "direct generation" method using **SOLID70** elements. Since the needle is symmetric, only half of the model is used in the analysis.

As shown in the figures, needle geometry is defined by the following main parameters :

nlg : needle length *m;*

rad(i) : needle radius on the "*i*th" section m, i = 1,2,3, ... ndiv ;

lgb : beginning position of the long groove *m;*

lge : end position of the long groove *m;*

hb : beginning position of the needle eye *m;*

he : end position of the needle eye *m;*

dp : punching-in length that the needle go in to the fabric *m;*

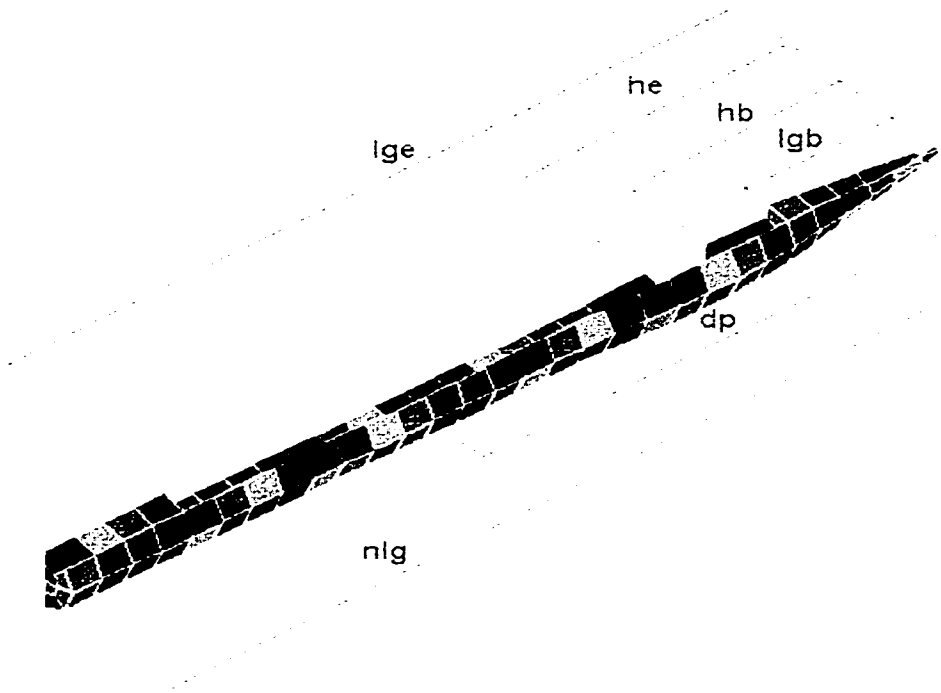

Figure 4.3 Needle meshing result

While generating needle mesh using "direct generation" method, half section of needle is generated first, then using the APDL strong features of "do-loop" and "if-then-else", other sections' nodes are generated, including the sections that has grooves and eye. In this method, one has complete control of the node number. It is then possible to make the element faces, experiencing heat flux and convection boundary conditions on the outer surface of the needle, as surface No.1. Referring to Figure 4.1, the first four nodes I,J,K,L, make up the element face No.1. This makes the program much easier in applying surface load.

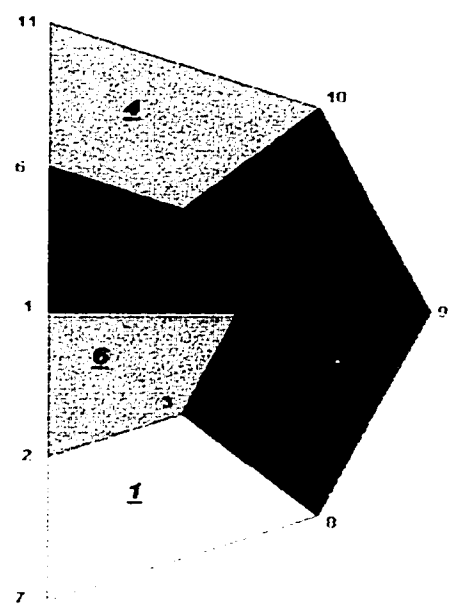

Figure 4.4 First section view of needle meshing

The number of section divisions along the needle length (expressed as *ndiv* in the program) determines the mesh size. If fast calculation is needed, *ndiv* can be smaller to make a rough mesh. If precise calculation is needed, *ndiv* can be bigger to make the mesh finer.

From the parameters described above, the needle lead shape, needle eye position and size, groove position and size, needle diameter, bulge dimension around the needle eye can be modified with different values. Then these parameters' effects on needle heating results can be obtained and analyzed.

4.2 Boundary Conditions

As discussed at the beginning, this thermal system has three types of boundary conditions: heat flux from the friction between fabric and needle outer surface, heat flow between thread and needle-eye, and convection from the needle's outer surface parts which are not in contact with the fabric. Since the boundary condition is time-dependent, multiple load steps are needed. In **ANSYS,** one cycle's time is divided into suitable small time steps, the specific boundary conditions relative to this time period are applied, then the problem is solved numerically step by step. This operation is repeated till the time point of equilibrium heating phase. In this model, because the sewing speed is high (500 rpm ~ 2000 rpm), in one cycle (punching and withdrawing) at least 12 load steps have to be applied. In order to get the temperature profile for 8 seconds, which is the time usually needed to go to steady phase, more than 1000 load steps are required.

Before applying the boundary conditions, some basic assumptions are made to simplify the model :

- The needle punching speed is uniform during the penetration and withdraw.
- The needle and fabric properties do not change during the sewing process.
- The top and bottom fabrics to be sewed have the same thermal properties, which means friction heat is generated uniformly over the contact area.
- Radiation is ignored, since it plays a minor role in needle cooling.
- Dynamic friction coefficient does not change with sewing speed.

The operating conditions used in the program for applying boundary conditions are:

rpm : rotation speed of the punching crank *revolution/minute* ;

th : fabric thickness *m* ;

dw : needle idling distance *m*;

fcoef : convection coefficient of the needle's outer surface $W/(m^2 \cdot ℃)$.

4.2.1 Heat Flux

1. <u>Applying the Time-Dependent Heat Flux Layer by Layer</u>

Figure 4.5 illustrates the process while the needle undergoes in one cycle, and explains how the heat flux boundary condition is changing with time and needle position.

In this program, the fabric "thickness" is used as a reference to piece the time period for each load step. The heat flux boundary condition is applied layer by layer. Since the needle penetrating speed is assumed uniform, therefore the speed and the ending time point of each acting load step can be expressed as :

$$spd = rpm \cdot \frac{(dp + dw) \cdot 2}{60} \tag{4.1}$$

$$Time = \frac{th}{spd} \cdot L_step \tag{4.2}$$

where, spd is needle punching speed m/s;

L_step is the index of multiple load step number.

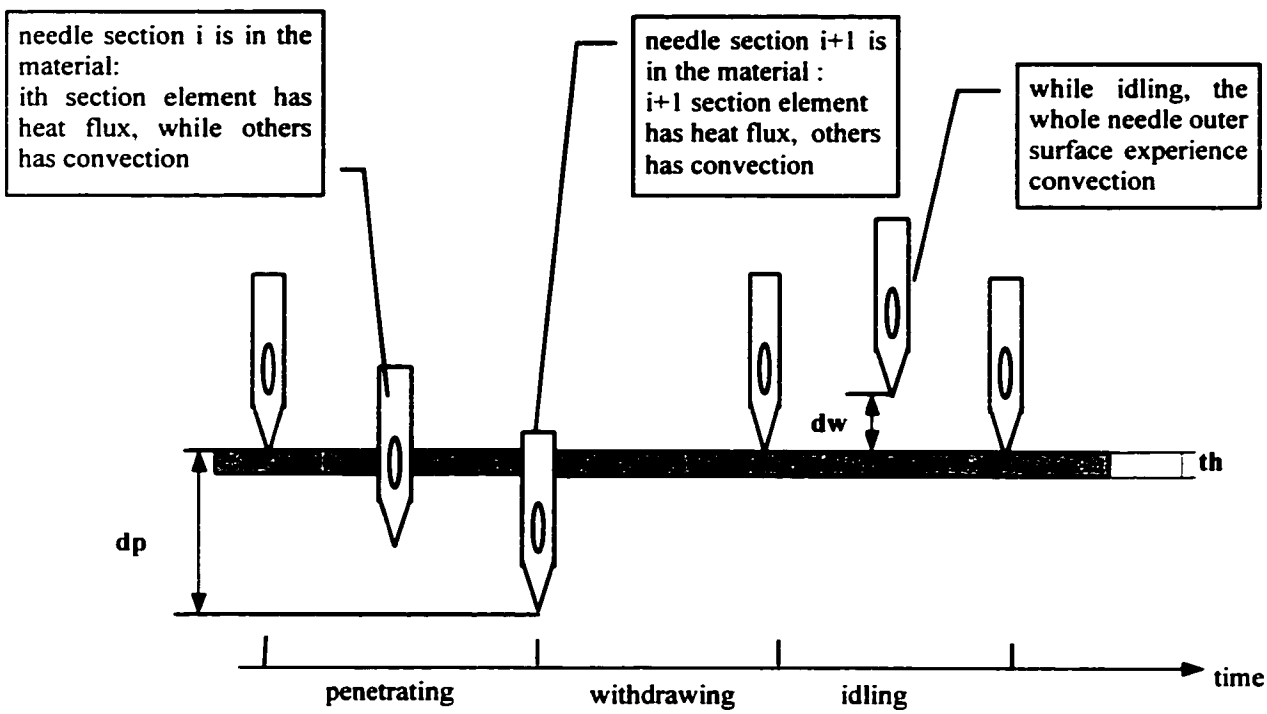

Figure 4.5 One cycle of needle sewing process

The number of needle element sections that experience heat flux at each load step is calculated as :

$$nshf = N\,\mathrm{int}(\frac{th}{n\lg} \cdot ndiv) \tag{4.3}$$

Where, *Nint(x)* is APDL function to calculate the nearest integer to *x*.

The number of load step while penetrating the fabric is:

$$kp = N\,\mathrm{int}(\frac{dp}{th}) \tag{4.4}$$

during these load steps the heat flux is taken in the needle.

The number of load step while the needle is in idle position:

$$kw = N\,\mathrm{int}(\frac{dw}{th}), \tag{4.5}$$

during these load steps there is no heat flux in the needle.

The total load step needed in one stroke is:

$$T_Load = 2 \cdot (kp + kw) \tag{4.6}$$

Figure 4.6 illustrates how the heat flux boundary conditions are applied layer by layer for each load step. In this case, the fabric thickness is 2 mm, and there are 30 divisions along the needle length.

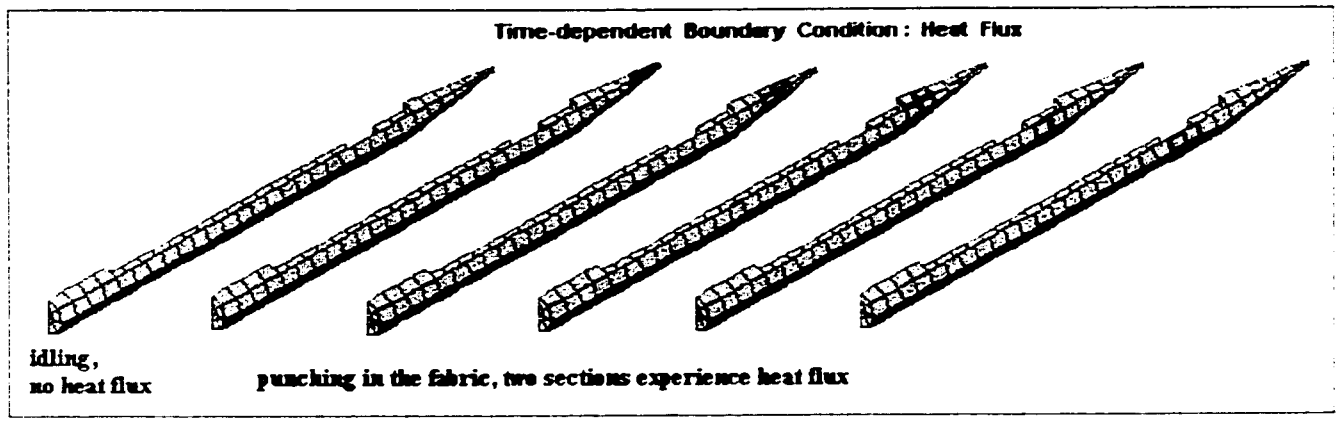

Figure 4.6 Applying heat flux boundary conditions layer by layer

2. Calculation of the Heat Flux

Heat is generated from the friction power, which can be expressed as:

$$P_f = f(t) \cdot v(t) \tag{4.7}$$

Where, P_f is the friction power generated while the needle penetrating the fabric W

$f(t)$ is the friction force between the needle and the fabric N

$v(t)$ is the needle punching speed m/s

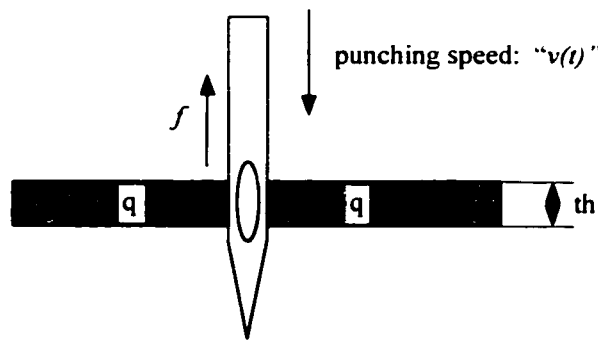

Figure 4.7 Sketch for heat flux calculation

The heat flux can then be obtained from:

$$q_{flux} = \frac{P_f}{A_{section}} = \frac{f(t)}{2\pi r \cdot th} \cdot v(t) \tag{4.8}$$

Where, q_{flux} is the heat flux W/m^2;

$A_{section}$ is the needle contact area that experience heat flux m^2;

r is the needle radius m;

Figure 4.8 illustrates friction force change with time in one cycle for a bulged needle [Mallet, E., 1997]. During the period when the needle lead goes in the fabric, the friction force is increasing linearly from 0 to some constant. As the bulged part goes into the fabric, the friction force is going to achieve the peak value. Then the flat part of shaft in the fabric, the friction force keeps constant.

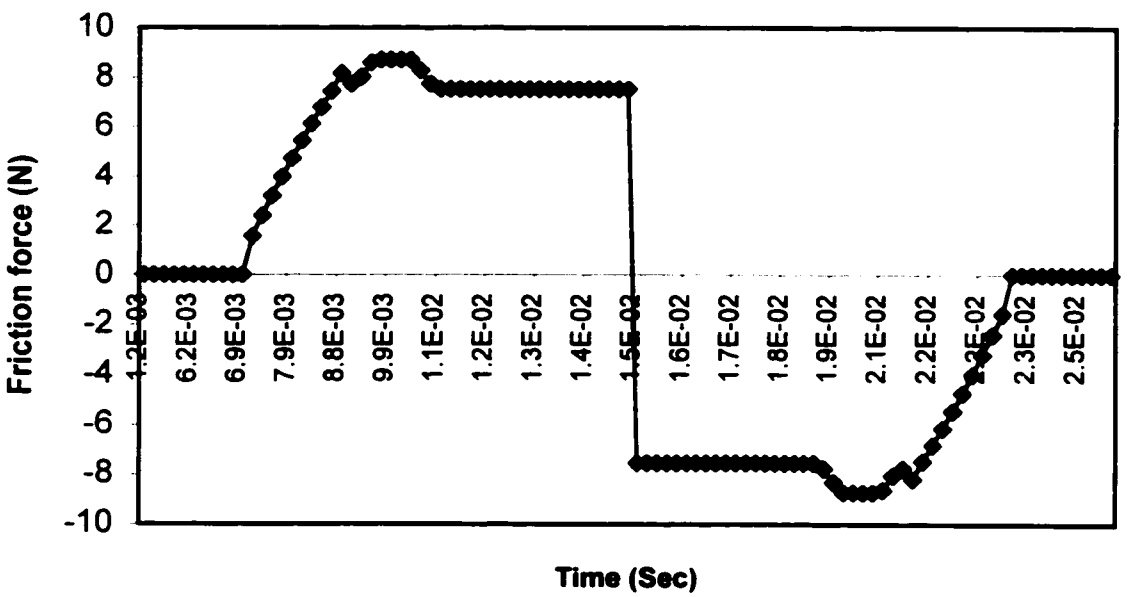

Figure 4.8 Friction force vs. time

When the needle flat part going through the fabric, the friction force is given by :

$$f = 2\pi r \cdot th \cdot p \cdot \mu \tag{4.9}$$

where, p is the unit normal force that fabric acts on the needle cylinder N/m^2

μ is the friction coefficient between fabric and needle surface

The concept "*friction force density*" used in the program is defined as :

$$f_{density} = \frac{f}{2\pi r \cdot th} = p \cdot \mu \tag{4.10}$$

$f_{density}$ is the unit friction force over the contact area between needle and fabric. It is a function of material properties, not dependent on the fabric thickness, or needle velocity [Mallet, 1997].

Figure 4.9 illustrates how the normal pressure along the needle changing with time during one cycle.

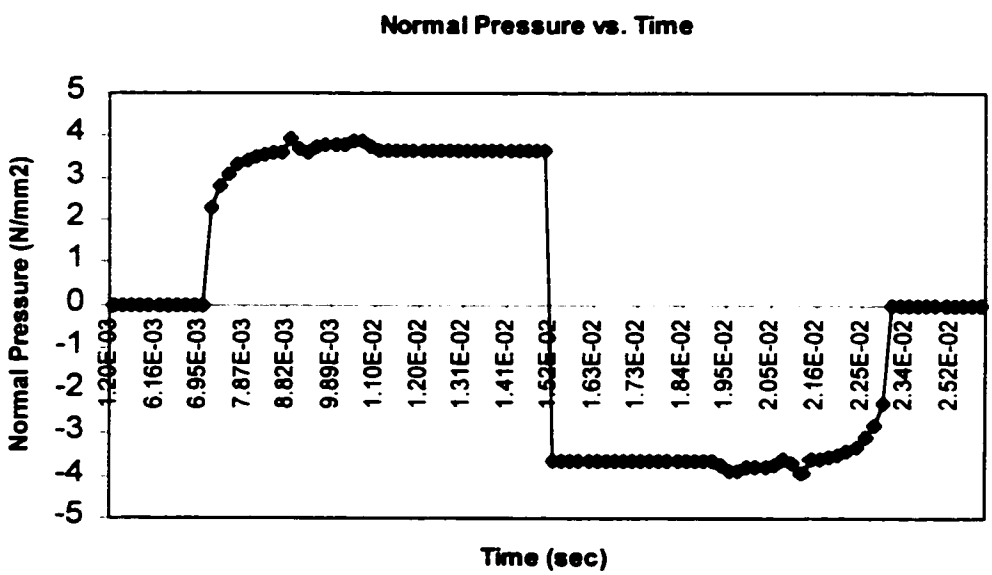

Figure 4.9 Normal pressure vs. time

Combining equation (4.9) and (4.10)one gets the heat flux when the needle shaft go in to the fabric with uniform punching speed :

$$q_{flux_flat} = f_{density} \cdot spd = p \cdot \mu \cdot spd \tag{4.11}$$

3. Friction Heat Partition Ratio Between Fabric and Needle

Assumptions are made as followings:

- The friction heat generated is conducted away into the bulk of the rubbing members, no loss to the surrounding.
- The proportion of the total heat flowing into each body is then determined by the criterion that the equations of heat flow for both bodies shall give the same average temperature over the contact area at the end of each cycle.

As studied in Chapter III, the friction heat partition ratio between needle and fabric can be determined by equation (3.22) with some modifications to adjust the assumptions. This friction partition ratio is of function of material properties of both needle and fabric, sewing speed, fabric thickness, needle diameter, initial temperature difference between needle and fabric (ΔT_0). In the sewing process, sewing speed, fabric thickness, and material properties won't change, therefore γ is only changing with the initial temperature difference at each new stitch. Figure 4.10 illustrates how γ changes with each stitch cycle at different sewing speed with different fabric. At the beginning of sewing needle temperature equals the ambient temperature, γ almost equals 1, all the friction heat going

to the needle. Then as sewing continues, more and more heat goes to the fabric since ΔT_0 increases.

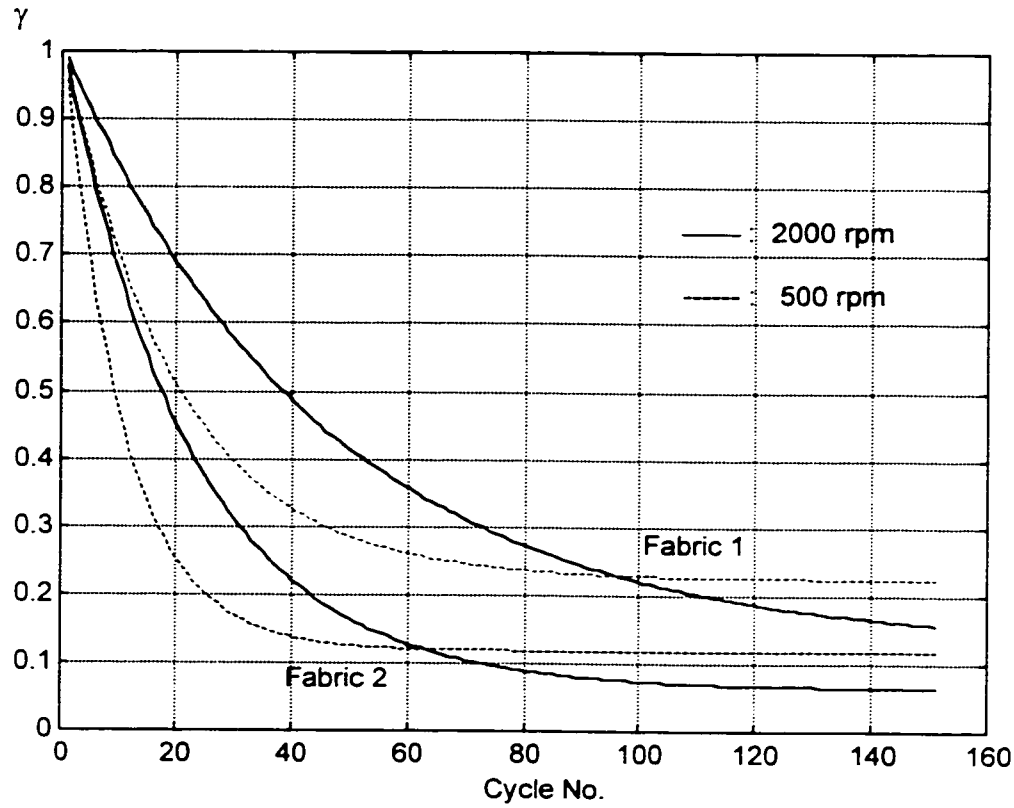

Figure 4.10 γ vs. sewing stitch cycle

4.2.2 Convection Boundary Condition

1. <u>Applying Time-Dependent Convection Boundary Condition</u>

Convection takes place between the needle outer surface and the environment air. Some assumptions are made, in order to apply the convection boundary conditions :

- Since the sewing speed is very high, the convection coefficient is assumed to be the same during the penetrating and withdrawal process.
- The settling time (the time period needed to go to the steady state) is very short (about 3 seconds) , therefore we can assume the convection coefficient doesn't change during the one operation.

Convection boundary condition is applied in a similar way as the heat flux in each load step: the outer surface of the needle sections that are not in the fabric experience convection boundary. See Figure 4.6, the sections that has no heat flux.

2. Determination of Convection Coefficient

Heat transferred by the convection can be expressed as:

$$Q = A\, h_c\, \Delta T \tag{4.11}$$

Where, A is the fabric area m^2 ;

h_c is convection coefficient $W/(m^2 \cdot K)$;

ΔT is the temperature difference between needle surface and environment, K.

The convection coefficient h_c is related to many factors, such as the properties of the fluid (k, ρ, μ, c_p), the needle shape, size, position, and fluid velocity, etc. In Perry's Handbook [Perry, J. H., ed. 1963], h_c is about 12 W/(m^2·K) for the natural convection from a vertical cylinder to air. For forced flow at a velocity of 3 m/sec past a single cylinder, h_c is about 170 W/(m^2·K).

From author's study, the final needle temperature won't make any obvious difference as h_c changes from 80 W/(m^2·K) to 120 W/(m^2·K), which corresponds to the

sewing speed from 500 rpm to 2000 rpm. In this thesis, a constant value for the convection coefficient is assumed.

4.2.3 Heat Flow

1. Heat Flow Boundary Condition

As stated in the introduction, thread plays a complicated role in needle heating problem. Depending on tension's change in thread, it can be a heat source when the thread is pulled tightly rubbing the needle eye; it can be a heat sink also when thread goes through the needle eye loosely, taking some heat from the needle eye. Therefore the thread motion in one cycle must be studied in order to apply correct boundary conditions.

Figure 4.11 illustrates the approximate motion of top thread, and indicates the thread tension's state. As illustrated, most of the time the thread is loosely in contact with the needle eye. Therefore the thread is more like a heat sink than a heat source.

The thread tension is generated before the needle punching into the fabric and after the needle withdrawing from the fabric. Figure 4.12 illustrates how the thread tension change with the crank rotation angle. As shown in the figure, thread tension is time-dependent, an average value will be taken in calculation of the heat flow generated from the thread. Heat flow boundary condition are going to apply step by step too.

2. Calculation of Heat Flow

(1) As a Heat Source

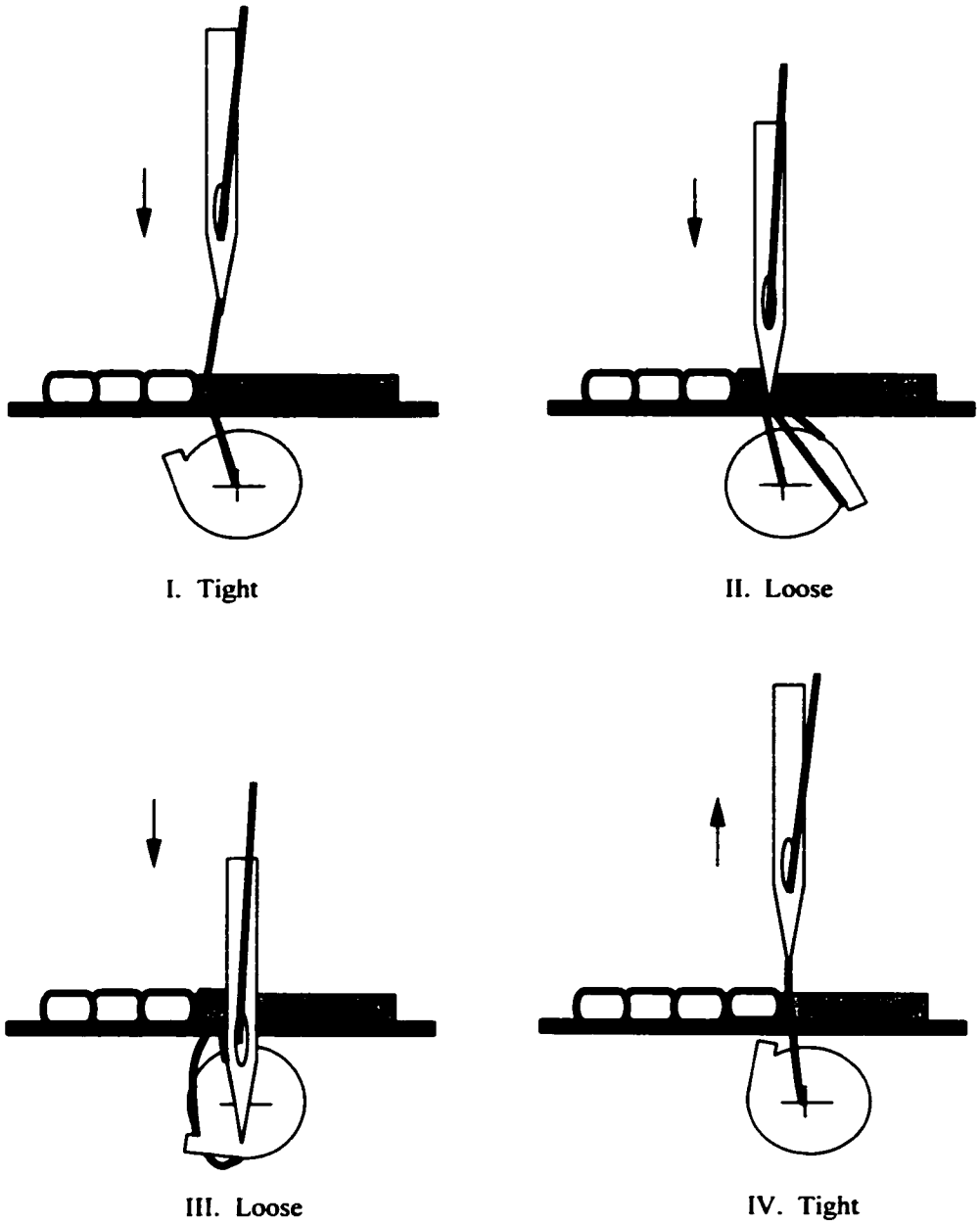

Figure 4.11 Sketch of thread motion and tension in the thread

Thread tension are generated during those periods: before needle penetrating the fabric and after needle withdrawing the fabric, specifically during the needle idling time. The thread is tightly pulled in this period.

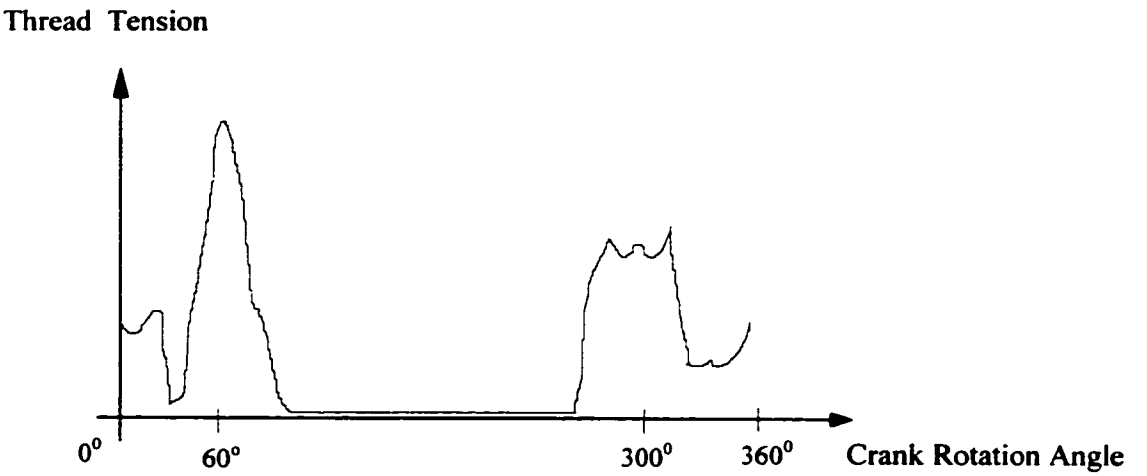

Figure 4.12 Sketch of thread tension vs. crank rotation angle

Assume the thread-protecting groove in the needle can accommodate the thread totally during the period when needle piercing fabric and withdrawing from the fabric, therefore the friction effect between thread and fabric is ignored. But when the thread diameter is in large size, this assumption won't apply. Then extra friction heat is generated between thread and fabric. That is the reason of the finding that the smaller size the thread, the less the heating problem [Hersh, 1969].

Refer to Figure 4.13. Suppose thread tension is T, the needle diameter is d, and the needle eye diameter is h, the normal force N can be calculated:

$$N = 2T \cdot \cos\{(\theta_1 + 90^\circ + \theta_2)/2\} \tag{4.12}$$

Where, $\theta_2 = arctg(h/d)$, $0^\circ < \theta_1 < 15^\circ$

Then the friction force

$$f = \mu \cdot N = \mu \cdot 2T \cdot \cos\{(\theta_1 + 90^\circ + \theta_2)/2\} \tag{4.13}$$

The friction power is expressed by:

$$P_{friction} = f \cdot V_{thread} \tag{4.14}$$

V_{thread} is the thread velocity relative to the needle. Actually during that pulling period, the thread is static, therefore V_{thread} is actually the velocity of the needle, which can be obtained from equation (4.1).

Similar to the heat flux generated from the friction between needle and fabric, the heat flow rubbed from thread and the needle eye is partitioned between thread and needle.

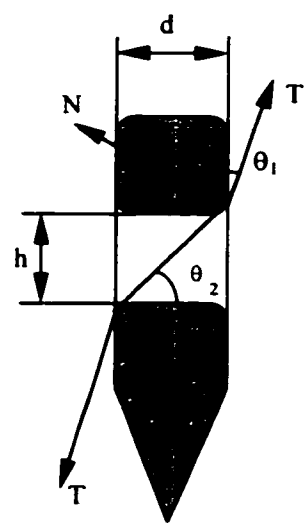

Figure 4.13 Sketch to calculate the heat flow

The partition ratio can be obtained from a similar way as γ , which depend on the thread material properties, sewing speed, initial temperature difference between thread and needle eye. Referring to Figure 4.9, author find the following equation give good approximate solution of γ_{thread} :

$$\gamma_{thread} = \frac{1}{e^{\beta_t \lambda_t (T - T_0)}} \tag{4.15}$$

Where, γ_{thread} is friction heat flow partition ratio between thread and needle;

β_t is the thread property coefficient;

λ_t is the speed coefficient, $0 < \lambda_t < 1$.

T_0 is the environment temperature K

T is the reference temperature of the needle K

At the beginning, it is assumed that the friction heat is absorbed totally by the needle because the thread is less sensitive to heat. With the increase of the needle temperature, more friction heat goes to the thread. The value of β_t , λ_t can be obtained from the experiment, or further theoretical analysis.

(2) <u>As a Heat Sink</u>

The thread motion when it is in loose state is still very complicated, because it keeps going through and coming out of the fabric. Sometimes thread may feed in to form the loop, while other time the thread is pulled out to form the final stitch. Therefore only the average calculation of its total effect being a heat sink is possible. In this study, this average effect in one cycle is studied.

Suppose after one cycle, the amount of the thread going through the needle eye is $\rho_t V_{olt}$, and average temperature in thread increases to T from T_∞, the reference temperature in the needle eye is T_e. The following equation gives a approximate estimation of thread cooling effect on the needle eye in one cycle:

$$\alpha_t = \frac{\xi_{vol} \cdot \rho_t c_t V_{olt} (T - T_\infty) / \Delta t}{T_e - T_{tt}} \tag{4.16}$$

Where, α_t is the thread cooling coefficient $W/℃$;

ξ_{vol} is thread volume coefficient indicating heat penetrating depth in thread;

Δt is the time in one cycle s;

T_{tt} is the thread temperature during the cycle, $T_\infty < T_{tt} < T$;

The numerator in equation (4.16) is the total heat absorbed in the thread during one cycle. α_t is determined by the thread properties, thread size, sewing speed. The average temperature in thread after one cycle can be obtained from experiment. Figure 4.14 is a typical image of needle heating results from experiment [Liasi, 1997].

In our experiment [Liasi, 1997], α_t for unbounded thread is about 0.004 $W/℃$, while for bounded thread is about 0.001 $W/℃$. The speed seems has little effect on α_t. The thorough examination of α_t can be carried out by complete experiment.

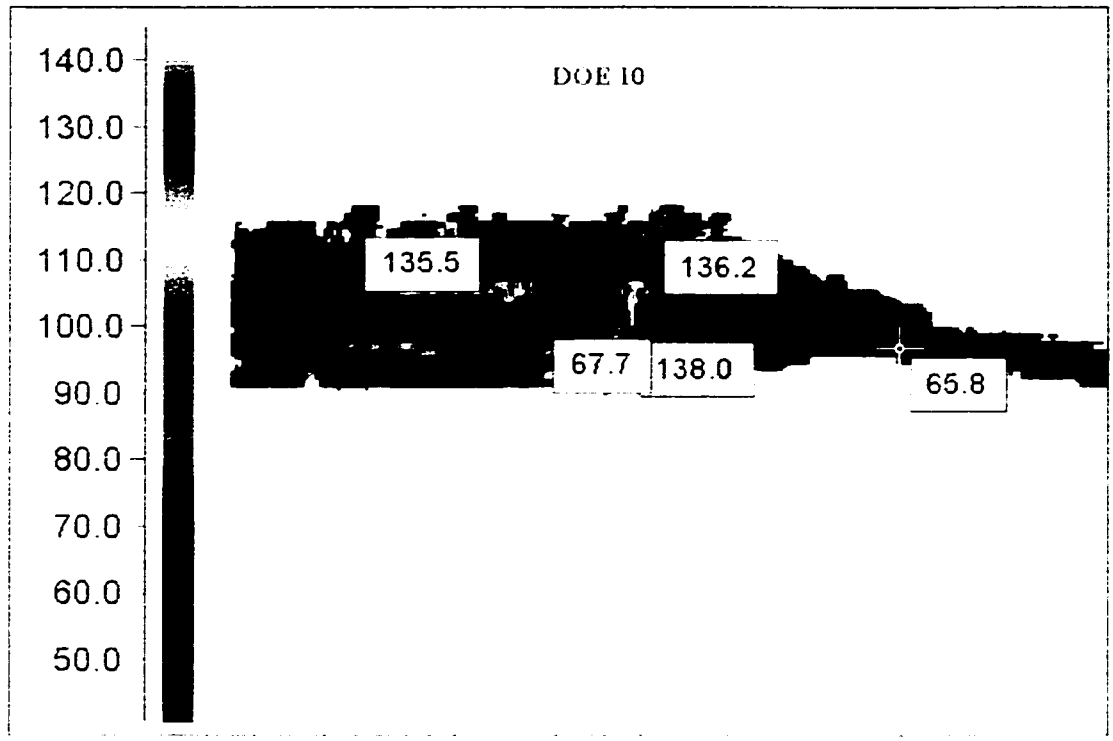

Figure 4.14 IR image of needle heating results [Liasi, 1997]

4.2 FEA Simulation Results and Discussions

4.3.1 Simulation Results

Simulations are done at sewing speed: 2000 rpm, 1000 rpm, 500 rpm, with fabric thickness of 4mm and 2mm. Figure 4.15 illustrates the typical node reference position. Figure 4.16, Figure 4.18 and Figure 4.20 are the simulation results of these nodes with respect to different speeds at fabric thickness 4mm. The experiment results under the corresponding situation are shown in Figure 4.17 , Figure 4.19 and Figure 4.21 [Liasi and et al., 1996].

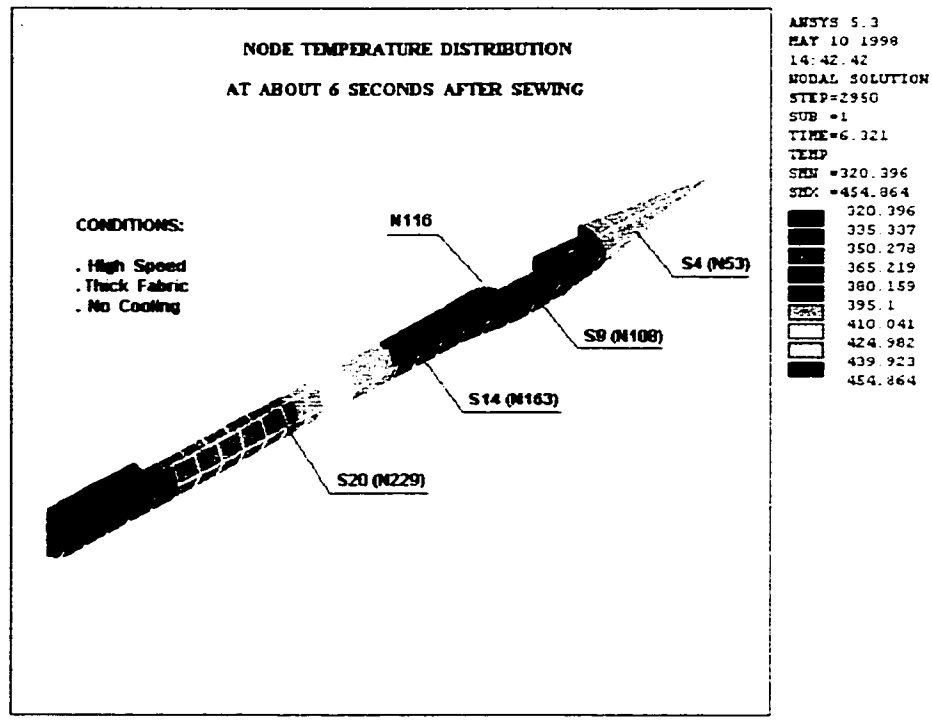

Figure 4.15 Reference nodes positions

Comparing the simulation results with the experiment results, it is found that the temperature curves from the simulation have the same trend as those from experiment:

- At the beginning, the temperature increases faster, after a time period the curves go steadily, approaching to steady state temperature.
- At the local point, the temperature curve varies within an interval, oscillating about the steady state, even though the trends is smooth and steady. This is caused by the

time-dependent boundary conditions. In the experimental results, temperature goes up and down slightly at the steady part of curve because of the same reason.

- The node at different position in the needle achieve the steady state at different time, the rear part of the needle attained steady state late. This may due to the different section of the bulged needle experience different friction heat.

Simulation errors are calculated as:

(1) *At high speed of 2000 rpm*: peak temperature from simulation is 453 K (180 ^{0}C), and peak temperature from experiment is 177 ^{0}C, therefore the relative error for the steady state temperature is about 2%. The time constant is about 0.6 second from simulation; and is 0.75 second from experiment.

(2) *At medium speed of 1000 rpm*: peak temperature from simulation is 400 K (127 ^{0}C), and the peak temperature from experiment is 117 ^{0}C, therefore the relative error for the sustained temperature is about 8 %. The time constant from experiment is about 1.4 seconds, and that from the simulation is about 0.8 seconds.

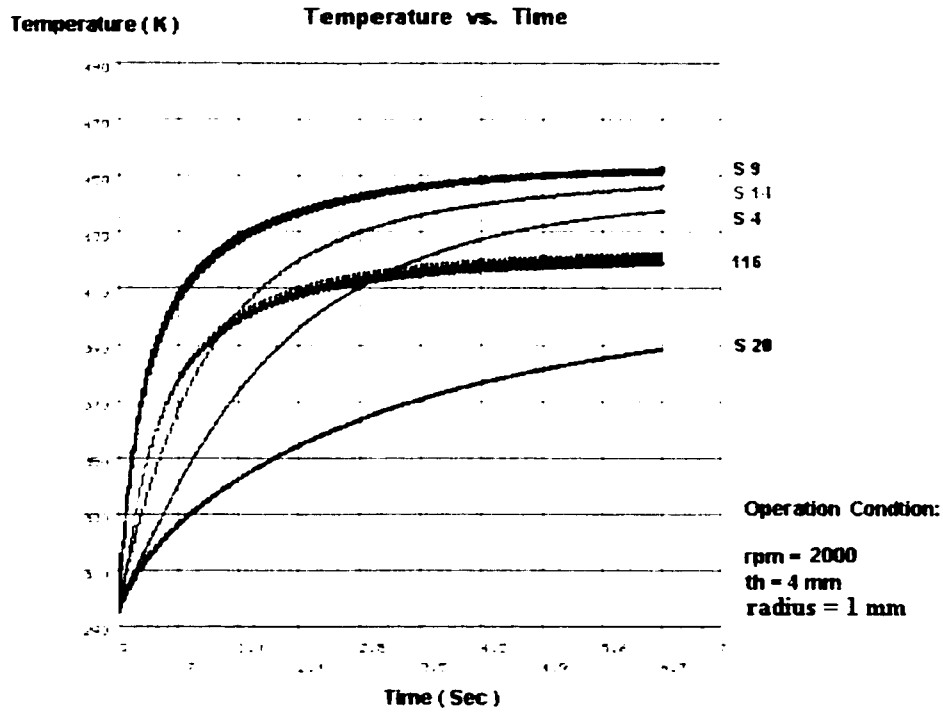

Figure 4.16 Temperature vs. time, 2000 rpm, th=4mm

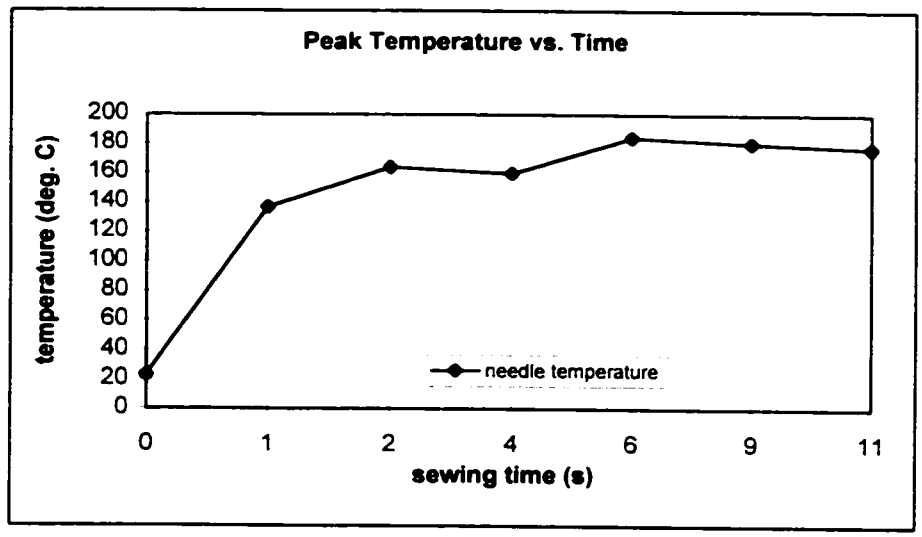

Figure 4.17 Experiment results of high speed sewing 2000 rpm

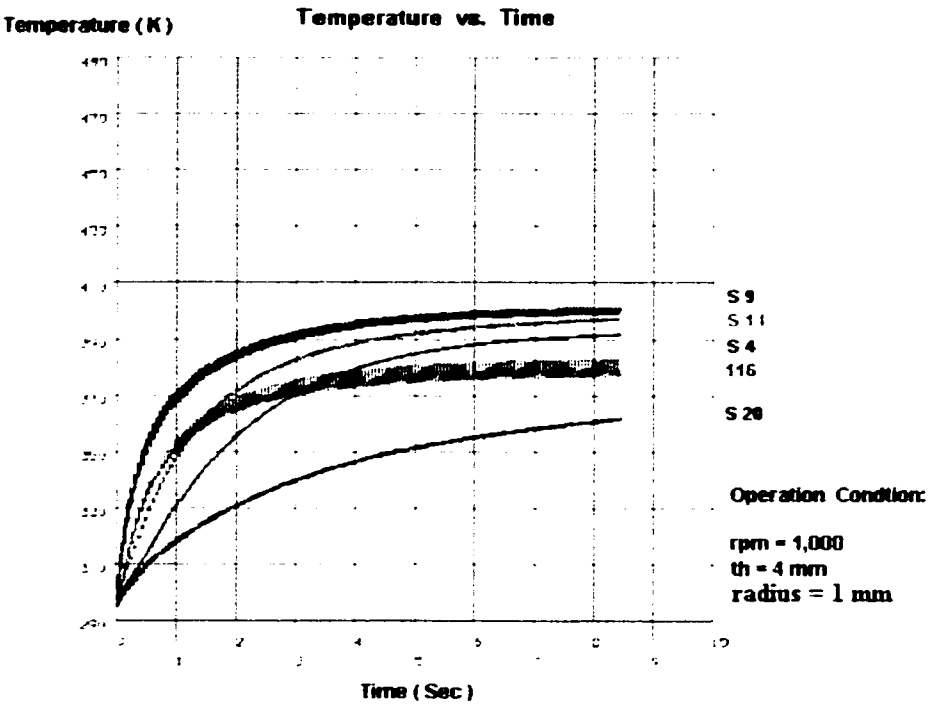

Figure 4.18 Temperature vs. time, 1000 rpm, th=4mm

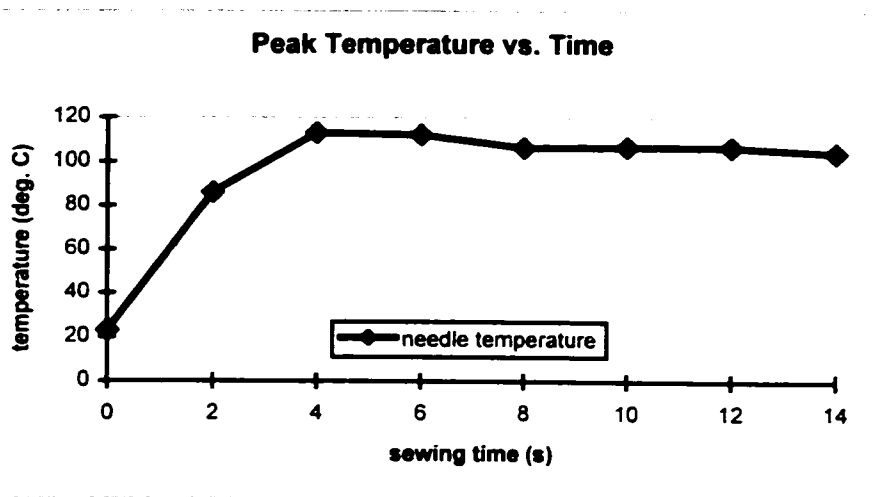

Figure 4.19 Experiment results of medium speed sewing 1000 rpm

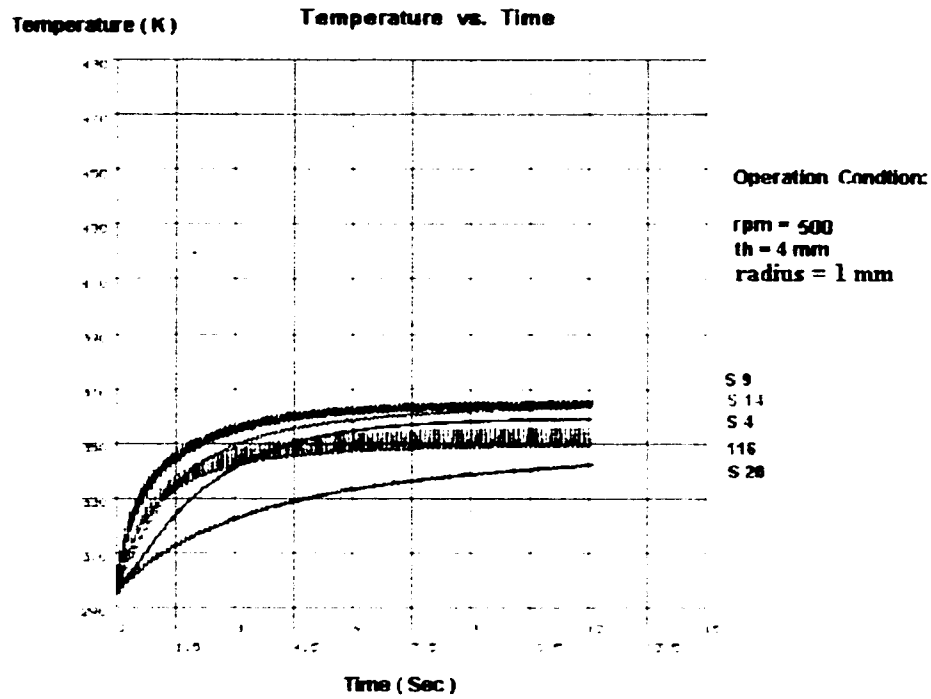

Figure 4.20 Temperature vs. time, 500 rpm, th=4mm

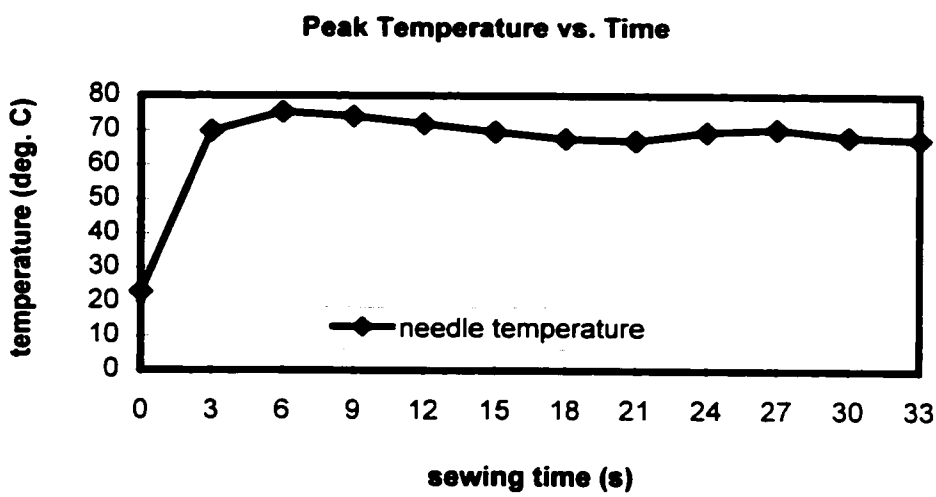

Figure 4.21 Experiment results of low speed sewing 500 rpm

(3) *At low speed of 500 rpm*: peak temperature from simulation is 360 K (87 ^{0}C), and the peak temperature from experiment is 77 ^{0}C, therefore the relative error is about 12 %. The time constant from the experiment is about 1.75 seconds, and that from the simulation is about 1.45 second too.

From the above comparison between the experimental results and the simulation results, one can conclude that the simulation model is reliable to some degree, and can be used to predict the needle heating results.

Table 4.1 is the summary of the simulation results for different kind of speed, thickness.

Table 4.1 Summary of simulation results for different sewing speed and thickness

Speed (rpm)	Thickness (mm)	Node Temperature (°C)			Time Constant (second)	Experiment	
		N53	N108	N163		P.T.	T.C.
2000	**4**	**162**	**180**	**170**	**0.6**	**177**	**0.75**
2000	2	110	127	120	0.75		
1000	**4**	**117**	**127**	**122**	**0.8**	**117**	**1.4**
1000	2	80	90	87	1.2		
500	**4**	**81**	**87**	**85**	**1.45**	**77**	**1.75**
500	2	60	65	63	1.8		

4.3.2 Parameters Effects on Needle Heating

From analysis study, it is found that operation conditions have important effects in needle heating. The effect from material properties of fabric, thread, needle on the

needle peak temperature and time constant are very obvious too. Specifically, these parameters are:

- sewing speed, the major factor of needle heating problem;
- fabric thickness;
- cooling condition, usually compressed air is used for cooling;
- material properties of needle, fabric, thread: conductivity, specific heat, density, friction coefficient, etc.
- needle geometry: diameter, point shape;

1. Effect of Sewing Speed

- For the same fabric thickness, as sewing speed increases, the peak temperature increases. The higher the speed, the more heat goes in to the needle during the unit time period, hence resulting the higher steady state temperatures.
- For the same fabric thickness, as sewing speed increases, the time constant decreases. The more heat taken by the needle within unit time period, the faster it reaches the steady state because heat absorption rate decreases with temperature going very high.

There is another important reason for these two results: friction heat partition ratio increases with sewing speed at the same fabric thickness [Appendix B Figure B.1]. As the sewing speed increases, more part of friction heat goes into the needle during each cycle, therefore the friction heat goes into the needle during the unit time is much bigger. Faster for the needle to achieve steady state with higher peak temperature.

2. Effect of Fabric Thickness

From table 4.1, it is found that:

- High speed (2000 rpm) with different fabric thickness (4 mm and 2 mm): When the fabric thickness is 4 mm, the maximum steady state temperature, which happened near needle eye, can reach 180 ^{0}C, and the time constant is 0.6 seconds, when the thickness is 2 mm, the maximum steady state temperature goes to 125 ^{0}C, which is 55 ^{0}C lower, and the time constant is 0.75 seconds, which is about 0.15 seconds longer.
- Medium speed (1000 rpm) with different thickness (4 mm and 2 mm): When the fabric thickness is 4 mm, the maximum steady state temperature can reach 127 ^{0}C, and the time constant is 0.8 seconds, when the thickness is 2 mm, the maximum steady state temperature goes to 90 ^{0}C , which is 37 ^{0}C lower, and the time constant is about 1.2 seconds, which is about 0.4 seconds longer .
- Low speed (500 rpm) with different thickness (4 mm and 2 mm): When the fabric thickness is 4 mm, the maximum steady state temperature can reach 87 ^{0}C, and the time constant is 1.45 seconds, when the thickness is 2 mm, the maximum steady state temperature goes to 65 ^{0}C, which is 22 ^{0}C lower, and the time constant is about 1.8 seconds, which is about 0.35 seconds longer .

From the above analysis, we found the fabric thickness plays a very important role in needle heating.

- When the fabric is thinner, the peak temperature will decrease greatly, ranging from 20 ^{0}C to 60 ^{0}C for each layer relating to different sewing speed. One reason is obviously because of less friction heat generated with thinner fabric.

The other reason is friction heat partition ratio γ is decreasing slightly as the fabric thickness decreases [Appendix B Figure B.2].

- With the higher speed, the peak temperature will make bigger difference with different thickness of the fabric. Because at high speed the needle takes in much more friction heat in the same time period and make bigger temperature difference for different fabric thickness.
- The time constant increases with thinner fabric thickness. The reason is thicker fabric generated much more friction heat, plus the friction heat partition ratio is bigger with thicker fabric, therefore needle can go to the steady state faster. This allows operator to continue the sewing time relatively longer when sewing thinner fabric, since it will take longer time to achieve the highest temperature.

3. Effect of Material Properties

Both needle material properties and fabric material properties will affect the peak temperature and time constant. The first parameter is the friction coefficient, which determines the friction force during needle penetrating and withdraw. Obviously, increasing needle surface smoothness, fining the textile structure, or using lubricant can always be a help to decrease the friction coefficient, and hence decrease the peak temperature to some degree.

The other major factor that affects peak temperature and time constant is the friction heat partition ratio, which is determined by both needle and fabric thermal properties. It is found that:

- With the increase of needle conductivity, the peak temperature will decrease to some degree in FEA model, which due to the conduction heat loss along the needle to the environment. But this effect of conductivity is not reflected in the lumped model, since the temperature in one section of the needle is assumed the same, and the conduction along the needle is not considered in the model.
- With the decrease of needle material density and specific heat, the time constant will decrease, but the peak temperature will not change too much. This is applicable to both lumped model and FEA model. But in sliding model, the peak temperature will decrease slightly.
- With the increase of fabric heat conductivity, the needle peak temperature will decrease and the time constant will increase too.
- With the increase of fabric density and specific heat, the peak temperature will decrease and the time constant will decrease too. This is because the friction heat partition ratio decrease with the increase of the ρ_2, c_2.

4. Effect of Needle Geometry

As shown in Figure 4.2, an industrial sewing needle is defined by some 15 parameters. There are a number of parameters that determine the behavior of needle heating. These parameters include:

- Needle punching-in length, which determines the total friction force that the needle experiences during penetration;
- The long thread protection groove position and size;

- The needle eye position and size;
- The total needle length; and the needle diameter.

Simulations are done with needle diameter at 0.0024 m, which shows the time constant is a little bit longer than that obtained from the smaller diameter of 0.002m, but the peak temperature makes no obvious difference. This is because the friction heat increases as the needle diameter increases, but convection heat loss also increases with the increased needle surface area. The net effect is almost negligible.

Further simulations may need to examine other geometry parameters' effect in needle heating.

4.4 Brief Comparison of FEA Model and Simplified Models

In sliding model and lumped model, the needle geometry is simplified as a cylinder. Only the surface part of the needle is included in the heat conduction across section in sliding model. And in the lumped model, the heat conduction along the needle is ignored. Therefore, the peak temperature obtained from these simplified model is slightly higher than that from FEA model.

In the FEA model, the major needle geometry parameters are included in the mesh, such as: needle diameter, needle point tip, thread grooves, needle eye position, bulge around needle eye. The thread effect as a heat sink and a heat source is considered also in FEA. Therefore the FEA simulation model gives more accurate results.

Figure 4.22 gives the comparison of the temperatures obtained from the points on the needle center line and on the outer surface. The "i" refers to center points, and the "o" refers to the outer surface points. It is found that the temperature on the center line points have pretty close temperature value as their counter parts on the outer surface. These results give some supports to the assumption of lumped model -- same temperature value in one section of the needle. Also it is found from the curve, temperatures on the outer surface oscillate bigger than that on the needle center line, which support the results from the sliding model to some degree.

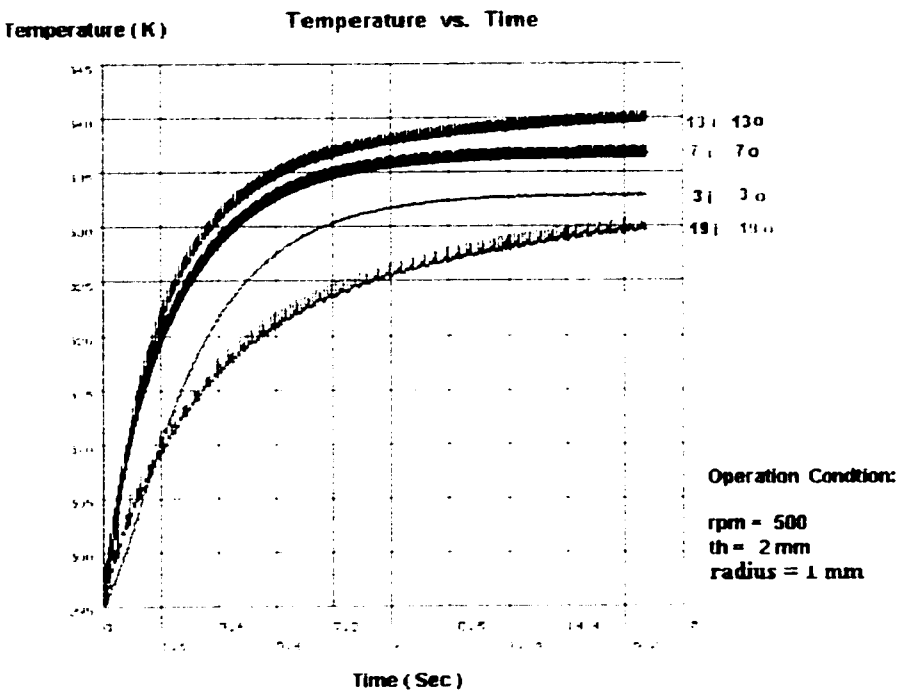

Figure 4.22 Comparison of temperature values on the needle center and outer surface

CHAPTER V

CONCLUSIONS AND FUTURE WORK

5.1 Conclusions

This thesis presented three simulation models of needle heating in industrial sewing: sliding model, lumped model, FEA model. Common assumptions are made for these simulation models, such as: sewing speed is uniform during the each cycle; fabric has uniform material properties; average thermal properties are taken for fabrics in different layers, radiation effect from the needle surface is ignored, etc.

Friction heat partition ratio between needle and fabric, which is an important factor affecting needle heating, was studied in detail in these models. These models correlate needle geometry, material properties with the sewing operation conditions, such as sewing speed, fabric thickness, and can trace the temperature increase in the needle till equilibrium state, and hence predict the peak temperature under different sewing conditions. The simulation results, which obtained at sewing speed 2000 rpm, 1000 rpm, 500 rpm with different fabric thickness, are presented as "Temperature vs. time" curves at the end of these chapters. The very close comparison between the simulation results and experimental results is readily apparent. The model reveal sewing speed and fabric thickness are the two major factors that affect peak temperature.

In sliding model and lumped model, needle geometry is simplified as an infinite cylinder, and the thread effect is ignored. The sliding model is based on the theory of moving plane heat source. While the lumped model is assumed the temperature at each point of one section in the needle are the same at one time. These two models give pretty good simulation result when sewing speed is under 3000 rpm and the fabric

thickness is less than 8 mm. At extremely highly speed and thick fabric sewing, the peak temperature tends to be higher than real case. Because the heat conduction across the needle and along the needle become important heat sink when temperature goes very high. These are not considered in sliding model and lumped model. But these two models give fast approximate calculation of peak temperature and time constant, they are very convenient in analyzing important parameters' effects on needle heating.

FEA simulation is carried out by ANSYS 5.3. Mesh of needle geometry is generated directly with solid 70 3-D thermal solid. The major needle geometry parameters are included in the mesh, such as: needle diameter, needle point tip, thread grooves, needle eye position, bulge around needle eye. The time dependent boundary conditions are applied by multiple load steps. The thread effect on needle heating as both heat sink and heat source are studied in detail. Heat flux and heat flow calculations are based on the sewing force model, thread tension experiment. The FEA model can present temperature distribution in the needle at any time point, which is an obvious advantage over the two simplified models. The FEA simulation model can be a foundation for optimization of sewing operations and needle design after combination with the sewing force model.

5.2 Future Work

Ranked by its importance, the future work may be as follows:

1. A total sewing process model. In the presented study, the needle heating is considered to be dependent on the sewing force obtained separately. Clearly, the

sewing force is also effected by the needle heating. Hence, a study on the combination of needle heating and the sewing force is very important.

2. The effect of the coolant. It has been reported that compressed air coolant is used in high speed sewing. The coolant effect is not included in the presented study and should be studied in the future.
3. Optimization of sewing operation. Based on a comprehensive computer simulation model, we can optimize sewing operations for efficient and quality sewing. Figure 5.1 shows an optimization model. The input information includes sewing specifications and initial sewing machine settings, such as: fabric type, layers to be sewn, thread type, thread tension setting, etc. The output of the model includes the desirable sewing speed.
4. The effect of the textile structure. In this study, it is assumed that the textile structure is uniform in all the directions. While it is true for the fabric such as vinyl and leather, it is may not satisfy well with the knitted fabric. The directional effect of the textile structural characteristic may affect the sewing force and hence affect the needle heating.

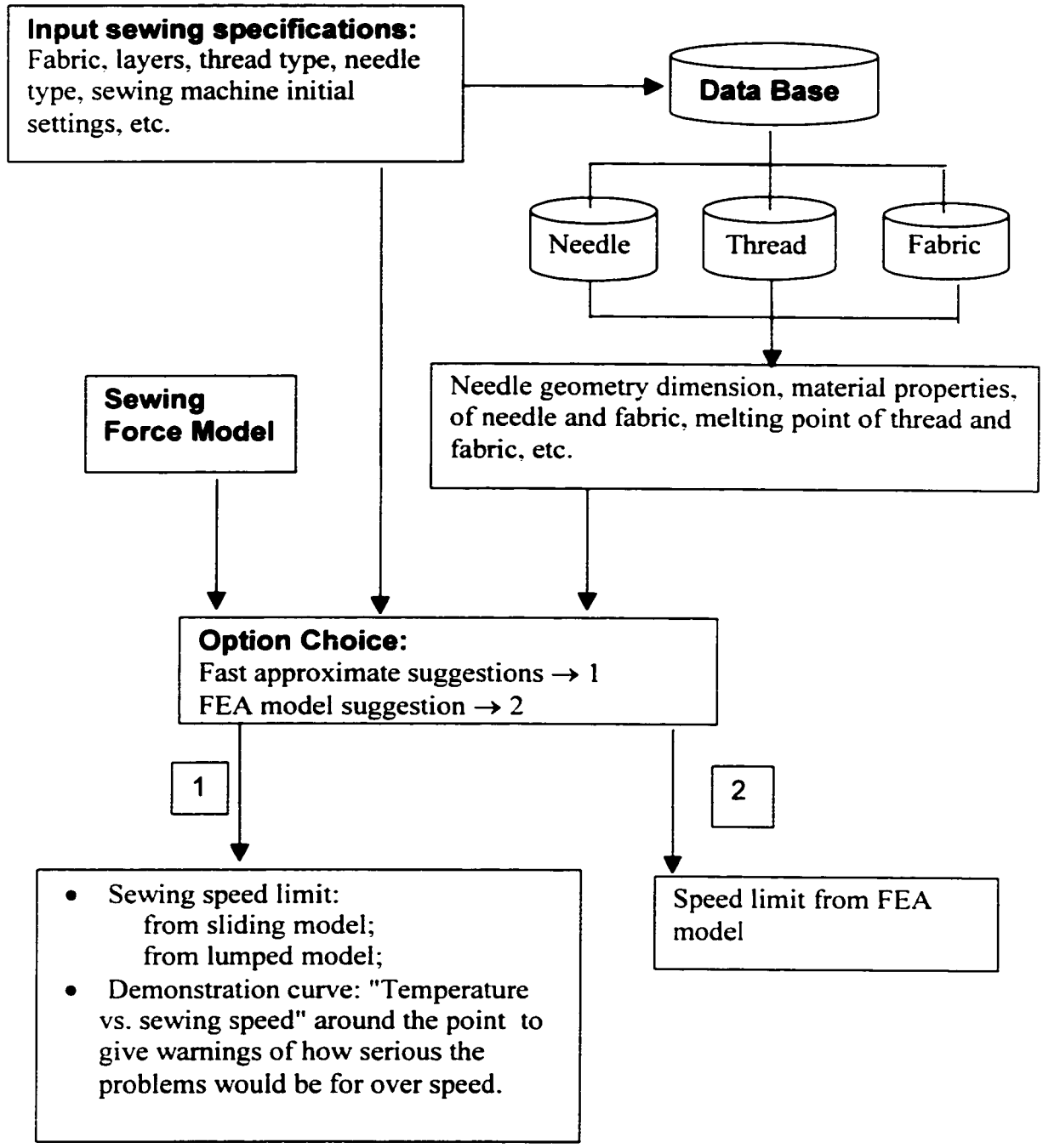

Figure 5.1 Proposed speed suggestion system

REFERENCES

Archard, J. F., "The Temperature of Rubbing Surfaces", *Wear,* Vol.2, 438-455, 1958

Armi, E. L., Johnson, J. L., Machler, R.C., "Application of the Sliding Thermocouple Method to the Determination of Temperature at the Interface of a Moving Bullet and a Gun Barrel", *Journal of Applied Physics,* Vol.18, 88-94, 1947

Arpaci, V. S., "Conduction Heat Transfer", *Addison-Wesley Publishing Company*, 1966.

Balakin, V. A., "Formation And Distribution of Heat in the Frictional Contact Zone Under Conditions of Non-Stationary Heat Exchange", *Wear*, Vol.72, 133-141, 1981

Bos, J., Moes, H., "Frictional Heating of Tribological Contacts", *Journal of Tribology*, Vol.117, 171-177, 1995

Bowden, F. P., Tabor, D., "The Friction and Lubrication of solids, Part II", *Oxford at the Clarendon Press,* 1964

Carr, W. W., Posey J. E., and Tincher W. C., "Frictional characteristics of apparel fabrics", *Textile Research Journal,* Vol.58, 129-136, 1988

Chantrenne, P., Raynaud, M., "A Methodology for the Experimental Estimation of The Thermal Dry Sliding Contact Model Parameters", *HTD-Vol. 312, 1995 National Heat Transfer Conference* - Vol.10, 71-78, ASME 1995

Charrler, J., Maki, J., "Penetration of Elastomeric Blocks by Needles", *ANTEC,* 761-764, 1986

Dorrity, Lewis, Olson, Howard, "Microprocessor-based System for Sewing Defect Detection", *Fifth Annual Academic Apparel Research Conference, Flexible Shop Floor Technology*, 4-ii, 1994

Elsayed, M.A., Wells, L.R., "Sewing Machine Dynamic Characterization Through Modal Analysis and Transfer Function Measurements",

Frederick, E. B., Zagieboylo, W., "Measurement of Needle Heat Generated During the Sewing of Wool and Wool Nylon Fabrics", *Textile Research Journal,* Vol.25, 1025-1029, 1955.

Galuszynski, S., "Fabric Tightness: "A Coefficient to Indicate Fabric Structure", J. *Textile Inst.* Vol. 72, 44-48, 1981.

Galuszynski, S., "Effect of Fabric Structure on Fabric Resistance to Needle Piercing", *Textile Research Journal,* Vol.56, 339-340, 1986.

Guyer, E., "Handbook of Applied Thermal Design", *McGraw-Hill Book Company*, 1989

Halling, J., "Principle of Tribology", *The Macmillan Press Ltd.*, 1975

Hearle, J., Sultan, M., "A Study of Needled Fabrics Part VI: The Mmeasurement of Punching Force During Needling", 237-242

Hersh, S. P., Grady, P. L., "Needle Heating During High-Speed Sewing", *Textile Research Journal,* Vol.39, 101-120, 1969.

Holm, R., "Calculation of the Temperature Development in a Contact Heated in the Contact Surface, and Application to the Problem of the Temperature Rise in a Sliding Contact", *Journal of Applied Physics,* Vol. 19, 361-366, 1948

Holm, R., Marys, ST., "Temperature Development in a Heated Contact With Application to sliding Contacts", *Journal of Applied Mechanics*, Sept, 369-374, 1952

Howard, G. M., Parsons, D., "Sewing Needle Temperature, Part I: Theoretical Analysis and Experimental Methods", *Textile Research Journal*, Vol.38, 606-614, 1968.

Howard, G. M., Sheehan, J. J., Mack, E. R., Virgilio, D. R., "Sewing Needle Temperature, Part II: The Effects of Needle Characteristics", *Textile Research Journal,* Vol. 41, 231-238, 1971.

Howard, G. M., Virgilio, D. R., Mack, E. R., "Sewing Needle Temperature, Part III: The Effects of Sewing Conditions", *Textile Research Journal*, Vol. 43, 651-656, 1973.

Howell, H. G., Mieszkis, K. W., Tabor, D., "Friction in Textiles", *London, Butterworths Scientific Publications*, 1959.

Hurt, F.N., Tyler, D.J., "Seam Damage in the Sewing of Knitted Fabrics", *HATRA Research Reports,* 35 - 36, 1975

Jaeger, J. C., "Moving Sources of Heat and the Temperature at Sliding Contacts", *Proceedings of Royal Society N.S.W.,* Vol. 76, 203-224, 1942

Kamata, Y., Tsunematsu, S., Kinoshita, R., Naka, S., "Needle-Fabric interaction during the sewing", *Sen-Igakkaishi,* Vol. 33, 157-165, 1977

Kelly, W. I., Smuts, S., Hunter, L., "The Sewability of Some Knitted Fabrics", *SAWTRI Technical Report*, No. 401, 1-22, 1978

Khan, R. A., Hersh, S. P., Grady, P. L., "Simulation of Needle-Fabric Interactions in Sewing Operations", *Textile Research Journal,* Vol.40, 489-498, 1970.

Laughlin, R. D., "Needle Temperature Measurement by Infrared Pyrometry", *Textile Research Journal,* Vol.33, 35-39, 1963.

Liasi, E., Du, R., "Final Report on the Experimental Study of Industrial Sewing Machines", *Experimental Report, Machine Automation Research Lab, University of Windsor,* 1996.

Liasi, E., Du, R., "A Study of Needle Heating in Industrial Sewing Using Infrared Radiometry", *Submitted to Int. J. of Clothing Science and Technology*, 1997.

Mallet, E., "Finite Element Simulation of Sewing Forces", *Research Report, Machine Automation Research Lab, University of Windsor,* 1997.

Matthews, B. Ann, and Little, Trevor J., Sewing dynamics, Part I : Measuring sewing machine forces at high speeds, *Textile Research Journal,* Vol. 58, 383-391, 1988.

Najafi, M., Smith, S.A., Dareing, D. W., Ye, H., "Temperature Reduction in Sewing Needles", *HTD-Vol. 310, 1995 National Heat Transfer Conference* - Vol. 8, ASME 1995.

Najafi, M., Smith, S. A., Ye, H., "Investigation of the Temperature Distribution in Sewing Machine Needles", *Fifth Annual Academic Apparel Research Conference,* 1994.

Perry, J. H., ed., "Chemical Engineers' Handbook", 4th ed., *New York, McGraw-Hill,* 1963.

Poulikakos, D., "Conduction Heat Transfer", *Prentice Hall, New Jersey*, 1994.

Scott, L. H., "Some Problems Relating to Sewing",

Shanghai Institute of Sewing Machine, "Operation Principles and Structure Analysis of Industrial Sewing Machine" (in Chinese), 1990

Singer Company, Improvements in Needle Design, *Bobbin*, Feb., 174 - 191, 1981

Simmons, S., Keller, A. Z., "A Physical Model of Needle Heating", *Clothing Res J.* Vol.2, 37-46, 1980

Simmons, S., "An analysis of Forces in a Fabric-Needle Sewing system", *Clothing Res J.* Vol.1, 51-59, 1979

Stylios, G., "A study of Problems Associated with Fabric Sewing in Commercial Garment Manufacture", *Ph.*D. *Thesis*, Leeds University, 1987

Stylios, G. Xu, Y.M., "An Investigation of the Penetration Force Profile of the Sewing Machine Needle point", *J. Text. Inst.* Vol.86, 48-163, 1995

Torrington Company, "Finding Solutions to Needle problems", *Bobbin*, 180. February, 1981

Varadi, K., Neder, Z., Friedrich, K., "Evaluation of the Real Contact Areas, Pressure Distributions and Contact Temperatures During Sliding Contact Between Real Metal Surfaces", *Wear*, Vol. 200, 55-62, 1996

Wang, S., Komvopoulos, K., "A Fractal Theory of the Temperature Distributionn at Elastic Contacts of Fast Sliding Surfaces", *Journal of Tribology*, Vol.117, 203-215, 1995

Wang, S., Komvopoulos, K., "A Fractal Theory of the Interfacial Temperature Distribution in the Slow Sliding Regime: Part I - Elastic Contact and Heat Transfer Analysis", *Journal of Tribology*, Vol.16, 812-823, 1994

Wang, S., Komvopoulos, K., "A Fractal Theory of the Interfacial Temperature Distribution in the Slow Sliding Regime: Part II - Multiple Domains, Elastoplastic Contacts and Applications", *Journal of Tribology*, Vol.116, 824-832, 1994

Weast, R. C., "Handbook of Chemistry and Physics", *The Chemical Rubber Co.*, Cleveland, Ohio, 1973

Yang, S. M., "Heat Transfer" (in Chinese), *Advanced Education Publish Ltd.* Beijing, P.R.China, 1984

Yevtushenko, A., Ivanyk, E., "Effect of the Rough Surface on the Transient Frictional Temperature And Thermal Stresses Near a Single Contact Area", *Wear*, Vol.197, 160-168, 1996

Yevtushenko, A., Ivanyk, E., "Determination of Temperatures for Sliding Contact with Applications for Braking Systems", *Wear*, Vol.206, 53-59, 1997

Yevtushenko, A., Ukkhanska, O., Chapovska, R., "Friction Heat Distribution Between a Stationary Pin and a Rotation Disc", *Wear*, Vol.196, 219-225, 1996

Appendix A: Matlab Program of Sliding Model

Main function to calculate the examined needle section temperature

---

```
function y=smain(y0,rou,c,ri,th,rpm,df,alf)

% y0 is the distance between the examined point to the needle tip
% rou is the needle material density
% c is the needle material specific heat
% th is the fabric thickness
% rpm is the sewing velocity
% df is the friction force per unit area
% alf is the cooling coefficient

% To is the environment temperature
% dp is the needle punching distance; dw is the needle idling distance.
To=295;
dp=0.02;
dw=0.008;

% vol is the volume of the needle section in contact
% area is the contact section area
vol=ri*ri*3.14*th;
area=2*3.14*ri*th;
pcv=rou*c*vol;

% vel is the average velocity of needle
vel=rpm*(dp+dw)*2/60;

% t1 and t3 are the time period the contact
% (con't)heat source goes through the examined point.

% t2 and t4 are the time period when the selected needle section not
% covered by the contact heat source during punching and withdraw.
t1=th/vel;
t2=2*(dp-th/2-y0)/vel;
t3=t1;
t4=2*(y0+dw-th/2)/vel;

%lmt2 is fabric heat conductivity
lmt2=0.25;

% lmt is the needle material heat conductivity
lmt=25;

%Calculation of heat dissipation coefficient α = k/ρc
emis1=lmt/(rou*c);

% qq0 is the total friction heat per unit area per unit time
qq0=df*vel;

T(1)=To;
time(1)=0;
```

```
for cycle=0:1:120,
   I=cycle*4+1;


% sama is the friction heat partition coefficient
   dt0=T(I)-To;
   sama(cycle+1)=sliding(dt0,rou,c,lmt,lmt2,th,rpm,df);

   qq=qq0*sama(cycle+1);

   T(I+1)=sheat(T(I),lmt,emis1,vel,th,qq);
   time(I+1)=time(I)+t1;

   T(I+2)=scool(To,T(I+1),area,pcv,rpm,alf,t2);
   time(I+2)=time(I+1)+t2;

   T(I+3)=sheat(T(I+2),lmt,emis1,vel,th,qq);
   time(I+3)=time(I+2)+t3;

   T(I+4)=scool(To,T(I+3),area,pcv,rpm,alf,t4);
   time(I+4)=time(I+3)+t4;

end

grid on
plot(time,T-273,'c')
hold on
```

Function to calculate friction heat partition ratio γ

```
function sama=sliding(dt0,rou1,c1,lmt1,lmt2,th,rpm,df)

% dp is the needle punching distance; dw is the needle idling distance.
dp=0.02;
dw=0.008;

% vel is the needle velocity; df is the friction force per unit area
vel=rpm*2*(dp+dw)/60;
q=df*vel;

%Calculation of heat dissipation coefficient α = k/ρc
emis=lmt1/(rou1*c1);

% Calculation of the friction partition ratio γ
sama=(0.946*q*th/lmt2-
dt0)/(1.064*q*sqrt(emis*th/vel)/lmt1+0.946*q*th/lmt2);
```

Function to calculate needle temperature in heating process

```
function y=sheat(Ti,lmt1,emis1,vel,th,q)
```

```
% Ti is the initial temperature when heating begin
% q is the part of friction heat goes to the needle

y=Ti+1.064*q*sqrt(emis1*th/vel)/lmt1;
```

Function to calculate needle temperature in cooling process

```
function y=scool(To,Ti,area,pcv,rpm,alf,t)

% Ti is the initial temperature when cooling begin
% To is the environment temperature
% t is the cooling time

% beta is the coefficient to adjust the needle volume active in heating
and cooling
beta=0.02*2000/rpm;
pcv0=beta*pcv;
y=To+(Ti-To)*exp(-alf*area*t/pcv0);
```

Appendix B: Some parameters that affect the friction heat partition ratio γ.

Following curves based on the equation (3.22) give a basic trend of how the γ is going to change with sewing speed, fabric thickness, material properties of both needle and fabric. Since assumptions have been made while deducing the equation, therefore the value may be modified when in real use.

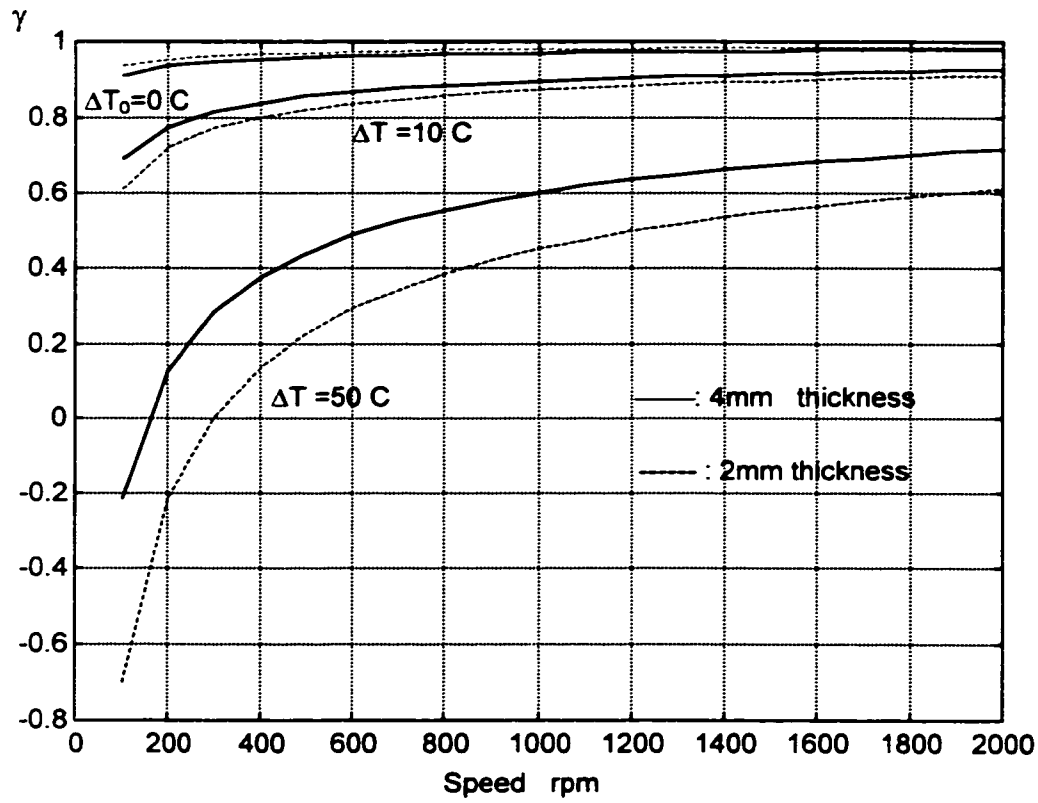

Figure B.1 γ vs. sewing speed at different fabric thickness

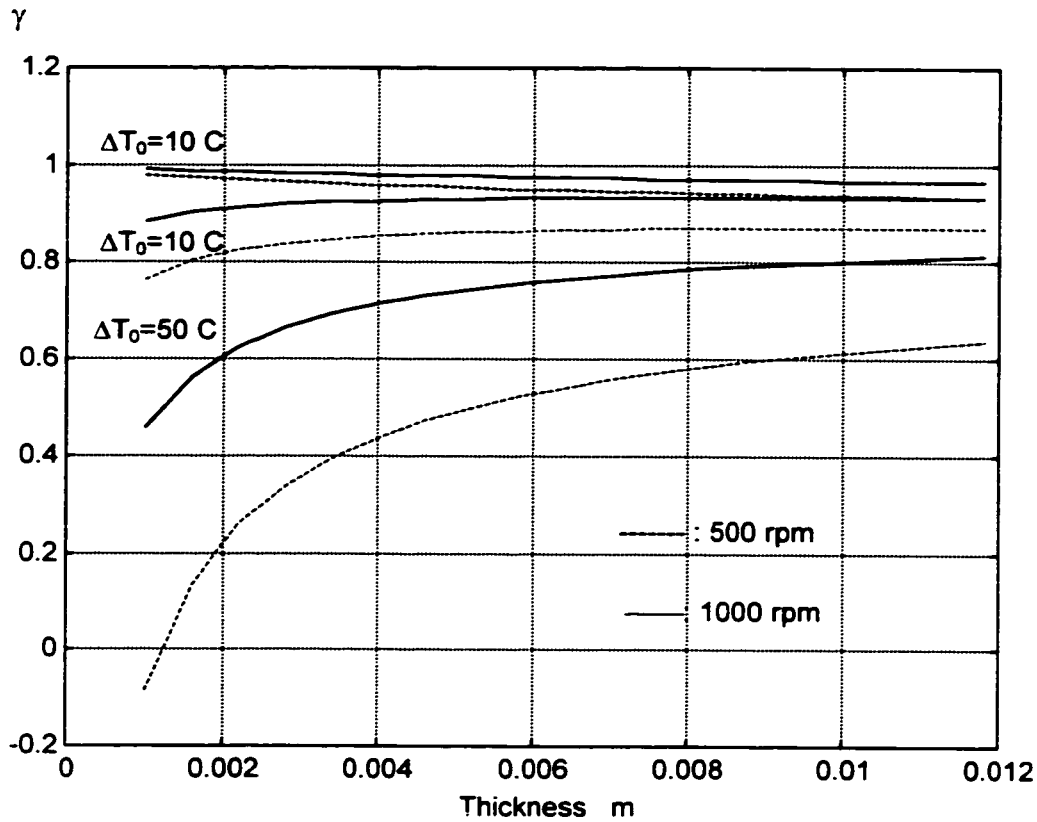

Figure B.2 γ vs. fabric thickness at different sewing speed

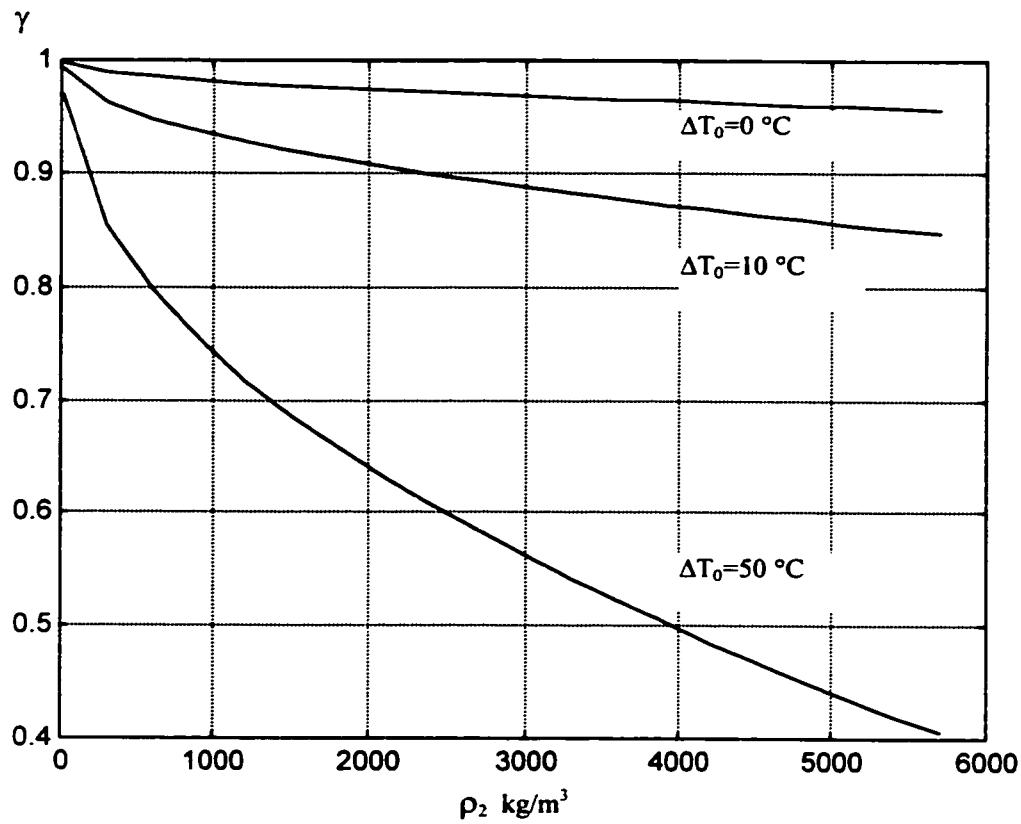

Figure B.3 γ vs. fabric density at different initial temperature difference

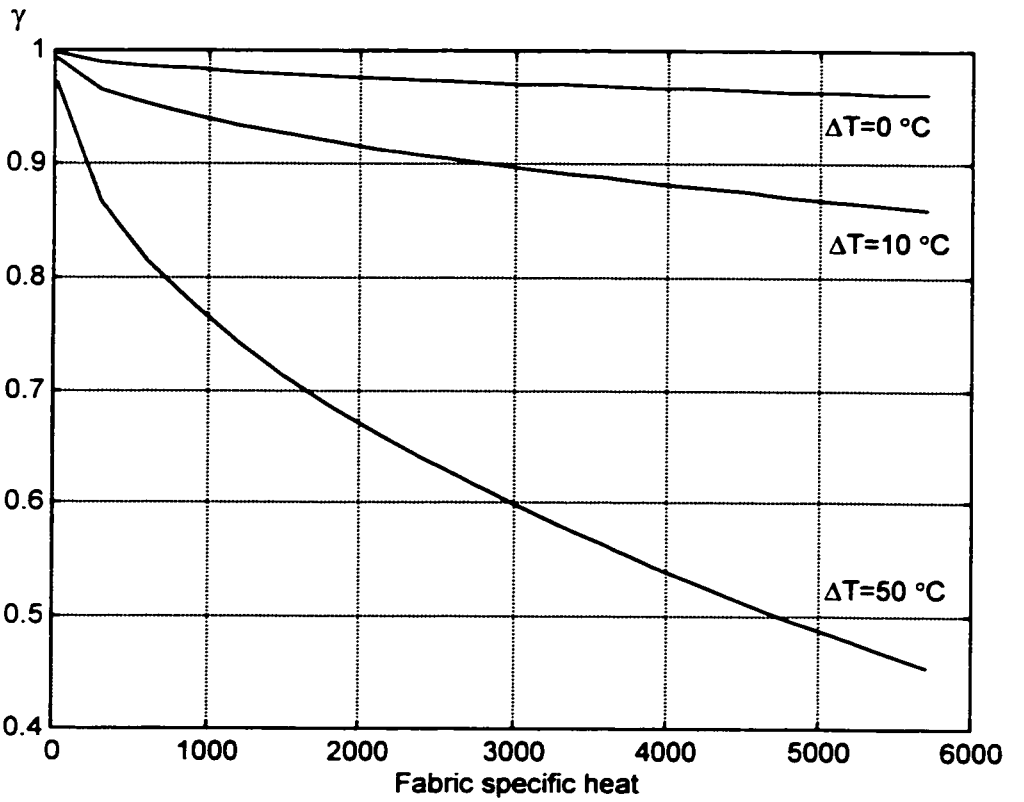

Figure B.4 γ vs. fabric specific heat

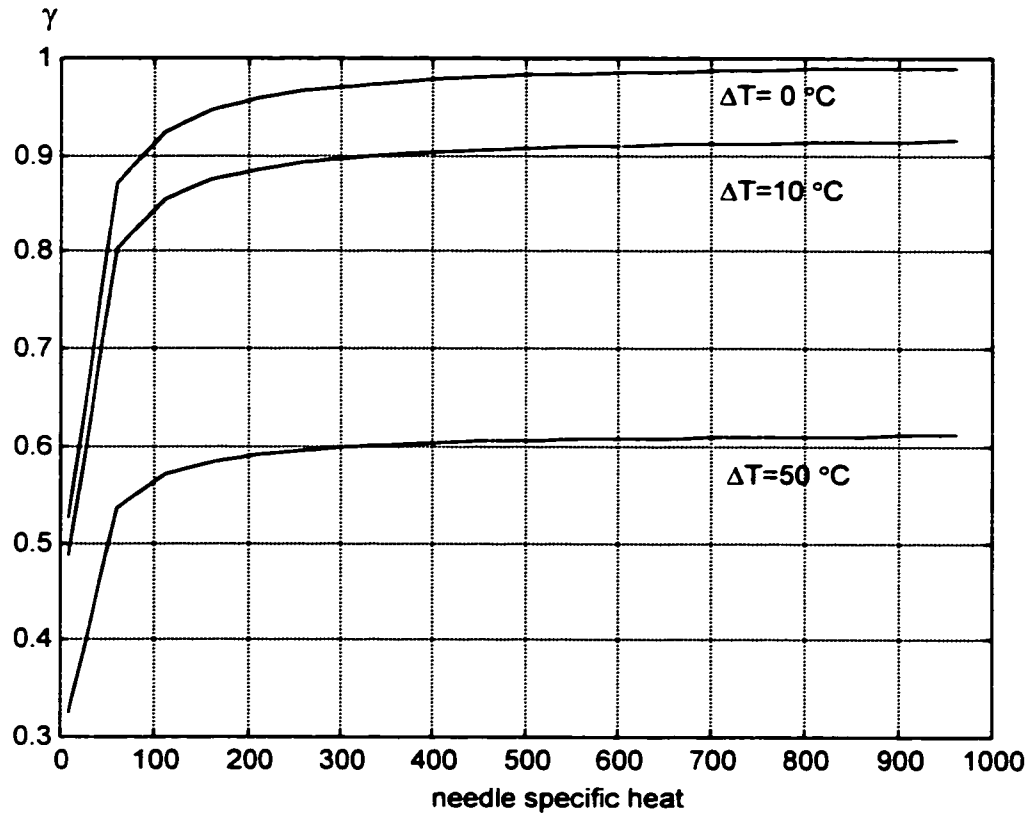

Figure B.5 γ vs. needle specific heat

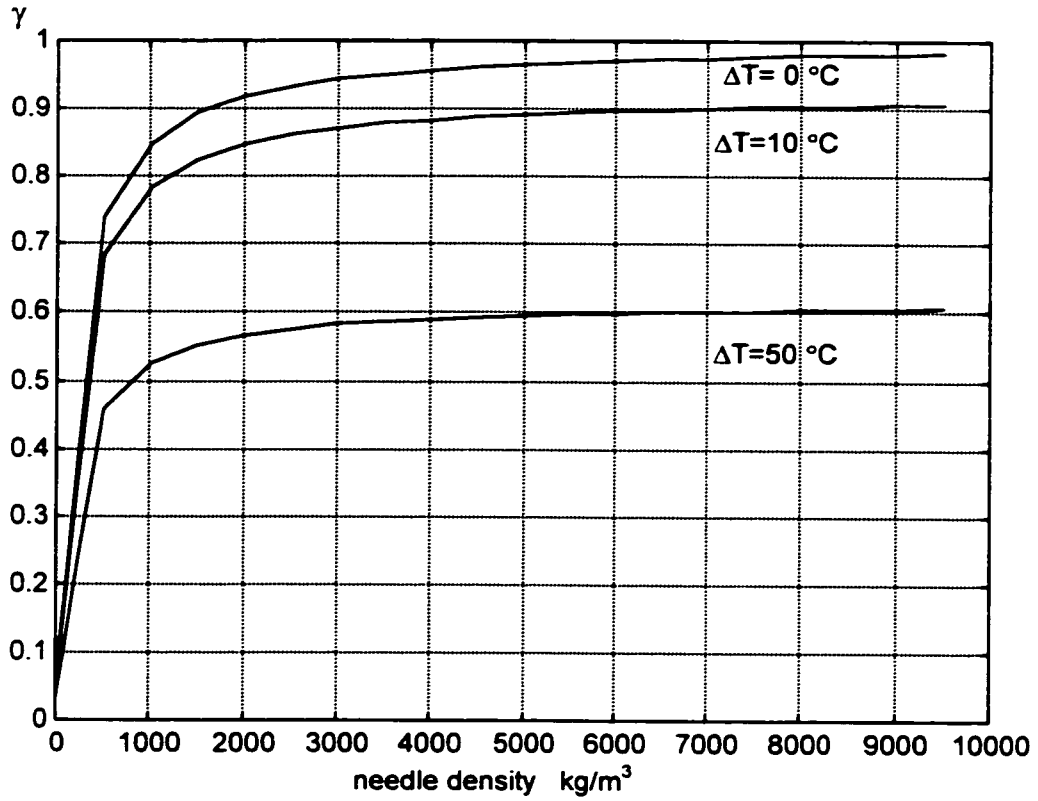

Figure B.6 γ vs. needle density at different ΔT_0

Appendix C: Matlab Program for Lumped Model

Main function to calculate the examined needle section temperature

---

```
function y=main(y0,rou,c,ri,th,rpm,df,alf)

% y0 is the distance between the examined point to the needle tip
% df is the friction force per unit area
% alf is the cooling coefficient

% To is the environment temperature
To=295;
dp=0.02;
dw=0.008;

% vol is the volume of the needle section examined
vol=ri*ri*3.14*th;
area=2*3.14*ri*th;
pcv=rou*c*vol;

vel=rpm*(dp+dw)*2/60;
% vel is the average velocity of needle

t1=th/vel;
t2=2*(dp-th/2-y0)/vel;
t3=t1;
t4=2*(y0+dw-th/2)/vel;
% t1 and t3 are the heating time
% t2 and t4 are the cooling time

% rou2, c2, lmt2 are fabric properties
lmt=17;
rou2=2500;
c2=3000;
lmt2=0.25;

% q0 is the total friction heat
q0=df*area*vel;

T(1)=To;
time(1)=0;

for cycle=0:1:40,
   I=cycle*4+1;

   dt0=T(I)-To;
   gama(cycle+1)=astot(dt0,rou,c,lmt,rou2,c2,lmt2,ri,df,th,rpm);

   q=q0*gama(cycle+1);

   T(I+1)=heat(T(I),q,pcv,t1);
```

```
    time(I+1)=time(I)+t1;

    T(I+2)=cool(To,T(I+1),area,pcv,alf,t2);
    time(I+2)=time(I+1)+t2;

    T(I+3)=heat(T(I+2),q,pcv,t3);
    time(I+3)=time(I+2)+t3;

    T(I+4)=cool(To,T(I+3),area,pcv,alf,t4);
    time(I+4)=time(I+3)+t4;

end

grid on
plot(time,T-273,'m')
hold on
```

Function to calculate friction heat partition ratio γ

```
function gama=astot(dt0,rou1,c1,lmt1,rou2,c2,lmt2,ri,df,th,rpm)

% sta1 is the coefficient to adjust the total equation
% sta2 is the coefficient to adjust the radius
sta1=0.9;
sta2=0.55;

% ri2 is the radius after adjusted
ri2=sta2*sqrt(ri*th);

area=2*pi*ri*th;
f=area*df;
a1=rou1*c1*(th*pi*ri*ri);

a2=2*lmt2*pi*ri2;
nt=lmt2/(rou2*c2*ri2*ri2);

vlci=rpm*2*0.028/60;
t=th/vlci;

x=nt*t;
z=1.0-exp(x)*erfc(sqrt(x));

gama=1.0-(dt0/(f*th)+1.0/a1)/(1.0/a1+z*sta1/(t*a2));
```

Function to calculate needle temperature in heating process

```
function y=heat(Ti,q,pcv,t)

% Ti is the initial temperature when heating begin
% q is the part of friction heat goes to the needle
% t is the heating time
```

```
y=Ti+q*t/pcv;
```

Function to calculate needle temperature in cooling process

```
function y=cool(To,Ti,area,pcv,alf,t)

% Ti is the initial temperature when cooling begin
% To is the environment temperature
% t is the cooling time
y=To+(Ti-To)*exp(-alf*area*t/pcv);
```

Appendix D: ANSYS Program for FEA Model

```
!*******
! Start
!*******
/BATCH

! /COM,ANSYS RELEASE  5.3    UP010997         13:48:19    18/04/1997
!/input,menust,tmp

!***********
!Parameters
!***********

!The array of heat flux coefficient

!"dtemp" is temperature difference between needle and fabric
*DIM,dtemp,ARRAY,500

!"ntemp" is needle reference temperature
*DIM,ntemp,ARRAY,500

!-------------------------------------------------------------
!Geometry of the needle

!Needle Radius
ri=0.001

!Length of the needle
nlg=0.03

!Location of the needle eye
hb=0.008
he=0.010

!Location of the short groove
sgb=0.006
sge=0.012
!Location of the long groove
lgb=0.006
lge=0.026

!dimension of bulge around the needle hole
bugl=0.0002

*DIM,rad,TABLE,7
rad(1)=0.0001,ri,ri,ri+bugl,ri+bugl,ri,ri
rad(1,0)=0,0.006,hb-0.002,hb,he,he+0.002,nlg
rad(0,1)=1

!-------------------------------------------------------
!Sewing parameters

!sewing speed
```

```
rpm=2000
!Distance of penetration
dp=0.02

!Distance of idling
dw=0.008

!Thickness of the fabric
th=0.004

!Needle punching speed
spd=rpm*(dp+dw)*2/60

!-------------------------------------------------------
!Meshing parameters

!Number of elements on the length
ndiv=30

!Number of sections experiencing heat flux at the same time
nshf=th/nlg*ndiv

!Number of load steps during punching
kp=dp/th

!Number of load steps during withdraw
kw=dw/th

!-------------------------------------------------------
!Thermal conditions

!Initial temperature
itemp=295

!Bulk temperature
btemp=295

!Heat flux
!friction force density
fric=900000

!Friction force
frcn=fric*2*3.14*ri*th

!friction power
fpower=fric*spd

!coefficient of adjusted friction due to bulge
fbt=(ri+bugl)/ri

*DIM,hheat,TABLE,7
hheat(1)=0,fpower/fbt,fpower,fpower*fbt,fpower*fbt,fpower,fpower/fbt
hheat(1,0)=0,ndiv/nlg*0.006,ndiv*(hb-
0.002)/nlg,ndiv*hb/nlg,ndiv*he/nlg,ndiv*(he+0.002)/nlg,ndiv
hheat(0,1)=1
```

```
! att (W/C) is the thread cooling coefficient
att=0.001
!thread absorption rate
btt=0.015

!heat_flow to needle eye (W)
hflow=0.02

!coefficient on outer face
fcoef=100
!coefficient on groove
gfcoef=50

!-------------------------------------------------------
!Fabric Properties

!Fabric density
rou2=2500
!Fabric Specific Heat
c2=3000
!Fabric Heat Conduction Coefficient
lmt2=0.25

!-------------------------------------------------------

!Nodes counter
nnb=1
!Elements counter
enb=1

!*************
!Preprocessor
!*************

/PREP7

!---Thermal analysis---
KEYW,PR_SET,1
KEYW,PR_STRUC,0
KEYW,PR_THERM,1
KEYW,PR_ELMAG,0
KEYW,PR_FLUID,0
KEYW,PR_MULTI,0
KEYW,PR_CFD,0
KEYW,LSDYNA,0
/PMETH,OFF

!---Element type---
ET,1,SOLID70
KEYOPT,1,2,0
KEYOPT,1,4,0
KEYOPT,1,7,0
KEYOPT,1,8,0
```

```
!---Material properties---
UIMP,1,EX, , ,
UIMP,1,DENS, , ,7500
UIMP,1,ALPX, , , ,
UIMP,1,REFT, , , ,
UIMP,1,NUXY, , ,0.3,
UIMP,1,PRXY, , , ,
UIMP,1,GXY, , , ,
UIMP,1,MU, , , ,
UIMP,1,DAMP, , , ,
UIMP,1,KXX, , ,20,
UIMP,1,C, , ,400,
UIMP,1,ENTH, , , ,
UIMP,1,HF, , , ,
UIMP,1,EMIS, , , ,
UIMP,1,QRATE, , , ,
UIMP,1,MURX, , , ,
UIMP,1,MGXX, , , ,
UIMP,1,RSVX, , , ,
UIMP,1,PERX, , , ,
UIMP,1,VISC, , , ,
UIMP,1,SONC, , , ,

TYPE,1,
MAT,1,
REAL,1,
ESYS,0,

!---Get Needle Material Properties---
*GET,roul,DENS,1,TEMP, ,
*GET,cl,C,1,TEMP, ,
*GET,lmtl,KXX,1,TEMP, ,

!---Constants Calculation for Gama---

! coefficient for fabric equation
sta1=0.9

! coefficient for radius
sta2=0.55

ri2=sta2*sqrt(ri*th)

a1=roul*cl*(th*3.14*ri*ri)
a2=2*lmt2*3.14*ri2
nt=lmt2/(rou2*c2*ri2*ri2)
tim=th/spd
ntt=1.1*sqrt(nt*tim)
z=sta1*(1.0-exp(-ntt))

!-----------------------------------------------------------

!---Meshing---

N,nnb,0,0,0
```

```
N,nnb+1,0,-rad(0)/2,0
N,nnb+2,rad(0)*0.707/2,-rad(0)*0.707/2,0
N,nnb+3,rad(0)/2,0,0
N,nnb+4,rad(0)*0.707/2,rad(0)*0.707/2,0
N,nnb+5,0,rad(0)/2,0
N,nnb+6,0,-rad(0),0
N,nnb+7,rad(0)*0.707,-rad(0)*0.707,0
N,nnb+8,rad(0),0,0
N,nnb+9,rad(0)*0.707,rad(0)*0.707,0
N,nnb+10,0,rad(0),0
nnb=nnb+11

*DO,I,nlg/ndiv,nlg,nlg/ndiv

N,nnb,0,0,I
N,nnb+1,0,-rad(I)/2,I
N,nnb+2,rad(I)*0.707/2,-rad(I)*0.707/2,I
N,nnb+3,rad(I)/2,0,I
N,nnb+4,rad(I)*0.707/2,rad(I)*0.707/2,I
N,nnb+5,0,rad(I)/2,I
N,nnb+6,0,-rad(I),I
N,nnb+7,rad(I)*0.707,-rad(I)*0.707,I
N,nnb+8,rad(I),0,I
N,nnb+9,rad(I)*0.707,rad(I)*0.707,I
N,nnb+10,0,rad(I),I

EN,enb+1,nnb-4,nnb-3,nnb+8,nnb+7,nnb-9,nnb-8,nnb+3,nnb+2
EN,enb+2,nnb-3,nnb-2,nnb+9,nnb+8,nnb-8,nnb-7,nnb+4,nnb+3

*IF,I,LE,hb,THEN
EN,enb+4,nnb-7,nnb-6,nnb+5,nnb+4,nnb-8,nnb-11,nnb,nnb+3
EN,enb+5,nnb-10,nnb-9,nnb+2,nnb+1,nnb-11,nnb-8,nnb+3,nnb
*ENDIF
*IF,I,GT,he,THEN
EN,enb+4,nnb-7,nnb-6,nnb+5,nnb+4,nnb-8,nnb-11,nnb,nnb+3
EN,enb+5,nnb-10,nnb-9,nnb+2,nnb+1,nnb-11,nnb-8,nnb+3,nnb
*ENDIF

*IF,I,LE,sgb,THEN
EN,enb,nnb-5,nnb-4,nnb+7,nnb+6,nnb-10,nnb-9,nnb+2,nnb+1
*ENDIF
*IF,I,GT,sge,THEN
EN,enb,nnb-5,nnb-4,nnb+7,nnb+6,nnb-10,nnb-9,nnb+2,nnb+1
*ENDIF

*IF,I,LE,lgb,THEN
EN,enb+3,nnb-2,nnb-1,nnb+10,nnb+9,nnb-7,nnb-6,nnb+5,nnb+4
*ENDIF
*IF,I,GT,lge,THEN
EN,enb+3,nnb-2,nnb-1,nnb+10,nnb+9,nnb-7,nnb-6,nnb+5,nnb+4
*ENDIF

nnb=nnb+11
enb=enb+6
```

```
*ENDDO

!---End of meshing---

!Initial temperature
*DO,J,1,nnb-1,1
IC,J,TEMP,itemp
*ENDDO
FINISH

!********
! Solver
!********

/SOLU
ANTYPE,4

!---Begin applying multiple load steps---

!-------------------------------------------------------------
*DO,CYCLE,0,245,1

!---Caculate friction heat distribution---
ntemp(CYCLE+1)=TEMP(ndiv/nlg*he*11+9)
dtemp(CYCLE+1)=ntemp(CYCLE+1)-itemp
gama=1.0-(dtemp(CYCLE+1)/(frcn*th)+1.0/a1)/(1.0/a1+z/(tim*a2))

*IF,gama,LE,0, THEN
      gama=0
*ENDIF

!---punching---

*DO,L_STEP, 2*(kw+kp)*CYCLE+1,(kw+kp)*(2*CYCLE+1),1

TIME, th/spd*L_STEP
AUTOTS,0
DELTIM,th/spd,0,0,0
KBC,1

!ttpp is the eye reference temperature
ttpp=TEMP(ndiv/nlg*he*11+6)
atcoe=EXP(-btt*(ttpp-itemp))

!Four nodes experience friction heat in idling steps

*IF, L_STEP,LE,2*(kw+kp)*cycle+kw,THEN

      F,ndiv/nlg*hb*11+2,HEAT,hflow*atcoe,
      F,ndiv/nlg*hb*11+3,HEAT,hflow*atcoe,
      F,ndiv/nlg*he*11+6,HEAT,hflow*atcoe,
      F,ndiv/nlg*he*11+5,HEAT,hflow*atcoe,
*ELSE
      F,ndiv/nlg*hb*11+2,HEAT,att*(itemp-ttpp),
      F,ndiv/nlg*hb*11+3,HEAT,att*(itemp-ttpp),
```

```
      F,ndiv/nlg*he*11+6,HEAT,att*(itemp-ttpp),
      F,ndiv/nlg*he*11+5,HEAT,att*(itemp-ttpp),
*ENDIF

!Convection in short groove_side
*DO,I,sgb/nlg*ndiv,sge/nlg*ndiv-1,1
SFE,6*I+2,5,CONV,0,gfcoef,
SFE,6*I+2,5,CONV,2,btemp,
*ENDDO

!Convection in short groove_bottom
*DO,I,sgb/nlg*ndiv,hb/nlg*ndiv-1,1
SFE,6*I+6,1,CONV,0,gfcoef,
SFE,6*I+6,1,CONV,2,btemp,
*ENDDO
*DO,I,he/nlg*ndiv,sge/nlg*ndiv-1,1
SFE,6*I+6,1,CONV,0,gfcoef,
SFE,6*I+6,1,CONV,2,btemp,
*ENDDO

!Convection in long groove_side
*DO,I,lgb/nlg*ndiv,lge/nlg*ndiv-1,1
SFE,6*I+3,3,CONV,0,gfcoef,
SFE,6*I+3,3,CONV,2,btemp,
*ENDDO

!Convection in long groove_bottom
*DO,I,lgb/nlg*ndiv,hb/nlg*ndiv-1,1
SFE,6*I+5,1,CONV,0,gfcoef,
SFE,6*I+5,1,CONV,2,btemp,
*ENDDO
*DO,I,he/nlg*ndiv,lge/nlg*ndiv-1,1
SFE,6*I+5,1,CONV,0,gfcoef,
SFE,6*I+5,1,CONV,2,btemp,
*ENDDO

!Convection in the hole
*DO,I,hb/nlg*ndiv,he/nlg*ndiv-1,1
SFE,6*I+2,6,CONV,0,gfcoef,
SFE,6*I+2,6,CONV,2,btemp,
SFE,6*I+3,6,CONV,0,gfcoef,
SFE,6*I+3,6,CONV,2,btemp,
*ENDDO

!Element 1-Exterior face load
*DO,I,0,sgb/nlg*ndiv-1,1
*IF,I,GE,(L_STEP-kw-1-2*(kp+kw)*CYCLE)*nshf,THEN
      *IF,I,LE,(L_STEP-kw-2*(kp+kw)*CYCLE)*nshf-1,THEN
            SFE,6*I+1,1,HFLUX , ,hheat(I)*gama,
      *ELSE
            SFE,6*I+1,1,CONV,0,fcoef,
            SFE,6*I+1,1,CONV,2,btemp,
      *ENDIF
*ELSE
      SFE,6*I+1,1,CONV,0,fcoef,
```

```
      SFE,6*I+1,1,CONV,2,btemp,
*ENDIF
*ENDDO

*DO,I,sge/nlg*ndiv,ndiv-1,1
*IF,I,GE,(L_STEP-kw-1-2*(kp+kw)*CYCLE)*nshf,THEN
      *IF,I,LE,(L_STEP-kw-2*(kp+kw)*CYCLE)*nshf-1,THEN
            SFE,6*I+1,1,HFLUX , ,hheat(I)*gama,
      *ELSE
            SFE,6*I+1,1,CONV,0,fcoef,
            SFE,6*I+1,1,CONV,2,btemp,
      *ENDIF
*ELSE
      SFE,6*I+1,1,CONV,0,fcoef,
      SFE,6*I+1,1,CONV,2,btemp,
*ENDIF
*ENDDO


!Element 2 and 3-Exterior face load
*DO,I,0,ndiv-1,1
*IF,I,GE,(L_STEP-kw-1-2*(kp+kw)*CYCLE)*nshf,THEN
      *IF,I,LE,(L_STEP-kw-2*(kp+kw)*CYCLE)*nshf-1,THEN
            SFE,6*I+2,1,HFLUX , ,hheat(I)*gama,
            SFE,6*I+3,1,HFLUX , ,hheat(I)*gama,
      *ELSE
            SFE,6*I+2,1,CONV,0,fcoef,
            SFE,6*I+2,1,CONV,2,btemp,
            SFE,6*I+3,1,CONV,0,fcoef,
            SFE,6*I+3,1,CONV,2,btemp,
      *ENDIF
*ELSE
      SFE,6*I+2,1,CONV,0,fcoef,
      SFE,6*I+2,1,CONV,2,btemp,
      SFE,6*I+3,1,CONV,0,fcoef,
      SFE,6*I+3,1,CONV,2,btemp,
*ENDIF
*ENDDO


!Element 4-Exterior face load
*DO,I,0,lgb/nlg*ndiv-1,1
*IF,I,GE,(L_STEP-kw-1-2*(kp+kw)*CYCLE)*nshf,THEN
      *IF,I,LE,(L_STEP-kw-2*(kp+kw)*CYCLE)*nshf-1,THEN
            SFE,6*I+4,1,HFLUX , ,hheat(I)*gama,
      *ELSE
            SFE,6*I+4,1,CONV,0,fcoef,
            SFE,6*I+4,1,CONV,2,btemp,
      *ENDIF
*ELSE
      SFE,6*I+4,1,CONV,0,fcoef,
      SFE,6*I+4,1,CONV,2,btemp,
*ENDIF
*ENDDO
```

```
*DO,I,lge/nlg*ndiv,ndiv-1,1
*IF,I,GE,(L_STEP-kw-1-2*(kp+kw)*CYCLE)*nshf,THEN
      *IF,I,LE,(L_STEP-kw-2*(kp+kw)*CYCLE)*nshf-1,THEN
            SFE,6*I+4,1,HFLUX , ,hheat(I)*gama,
      *ELSE
            SFE,6*I+4,1,CONV,0,fcoef,
            SFE,6*I+4,1,CONV,2,btemp,
      *ENDIF
*ELSE
      SFE,6*I+4,1,CONV,0,fcoef,
      SFE,6*I+4,1,CONV,2,btemp,
*ENDIF
*ENDDO

LSWRITE,L_STEP,
SOLVE

SFEDELE,ALL,ALL,ALL
FDELE,ALL,ALL

*ENDDO
!---end of punching---

!-----------------------------------------------------

!---withdraw----

*DO,L_STEP,(kw+kp)*(2*CYCLE+1)+1,(kw+kp)*(2*CYCLE+2),1

TIME, th/spd*L_STEP
AUTOTS,0
DELTIM,th/spd,0,0,0
KBC,1


ttpp=TEMP(ndiv/nlg*he*11+6)

!Four nodes experience cooling

F,ndiv/nlg*hb*11+2,HEAT,att*(itemp-ttpp),
F,ndiv/nlg*hb*11+3,HEAT,att*(itemp-ttpp),
F,ndiv/nlg*he*11+6,HEAT,att*(itemp-ttpp),
F,ndiv/nlg*he*11+5,HEAT,att*(itemp-ttpp),

!Convection in short groove_side
*DO,I,sgb/nlg*ndiv,sge/nlg*ndiv-1,1
SFE,6*I+2,5,CONV,0,gfcoef,
SFE,6*I+2,5,CONV,2,btemp,
*ENDDO

!Convection in short groove_bottom
*DO,I,sgb/nlg*ndiv,hb/nlg*ndiv-1,1
SFE,6*I+6,1,CONV,0,gfcoef,
SFE,6*I+6,1,CONV,2,btemp,
*ENDDO
```

```
*DO,I,he/nlg*ndiv,sge/nlg*ndiv-1,1
SFE,6*I+6,1,CONV,0,gfcoef,
SFE,6*I+6,1,CONV,2,btemp,
*ENDDO

!Convection in long groove_side
*DO,I,lgb/nlg*ndiv,lge/nlg*ndiv-1,1
SFE,6*I+3,3,CONV,0,gfcoef,
SFE,6*I+3,3,CONV,2,btemp,
*ENDDO

!Convection in long groove_bottom
*DO,I,lgb/nlg*ndiv,hb/nlg*ndiv-1,1
SFE,6*I+5,1,CONV,0,gfcoef,
SFE,6*I+5,1,CONV,2,btemp,
*ENDDO
*DO,I,he/nlg*ndiv,lge/nlg*ndiv-1,1
SFE,6*I+5,1,CONV,0,gfcoef,
SFE,6*I+5,1,CONV,2,btemp,
*ENDDO

!Convection in the hole
*DO,I,hb/nlg*ndiv,he/nlg*ndiv-1,1
SFE,6*I+2,6,CONV,0,gfcoef,
SFE,6*I+2,6,CONV,2,btemp,
SFE,6*I+3,6,CONV,0,gfcoef,
SFE,6*I+3,6,CONV,2,btemp,
*ENDDO

!Element 1-Exterior face load
*DO,I,0,sgb/nlg*ndiv-1,1
*IF,I,GE,(2*kp+kw-L_STEP+2*(kp+kw)*CYCLE)*nshf,THEN
      *IF,I,LE,(2*kp+kw-L_STEP+1+2*(kp+kw)*CYCLE)*nshf-1,THEN
            SFE,6*I+1,1,HFLUX , ,hheat(I)*gama,
      *ELSE
            SFE,6*I+1,1,CONV,0,fcoef,
            SFE,6*I+1,1,CONV,2,btemp,
      *ENDIF
*ELSE
      SFE,6*I+1,1,CONV,0,fcoef,
      SFE,6*I+1,1,CONV,2,btemp,
*ENDIF
*ENDDO

*DO,I,sge/nlg*ndiv,ndiv-1,1
*IF,I,GE,(2*kp+kw-L_STEP+2*(kp+kw)*CYCLE)*nshf,THEN
      *IF,I,LE,(2*kp+kw-L_STEP+1+2*(kp+kw)*CYCLE)*nshf-1,THEN
            SFE,6*I+1,1,HFLUX , ,hheat(I)*gama,
      *ELSE
            SFE,6*I+1,1,CONV,0,fcoef,
            SFE,6*I+1,1,CONV,2,btemp,
      *ENDIF
*ELSE
      SFE,6*I+1,1,CONV,0,fcoef,
      SFE,6*I+1,1,CONV,2,btemp,
```

```
*ENDIF
*ENDDO


!Element 2 and 3-Exterior face load
*DO,I,0,ndiv-1,1
*IF,I,GE,(2*kp+kw-L_STEP+2*(kp+kw)*CYCLE)*nshf,THEN
      *IF,I,LE,(2*kp+kw-L_STEP+1+2*(kp+kw)*CYCLE)*nshf-1,THEN
            SFE,6*I+2,1,HFLUX , ,hheat(I)*gama,
            SFE,6*I+3,1,HFLUX , ,hheat(I)*gama,
      *ELSE
            SFE,6*I+2,1,CONV,0,fcoef,
            SFE,6*I+2,1,CONV,2,btemp,
            SFE,6*I+3,1,CONV,0,fcoef,
            SFE,6*I+3,1,CONV,2,btemp,
      *ENDIF
*ELSE
      SFE,6*I+2,1,CONV,0,fcoef,
      SFE,6*I+2,1,CONV,2,btemp,
      SFE,6*I+3,1,CONV,0,fcoef,
      SFE,6*I+3,1,CONV,2,btemp,
*ENDIF
*ENDDO

!Element 4-Exterior face load
*DO,I,0,lgb/nlg*ndiv-1,1
*IF,I,GE,(2*kp+kw-L_STEP+2*(kp+kw)*CYCLE)*nshf,THEN
      *IF,I,LE,(2*kp+kw-L_STEP+1+2*(kp+kw)*CYCLE)*nshf-1,THEN
            SFE,6*I+4,1,HFLUX , ,hheat(I)*gama,
      *ELSE
            SFE,6*I+4,1,CONV,0,fcoef,
            SFE,6*I+4,1,CONV,2,btemp,
      *ENDIF
*ELSE
      SFE,6*I+4,1,CONV,0,fcoef,
      SFE,6*I+4,1,CONV,2,btemp,
*ENDIF
*ENDDO

*DO,I,lge/nlg*ndiv,ndiv-1,1
*IF,I,GE,(2*kp+kw-L_STEP+2*(kp+kw)*CYCLE)*nshf,THEN
      *IF,I,LE,(2*kp+kw-L_STEP+1+2*(kp+kw)*CYCLE)*nshf-1,THEN
            SFE,6*I+4,1,HFLUX , ,hheat(I)*gama,
      *ELSE
            SFE,6*I+4,1,CONV,0,fcoef,
            SFE,6*I+4,1,CONV,2,btemp,
      *ENDIF
*ELSE
      SFE,6*I+4,1,CONV,0,fcoef,
      SFE,6*I+4,1,CONV,2,btemp,
*ENDIF
*ENDDO

LSWRITE,L_STEP,
SOLVE
```

```
SFEDELE,ALL,ALL,ALL
FDELE,ALL,ALL

*ENDDO
!---End of withdraw---

*ENDDO

!---Multiple Punching Load steps done---

!-----------------------------------------------------------
SAVE

FINISH

/EXIT,ALL
```

Appendix E: FEA Simulation Results with Fabric Thickness at 2 mm

Following curves are the FEA simulation results of different speed at 2 mm fabric thickness, from where part of the Table 4.1 are filled.

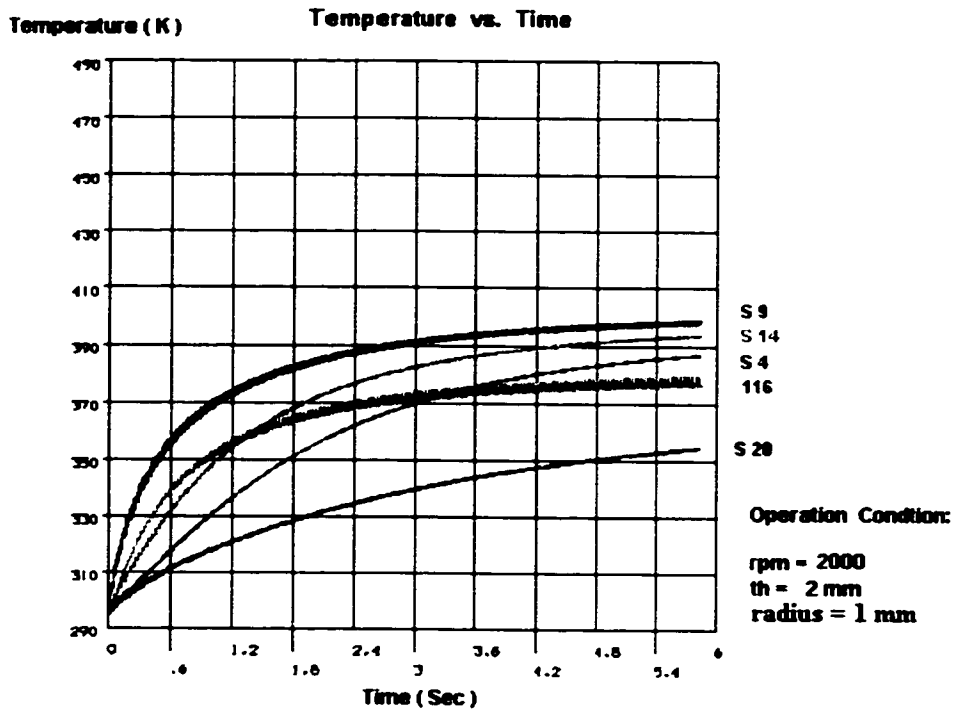

Figure E.1 Temperature vs. time, 2000 rpm, th = 2 mm

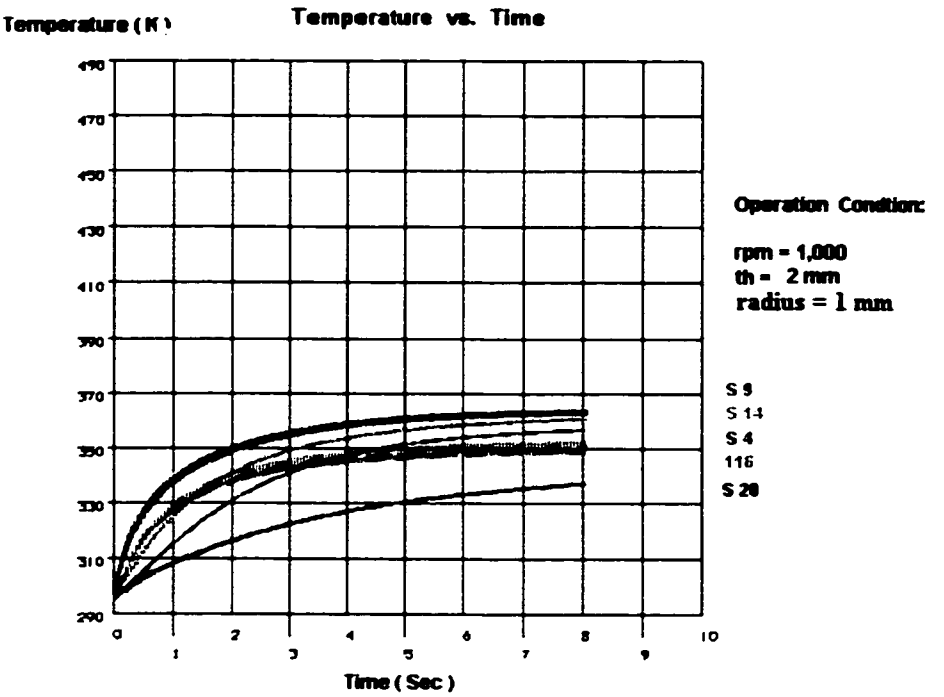

Figure E.2 Temperature vs. time, 1000 rpm, th = 2 mm

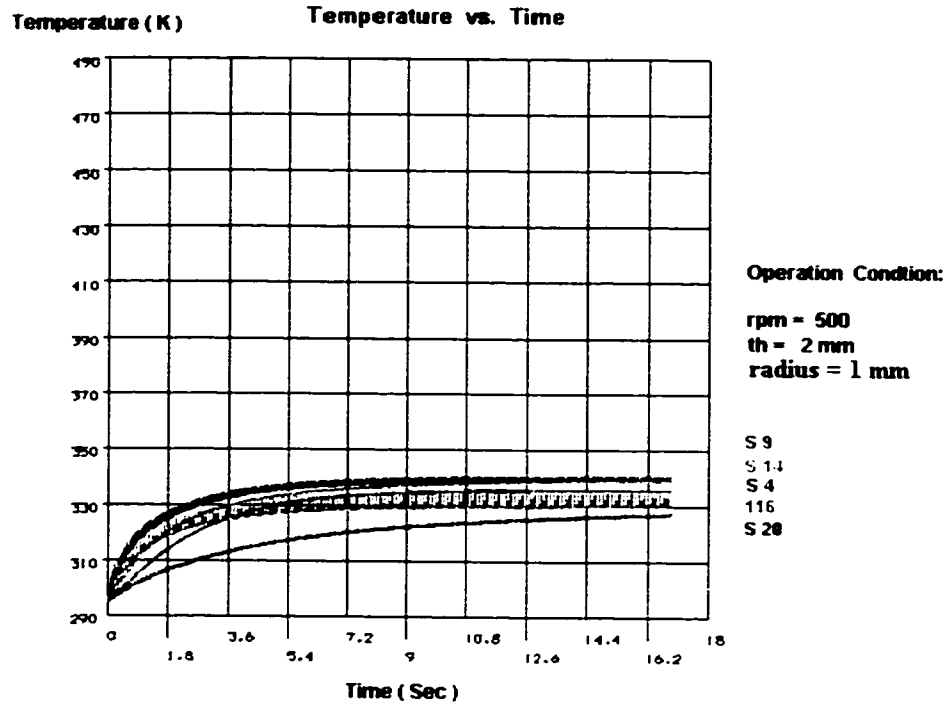

Figure E.3 Temperature vs. time, 500 rpm, th = 2 mm

VITA AUCTORIS

NAME:	Qingwen Li
PLACE OF BIRTH:	Tangshan, Hebei, China
EDUCATION:	University of Windsor, Windsor, Ontario 1996 - 1998 M.A.Sc.
	Xi'an Jiaotong University, Xi'an, P.R.China M.A.Sc. 1991
	Xi'an Jiaotong University, Xi'an, P.R.China B.E. 1988